GPS/INS INTEGRATION FOR PEDESTRIAN NAVIGATION

THÈSE N° 2704 (2002)

PRÉSENTÉE À LA FACULTÉ ENVIRONNEMENT NATUREL, ARCHITECTURAL ET CONSTRUIT

SECTION DES SCIENCES ET INGÉNIERIE DE L'ENVIRONNEMENT

ÉCOLE POLYTECHNIQUE FÉDÉRALE DE LAUSANNE

POUR L'OBTENTION DU GRADE DE DOCTEUR ÈS SCIENCES TECHNIQUES

PAR

Vincent GABAGLIO

ingénieur du génie rural diplômé EPF
de nationalité suisse et originaire de Ligornetto (TI)

acceptée sur proposition du jury:

Prof. B. Merminod, directeur de thèse
Dr M. El-Khoury, rapporteur
Dr C. Marselli, rapporteur
Prof. Ph. Robert, rapporteur

Lausanne, EPFL
2003

Abstract

This research has been sponsored by the Centre Suisse d'Electronique et de Microtechnique (CSEM) in Neuchâtel, Switzerland. It introduces a system and the algorithms for *Pedestrian Navigation* using a combination of sensors. The main objective is to localise a pedestrian anywhere and at any moment. The equipments utilised to fulfil this requirement are a Global Navigation Satellite System (GNSS) receiver and inertial sensors, which are attached to the person and as such need to be portable.

An overview of *Pedestrian Navigation* constitutes the first part of the document. This new domain is examined from four different views: applications, tools (or sensors), architecture of the system and finally environment in which the pedestrian is travelling. As part of this process, the 'state of the art' situation is presented.

The approach followed in order to aid pedestrian to navigate is based on the Dead Reckoning technique coupled with GNSS. Consequently, the resolution of the travelled 'distance' is separated from the resolution of the orientation of the walk. For the computation of the distance, a new technique based upon accelerometers and GNSS has been developed and demonstrated. The accelerometers are not used as a classical pedometer (counter of the number of steps) and the technique is not based on the double integration to obtain successively speed and distance. Instead, signal processing allows, considering individual parameters, the walking speed to be obtained directly from the signal of the accelerometers. This process, as well as the manner to determine the individual parameters, is presented in detail. The development of the algorithms is based on research performed in both the navigation and the medical domains (mainly in physiology).

The computation of the orientation is more classical. It is based on the measurements made by a gyroscope and a GNSS receiver. The particularity of this study is the use of a single gyroscope to determine the orientation of the walk instead of three for the classical technique of inertial navigation. The influence of body movement on the gyroscope output has been deeply

examined to determine the most appropriate way to process the signal of the gyroscope. The feasibility of the use of a single gyro, in the context of pedestrian navigation, is demonstrated. The potential added value for introducing a magnetic compass in the system is also evaluated.

Finally a centralised Kalman filter has been designed and tested to merge all the sensors outputs, to combine the distance and the orientation, to integrate the Dead Reckoning solution and the GNSS solutions and to estimate all the parameters in a close to real-time process. The efficiency of this filter is demonstrated through different tests.

Résumé

Cette recherche a été financée par le Centre Suisse d'Electronique et de Microtechnique (CSEM) à Neuchâtel, Suisse. Elle présente un système et des algorithmes pour la navigation pédestre en utilisant une combinaison de capteurs. La principale demande est de localiser en tout temps et en tout lieu une personne. Les instruments utilisés pour répondre à ce besoin sont les récepteurs de système global de navigation par satellites GNSS et des capteurs inertiels.

Une vue d'ensemble de la navigation pédestre constitue la première partie de ce document. Ce nouveau domaine est examiné sous quatre différentes approches: les applications, les instruments (ou capteurs), l'architecture du système et finalement l'environnement dans lequel évolue le piéton. Par la même occasion, l'état de l'art dans ce domaine est présenté.

L'approche suivie pour aider un piéton à naviguer est basée sur la technique de la navigation à l'estime. En conséquence, la résolution de la distance parcourue est séparée de la résolution de l'orientation.

Pour le calcul de la distance, une nouvelle technique basée sur l'accélérométrie et le GNSS a été développée et démontrée. L'accéléromètre n'est pas utilisé comme un simple podomètre (compteur du nombre de pas) et il n'y a pas de double intégration pour obtenir successivement vitesse et distance. Un traitement de signal permet d'obtenir directement la vitesse de marche par l'intermédiaire de paramètres individuels. Ce traitement est présenté en détail ainsi que la manière de déterminer les paramètres individuels. Le développement des algorithmes se base sur les recherches dans le domaine de la navigation et dans le domaine médical (principalement la physiologie).

Le calcul de l'orientation est plus classique. Il utilise un gyroscope et un récepteurs GNSS. La particularité de cette étude réside dans l'utilisation d'un unique gyromètre pour déterminer l'orientation au lieu de trois en technique classique de navigation inertielle. L'influence du mouvement du corps

sur la sortie du gyromètre a été étudiée en détail afin de déterminer la manière la plus appropriée pour traiter le signal du gyro. La faisabilité de l'utilisation d'un unique gyromètre dans le contexte de la navigation pédestre est démontrée. La valeur ajoutée potentielle pour le système d'un compas magnétique est présentée.

Finalement, un filtre de Kalman centralisé a été conçu et testé afin de fusionner les sorties des capteurs, de combiner la distance à l'estime et l'orientation à l'estime, d'intégrer la solution de navigation à l'estime avec la solution GNSS et de compenser tous les paramètres. L'efficacité de ce filtre est démontrée par différents tests.

Abbreviations and notation

Abbreviations are often used in this thesis. The following section allows the readers to keep a good understanding of the text. The notation used in this thesis is a compromise between all the notations used by the reference authors. It is based on the notation used in the Institute of Geomatics at the Swiss Federal Institute of Technology in Lausanne. However, some concessions are made to the American notation for the least square adjustment. The same letter may be used twice for different meanings. In all such instances, clarifications are made within the text to avoid any confusion.

Abbreviation

BS	Base Station
CSEM	Centre Suisse d'Electronique et de Microtechnique
DGPS	Differential GPS
DME	Distance Measurement Equipment
DoD	US Department of Defense
DOP	Dilution Of Precision
DR	Dead Reckoning
EGNOS	European Geostationary Navigation Overlay Service
ENU	East-North-Up (right-handed coordinate axes)
EPFL	Ecole Polytechnique Fédérale de Lausanne
E-OTD	Enhanced Observed Time Difference
FDSS	Fall Detection Sensors System
FIR	Finite Impulse Response
FOG	Fibre Optic Gyro
GIS	Geographic Information System
GNSS	Global Navigation Satellite System
GPRS	General Packet Radio Service
GPS	Global Positioning System
GSM	Global System for Mobile communications
Gyro	Gyroscope
HDOP	Horizontal Dilution of Precision
IGEO	Institut de Géomatique
INS	Inertial Navigation System
IMU	Inertial Measurement Unit
KF	Kalman Filter
LBS	Location Based Services
LORAN	Long Range
MEMS	Micro-Electromechanical Systems
MIMU	Miniature Inertial Measurement Unit or MEMS IMU
MS	Master Station
MSPC	Multi-Variate Statistical Process Control
NAVSTAR	Navigation Satellite Timing and Ranging
NED	North-East-Down (right-handed coordinate axes)
PCA	Principal Component Analysis
PDA	Personal Digital Assistant

RAIM   Receiver Autonomous Integrity Monitoring
RF   Radio Frequency
RLG   Ring Laser Gyro
RMS   Root Mean Square
RTK   Real Time Kinematic
SA   Selective Availability
SARSAT   Search And Rescue Satellite
TDOA   Time Difference of Arrival
TOA   Time of Arrival
TOPO   Unité de Topométrie
UMTS   Universal Mobile Telecommunications System
UWB   Ultra Wide Band
VHF   Very High Frequency
VLF   Very Low Frequency
VOR   VHF Omnidirectional Range
WAAS   Wide Area Augmentation System
WGS-84   World Geodetic System (1984)
ZUP   Zero Velocity Update
2D   2 dimensions
3D   3 dimensions
2G   Second communication generation (GSM-GPRS)
3G   Third communication generation (UMTS)

Notation

Vectors

ℓ Vector of observation
$\mathbf{g}$ Earth's gravity field
$\mathbf{v}$ Observation residual
$\tilde{\mathbf{v}}$ Predicted error
$\mathbf{x}$ State vector
$d\mathbf{x}$ Increment of the state vector
$\overset{\circ}{\mathbf{x}}_k$ Approach value of the state vector at time k
$\tilde{\mathbf{x}}_k$ Predicted state vector at time k
$\hat{\mathbf{x}}_k$ Estimated state vector at time k
$\hat{\hat{\mathbf{x}}}_k$ Smoothed state vector at time k
$\mathbf{z}$ Vector of observation error $(\mathbf{z} = \ell - \mathbf{F}(\mathbf{x}))$
$\mathbf{\Omega}$ Rotation vector

Matrices

$\mathbf{C}_{\ell\ell}$ Covariance matrix of the observation ℓ
$\mathbf{C}_{\mathbf{xx}}$ Covariance matrix of the vector $\mathbf{x}$
$\mathbf{D}$ Differential matrix
$\mathbf{F}$ Matrix of elements of a linear equation $(\mathbf{y} = \mathbf{F} \cdot \mathbf{x})$
$\mathbf{F}$ Kinematic matrix (also called dynamic matrix)
$\mathbf{G}$ Input coupling matrix
$\mathbf{H}$ Design matrix
$\mathbf{I}$ Unit matrix
$\mathbf{K}$ Gain matrix
$\mathbf{P}$ Weight matrix
$\mathbf{Q}_{ww}$ Process noise covariance matrix
$\mathbf{Q}_{\mathbf{xx}}$ Cofactor matrix $(C_{xx} = \sigma_o^2 \cdot Q_{xx})$
$\mathbf{R}$ Attitude matrix
$\mathbf{\Phi}$ State transition matrix

Scalars

a	Acceleration
$\bar{a}$	Averaged acceleration
A	Amplitude
A, B, C	Individual parameter for distance computation
az	Azimuth of satellite
b	Bias (gyro)
c	speed of light
C	mean acceleration
D	Phase shift
$dist$	Travelled distance
$dt, \Delta t$	Time increment
E, N, U	East, North and Up coordinate (Navigation Frame)
el	Elevation of satellite
F	Frequency
g	Value of the Earth's gravity
ℓ	Observation
odo_{count}	Count of wheel turn made by an odometer
r	Radius of the wheel
u	White noise
$s, speed$	Speed
t	Time
$\Delta t, dt$	Time increment
v	Residual
v_e	Tension (voltage)
w	Process noise and system noise
x, y, z	Body frame axis
z	Observation error $(z = \ell - f(\mathbf{x}))$
α	Correlation time of a Gauss-Markov process
λ	Scale factor
ϕ	Azimuth
ρ	Correlation
σ_o	Mean error on unit weight
ω_x	Angular rate measured by the x-axis gyro
Ω	Angle rate for a single-axis rotation
ϕ, θ, ψ	Euler angle for attitude computation
VAR	Averaged quadratic acceleration amplitude
RMS	Square-root of VAR
ABS	Average of the absolute acceleration amplitude
AMP	Mean amplitude of the acceleration peak
$FREQ$	Step frequency (pace of the walk)

Contents

List of Figures

List of Tables

Chapter 1

Introduction

The word navigation, from a technical point of view, was until a hundred years ago used exclusively to define the way to guide a boat to the desired location. Even if it had a meaning for people on the ground, all the researches and investigations in the navigation domain were oriented towards maritime applications. Then, after the invention of the first aircraft, the word was also used for aeronautics, opening the door to the development of new systems.

During the last century, the nature of navigation sensors technology and in processor performance has kept the scope of the applications based on these to costly high-end ones. Developments and researches were dedicated to military applications before being partially introduced in civil applications. The last 30 years have seen significant advancement in both the sensors technology and the processor performances, with for example the progress in the domain of semiconductors leading to the advent of microprocessors. These advances, combined with a decrease in sensor and processor costs, has opened the door to new applications, especially in the terrestrial fields. The potential number of new users is huge and researches are today also performed to develop systems for non-military application.

Car navigation has been the first commercial target for low-cost navigation systems. Today, existing sensors also allow consideration of offering such navigation systems to an individual: to provide him with information on position and to aid with guidance. These considerations inspire the work performed in this thesis.

The scope of this study is to investigate a system and algorithms able to provide continuous positioning information of a walking person at all times and in all environments. The applications pointed to by this definition are identified under the generic term of *Pedestrian Navigation*.

To better understand this concept, the definition of the word navigation is given from a general point of view. Navigation is generally defined as the act of guiding an object or a person from its present location to a desired point. The object is generally a vehicle (boat, car, airplane ...)

From a functional point of view, navigation includes two separate tasks:

- localisation

- guidance

Localisation is the way to obtain the position of the object in a defined referential. This function can be performed by different means. In chapter 2, different modern techniques of localisation and positioning will be presented.

Guidance is the part of navigation that interacts with the drivers of a vehicle (boat, car, airplane...) or with a pedestrian. It includes different aspects:

- computation of the way to go from the present point to the desired one. Algorithms in this domain are now common and well known. They allow the user to choose between different options: shortest or fastest way, point of interest. This task entails of course the availability of geographic information such as road, building, point of interest, addresses, gas station...

- communication to the driver: if the driver is a human then different vectors of communication can be used. In the current navigation system, the followings are mainly utilised: voice, maps or symbolic representation. When the guidance of the object is made in an automated way (processor and motors) then the guidance information is given immediately to the motors.

The guidance task is not investigated more deeply in this thesis. The focus is on the way (sensor and algorithm) to localise the person.

In complement to localisation and guidance, other notions can be added to complete the definition of navigation:

- Real time. The real time aspects are derived immediately from the guidance. To interact with the driver, it is obvious that information on position must be computed in real-time to allow an efficient guidance.

- GIS is also an important element strongly linked to the guidance. This component is not used only to represent information on a map. The georeferenced information of roads and of targets is needed for guidance. GIS offers the possibility to include many other types of information such as point of interest. GIS is also often used as a sensor. This aspect will be developed in more details in the next chapter.

The principles of navigation can be applied to different types of vehicles or moving objects. The application of the modern navigation technique to a person is more recent, even if personal's navigation is existing already with magnetic compass and maps. However, the utilisation of these instruments is not simple for everyone and electronic navigation has a lot of interest for a large number of persons with different profiles.

To perform the mentioned function of navigation several types of instruments can be used. The approach chosen in this study focused on pedestrian navigation is an hybridisation of the following sensors:

- GNSS receiver

- accelerometers

- gyroscope

Of course other possibilities have been investigated and are reported in the Chapter 2.

The structure of this document reflects the logic of the study. In the next chapter different aspects of the pedestrian navigation are explained. The requirements for the studied system are developed and the system is designed. The reasons for the choice are also explained. In the three following chapters (Chapter 3, Chapter 4 and Chapter 5), the system and algorithms are described in detail. Chapter 3 shows the way to determine the distance travelled by the person. Chapter 4 defines the techniques to determine the orientation of his walk. Chapter 5 aims at describing the sensors fusion to obtain an operational system. The algorithm and the chosen system architecture are validated by trials and tests as illustrated in the last part of chapter 5. Concluding remarks and a discussion on the possible perspectives take place in the Chapter 6.

Chapter 2

Pedestrian navigation: concept and state of the art

The objective of this chapter is to present the concept of *Pedestrian Navigation*. Each person, depending on his background and his knowledge, will present such a concept in a different way. The methodology adopted here considers not only the apparatus and the algorithm (which will be the main topic of the next chapters) but considers also the *pedestrian navigation* under the following four approaches:

- the spectrum of applications,

- the relevant sensors and technologies,

- the different applicable concepts for the system architecture and finally

- the different types of environmental conditions in which the pedestrian moves about.

These four elements are considered in the first part of this chapter. It aims to provide a synthetic overview with a scope as large as possible. The information comes from different sources such as the internet, proceedings of symposium and conferences, industrial advertisement and several research and development projects. The list made below for each element is obviously a non-exhaustive one and is subject to evolution. The navigation environment is today fertile and, to some extent, an unpredictable terrain for new applications and tools.

The second part of this chapter focuses on two different techniques that are classically used within the navigation community: the Inertial Navigation

System (INS) and the Dead Reckoning system (DR). These two techniques use some of the tools presented in the first part.

The third part of the chapter presents the requirements and the system design. First the user requirements are determined and the system design (choice and placement of sensors, architecture...) is performed consequently, with the aim of fulfilling the requirements.

The last part of the chapter compares the chosen system design and architecture with other products available on the market or under development in different research laboratories all over the world.

2.1 Concepts for pedestrian navigation

In this section the concept of pedestrian navigation is approached through four different elements explained above.

2.1.1 Applications

As the capabilities of positioning a person has recently increased, the number of applications or services is permanently growing [Legat00]. This section presents a few of them. They are sorted starting from some applications aimed to reach a large public (with mass-market perspectives), to others that focus on specific applications, with associated smaller market potential.

Emergency call

The E-911 initiative in the United States and the European equivalent E-112 aim at locating every emergency call, even those provided from mobile phones. In the US, E-911 has already been upgraded several times and requirements have been established depending on the used technologies: network based (E-OTD, TDOA) or handset based (GNSS, A-GPS). In Europe the studies LOCUS [Locus01] and C-GALIES [Cgali02] have provided guidelines to the European Commission for the settlement of a new E-112 directive.

The introduction of such a requirement to locate all emergency calls will offer positioning capabilities in every mobile phone. It will help to open the market to other positioning services using mobile phones: the Location Based Services (LBS).

LBS: Location based services

LBS (Location Based Services) is a common terminology that encompasses numerous activities of different types. The driving concept is that better or new services can be proposed to a consumer if the service provider knows his position. Of course a communication link between the client (the pedestrian) and the provider must exist. The palette of services goes from medical services - to provide efficient emergency interventions - to purely commercial ones: to inform the client about the promotion in the shop in front of him or to guide him to the next pizzeria. This last example became the paradigm of the LBS. For further information about this type of applications the reader can refer to [Lechn01].

GIS, data collection

Geographic information system is now a common tool for numerous applications. However the cost of data acquisition remains often one of the main obstacles to increased availability and utilisation of such a tool. Pedestrian navigation system can offer a new possibility to acquire, in different environments, geo-determined information at a lower cost. For example a botanist will record the location of all the observed plants at the same time he is performing his usual work and will integrate the information directly in his database. The same logic can be applied to different scientific fields, such as geology, but also to other professional domains such as maintenance and construction of roads, electricity grids and water networks.

Integration in the field and in real-time of both tools (GIS and navigation) can open interesting perspectives. For example, a GIS containing the plan of underground pipes, combined with a pedestrian navigation system and virtual reality, can offer employees a virtual view (through special glasses) of the underground pipe directly on the terrain [Rober01]. This can facilitate and improve considerably the efficiency of their work.

Tourism

Tourism is another application for pedestrian navigation. Several projects have developed automated tour guide [Feine97, Yang99] to offer services to the tourist whilst travelling in a city or in a natural park. The purpose is always to provide him with the necessary or required information when he is passing near an interesting picture, sculpture, building or area. The system could also combine different applications to offer a more complete service.

For example, the same system can serve as a guide for mountain hiking and help the tourist in case of emergency [Loehn01].

Rescue

Emergency and security services (police, fire brigade) need location information to improve the efficiency of their operation and facilitate the management of the policemen, firemen and medical staff involved. Their cars are now usually equipped with navigation systems. However, during an operation they may need to leave their vehicle and to pursue their activities on foot. Then, to obtain continuity in the management of the operation and to improve the security of the persons, pedestrian navigation capabilities are needed.

Military

In the military sector, the knowledge of the location of each vehicle and soldier is strategic and of paramount importance. This capability is already achieved for vehicle and is foreseen to be a reality for soldiers soon. The pedestrian navigation finds here a direct application. Some research programs, such as the Exoskeletons in DARPA [Garci00], show clearly the advantages that pedestrian navigation could bring in this specific domain, which has not been further investigated in the scope of this thesis.

Medical studies

Applications for pedestrian navigation exist also in the medical domain. For example, the system can be used in the medical domain, or, more specifically, in physiology and biomechanics [Hoffm01, Schut97]. The main principle is to monitor during a certain period of time (generally at least one day) the activity of a person measured in terms of travelled distance associated with the walking speed and the incline of the travelled path. These parameters are then utilised to compute the energy expenditure or other physiological parameters important for fundamental research in this domain.

Navigation for the blind

Different projects and technologies have been already developed to help blind people to navigate in unknown environment [Petri96, Ram98, Dodso99,

Helal01, Garaj01]. Navigation tools can be used to offer different services to visually impaired persons: from obstacle avoidance to basic information about their position and orientation. In this domain, the acceptance by the blind community of any new device requires that it does not interfere with the sense of hearing or touching. Indeed these senses are primordial for their every day life.

Leisure

Leisure activities represent also an interesting and varied domain of applications for pedestrian navigation systems. In this domain, the cost of the system becomes a key-issue to ensure a good market penetration. One example of a leisure application is to add localisation information to the movies or pictures taken during a trip [Campb99]. New games based on the possibilities of knowing all the time the position of different people can be developed: treasure hunt, find a friend, etc.

This last example concludes this non-exhaustive list of applications for pedestrian navigation systems. Each application has different requirements in terms of accuracy, availability, integrity or continuity. Different technologies exist and can be applied. Each one has its own advantages and drawbacks. The next section aims to present different techniques able to fulfil, even partially, the requirements of these applications.

2.1.2 Tools

Electronics tools for surveying and navigation are not new. Different sensors, based on different techniques, using different algorithms have been developed in the past 50 years. The reason for choosing one or another technique for pedestrian navigation will be guided by considerations given at the end of this chapter. The present section lists different systems or sensors.

GNSS

Global Navigation Satellite System is today a well-known system. The reference system is the Global Positioning System (GPS) [Parki95]. It is composed of a nominal constellation of 24 satellites. This system offers to the

civilian a positioning service with an accuracy of around 10 meters since the turn-off of the selective availability (SA) in May 2002. Augmentation systems, Ground-Based Augmentation System (GBAS as some differential GPS networks-DGPS) or Satellite Based Augmentation System (SBAS as the WAAS or EGNOS), offer also an integrity service and improve the accuracy of the civil service.

Russian engineers have developed, in parallel, a similar GNSS: GLONASS. This system has currently a poor coverage. In 2002, only 9 satellites are in orbit for a nominal number of 24.

The European Space Agency and the European Union are now developing a system named Galileo which aims to offer in 2008 a variety of services for the civil community [Bened02].

The basic principle of this technique is to measure the propagation time of the signal from the transmitter (the satellite) to the user's receiver. Signals of four satellites are needed to determine the four unknown parameters: East and North coordinate, altitude and the error of the receiver clock (synchronisation).

The evolution of GNSS is constant. This trend is visible at different levels. Firstly, at system level, available satellites have more precise clocks on-board. GPS modernisation and the GALILEO program both plan strong improvements of the system which will offer better accuracy.

At receiver level, the improvements are made for different purposes:

- Miniaturisation. This process facilitates the integration of small receivers in other devices such as mobile phones, watches or Personal Digital Assistants(PDA).

- Power consumption. This aspect is linked to the previous one. The autonomy of a mobile phone or PDA is a key-element in term of marketing. If the autonomy is not sufficient, the product does not succeed. Hence the introduction of a GNSS receiver into such a device must not decrease too much its power autonomy.

- Accuracy. The research and development activities in the domain of the algorithms contribute to the improvement of accuracy. The improvement is not significant for absolute positioning using code measurement. However, for phase measurement in differential mode (also named Real-Time Kinematic - RTK), the development of ambiguity resolution techniques [Mermi88, Sauer94] today allows having an accuracy at centimetre level within only a few seconds [Han97, Tiber97].

- Sensitivity. The sensitivity of a receiver is defined as its capability to acquire and track weak signals. Evolution during the last years has shown that GNSS positioning is possible inside a building or in a forest [Haddr01]. The GNSS signal power on the earth surface is -160dBW. The building attenuation is generally about 20 dB.

- Software receiver. This type of receiver replaces hardware components by software for specific functions (mainly acquisition and tracking). This will increase the flexibility of the receiver to combine different signals. However, to obtain full software receiver implemented today in handset, evolution of the microprocessor is needed to obtain receiver with limited power consumption.

No further explanation is given about GNSS technology in this thesis. Interested readers can refer to one of the numerous existing books on the subject [Parki95, Stran97].

GSM or UMTS

GSM, or next generation UMTS, are conceived for communication purposes. However, it is also possible to compute position using different characteristics of these systems. Already in the early 90's Wickman [Wickm90] proposes a method for localisation with GSM. The different applicable techniques are now presented. This information is provided by various authors [Drane98, Hein01, Vidal01].

- Cell-id. The mobile location is simply determined by the position of the master station (MS for GSM) or base station (BS for UMTS). The accuracy of these technique is directly linked with the density of the MS/BS network. This means that the accuracy is good in urban area and weaker in rural or mountain area.

- Signal strength. The strength of the received signal is inversely proportional to the distance between the MS/BS and the mobile. The intersection of several distances (three to have a unambiguous 2D position) allows the mobile position to be determined. The accuracy of this technique depends greatly on the environment. The relationship between the strength of the signal and distance is only valid in ideal environments without obstacles, which is rarely the case.

- Angle of arrival. The position is determined by the intersection of straight lines which originate at the MS/BS and which are orientated according to the antennas at Base Station. No precise synchronisation of the different BS is necessary. Angle of arrival technique is often combined with signal strength. The first one gives the orientation, the second one the distance.

- Timing measurement. The previous techniques are based on geometrical aspects that do not require any time measurement or synchronisation between MS/BS and mobiles. However the obtained accuracy is often weaker than 100 meters. The time measurement techniques need synchronisation between elements of the network.

  - TOA : Time of Arrival. This technique is based on the measurement of the propagation time of the signal between the MS/BS and the mobile. The geometrical solution is given by an intersection of circles. A precise synchronisation of the BS/MS with the mobile is mandatory (as for the GNSS satellites).

  - TDOA (for GSM) and E-OTD (for UMTS): Time difference of arrival. The basic measurement is the difference of the time of arrival of a same signal emitted by different BS/MS. From a geometrical point of view, the solution is given by the intersection of hyperboles. The precise synchronisation of BS/MS is needed.

Tab.2.1 presents the error budget of GSM and UMTS, this table is proposed by [Heinr01].

error source	GSM	UMTS
resolution	270 m	18 m
multipath	0-250 m	0-17 m
troposphere	0.3-3m	0.3-3 m
network/hanset synch.	3-6 m	3-6 m
oscillation error	7.5 m	7.5 m
total error (1σ)	270-380 m	19-26 m

Table 2.1: Error budget for GSM and UMTS techniques

MEMS

The Micro-Electro-Mechanical Sensors Systems are subject of intensive research conducted by different laboratories all around the world. The sensors (accelerometers and gyroscopes) for navigation are part of this trend. Barbour, in [Barbo01a], Kourepenis, in [Koure98], and Yazdi, in [Yazdi98], give a clear view of the past, present and future evolution of the MEMS.

Concerning the accelerometers, the miniaturisation process has already produced effects. The sensors have reached a small size whilst maintaining sufficient performances to be integrated in small navigation devices. Accelerometers are also extensively used in other domains.

For the gyroscopes the challenge is more difficult. Indeed, for almost all types of architecture and principles, a physical relation exists between the size and the performance which is generally characterised through the stability of the bias and scale factor [Yazdi98]. The limits of the actual sensors have been described in [Ansel98]. However, new manufacturing techniques are currently being investigated [Ayazi01, Geige98]. They offer interesting perspectives. The possibilities of utilisation of MEMS for pedestrian navigation will be described in detail in the next chapter.

Magnetic compass

The properties of the Earth's magnetic field have been used for centuries by the navigators. This field can be measured by flux gate or magneto-resistance sensors [Denne79]. Most performing devices available today includes tilt sensors to provide sub-degree accuracy [Gnepf99, Carus00]. To maintain this accuracy, the anomaly of the Earth's magnetic field has to be taken into account. The main drawback of magnetic sensors is their sensitivity to magnetic sources others than the Earth's magnetic field. These sources are frequent in urban environments as they are mainly produced by electricity lines (for public transport) or the metallic structure of buildings. They are strongly dependent on the time and location. It is therefore not possible to adjust them for in a model.

Barometer

Barometers can also be considered as navigation sensors even if, basically, they offer only the vertical solution of the problem. Coupled with 3D digital terrain models, knowledge of the altitude can offer, for terrestrial application,

useful information about localisation. The altitude defines a line on the map and then limits the number of possible solutions. The accuracy of a barometer depends on the stability of the atmospheric pressure in one location. Thus, meteorological changes produce errors in the altitude determination if they are not taken into account and compensated.

Differential barometers can offer altitude with one meter accuracy. For pedestrian navigation, the use of a barometer can improve the accuracy of pedestrian navigation systems by measuring the walking slope. This can be critical for slopes exceeding a percentage of 7-8% [Perri00].

Visual recognition

Visual recognition is a technique that can be used for different applications. Numerical photogrammetry is one classical example. This technique consists in comparing a picture taken by a camera with elements in a database. These elements can also be pictures but are more generally 3D models of reality composed of structural lines like the edge of a building or the border of a road. When the structural lines, extracted from the picture, match the elements of the database, which are geo-referenced, the system knows where the person is and also what is their angle of view. Different systems have been developed based on camera only [Aoki99] or combining different sensors with the camera [Chen99].

GIS, map matching

Maps and road databases are extensively used in car navigation systems. Map matching is a technique based on comparison between the computed trajectory (position) of the vehicle and the elements contained in the map (or more generally in the GIS). For example, when a car turns 90 degrees, it means that it has reached an intersection. The system can then allocate the location of the intersection (furnished by the map) to the vehicle as well as the orientation of the street to the orientation of the vehicle. This technique is able to replace GNSS in poor coverage area such as tunnels, cities or forests.

A geographic information system can also be considered as a tool for pedestrian navigation. The identification and organisation in a database of walking data such as pavements, pedestrian crossings, corridors inside a building or paths in rural or mountains areas, can improve the pedestrian navigation system by providing a position (map matching) or an orientation (map aiding). The coupling of pedestrian systems with GIS has been the subject of experimentation by Golledge [Golle91, Golle98].

Indoor navigation

Indoor Navigation can be considered in the frame of this thesis as a subdomain of pedestrian navigation. Indoor navigation is sometimes named *In-Building* navigation. It concerns all navigation techniques and algorithms necessary to navigate (i.e. locate and guide) a person or an object when indoors (in building, in tunnels, under ground...). Language extension tends to classify almost all non-GNSS techniques as Indoor techniques. The following sections lists different localisation techniques that are applicable indoors. They are mainly taken from [Heinr01] and [Viita99].

- Pseudolite. A pseudolite is a ground based transmitter that simulates the signal of a GNSS satellite and that can be used by a GNSS receiver for ranging [Kee01]. A receiver-transparent use of pseudolites in confined environments has still some problems due to multipath and near-far problems, where the signal of the nearest pseudolite covers the signal of the other ones (jamming).

- Ultra-sound sensors. These sensors are able to provide information such as distance to the next wall. They are also used for obstacle avoidance applications.

- Local RF. RF location based systems consist of transmitters that send messages continuously using microwave frequency ($\sim$2.5 GHz). A transmitter is attached to the asset to be tracked. When the asset comes in the field of a transponder (reader), the message is sent to a central computer, which deduces the position of the asset. Different variants of this technique exist [Want92], depending on the network architecture. For example, the readers can be attached to the moving asset and the transmitters fixed to the building. The accuracy obtain is between 1.5 to 15 m. Today, RF transmitters are generally integrated into identification badges used in numerous offices [Harte94, Ward97].

- Infrared or fluorescent light detector. Generally, infrared transmitters and receivers are used when RF technology is not applicable because of the interference with instruments using a narrow frequency, e.g. hospitals or electronic factories.

- Ultra Wide Band (UWB). This technique has the potential to obtain precision under 30 cm [Opsha01, Fonta01]. However, problems of interference with other systems are important and the power must stay limited.

Other techniques for pedestrian or indoor navigation

Loran-C is an existing structure put in place for maritime and aviation navigation. The principle is based on the difference in the time of arrival of radio frequency pulses broadcast by three or more transmitting stations. Integration of Loran-C with GNNS has been, and is still, under evaluation [Brown88, Glori01]. The accuracy of this system is about 460m and the repeatability is 50m. Loran-C receivers are today too large and heavy for pedestrian navigation. They are mainly developed for maritime and avionics applications. However, some manufacturers have started to develop low size Loran-C receivers [Nels01].

Other systems are, or were, used for navigation [Lauri76]. They are briefly presented in the following paragraph.

- Omega. This technique uses hyperbolic position fixing by phase comparison techniques on Very Low Frequency (VLF) continuous wave electromagnetic signals.

- Decca. This hyperbolic method also consists in transmitting signal at VLF (similar to Omega).

- Transit. This is the direct ancestor of the American GPS. It is based on Doppler measurements. This technique is still used for search and rescue services (such as COSPAR-SARSAT).

- VOR-DME (VHF Omnidirectional Range and Distance Measurement Equipment). These instruments are mainly used for aviation. They provide a constant orientation (VOR) or a distance to a beacon (DME).

2.1.3 System architecture

The system architecture for pedestrian navigation is determined by the following questions:

- Where is the position computed?

- Where are the measurement tools placed?

- Where is the information displayed?

There are two possible responses to the first question. The position can be computed directly by the person or by a processing facility owned by a service provider or by an institutional entity. For example, GSM positioning techniques offer a possibility to compute position in the device or in the master control centre. Several legal issues state behind this conceptual aspect. There is no intention in this report to cover the legal aspect of the pedestrian navigation, as it would be a self-contained thesis subject and it depends upon the applicable legislation, which changes from country to country. However, it can broadly be stated that the knowledge of the position of a person is protected by a fundamental right: the *private life protection*. Generally, this right can be reduced in certain cases when conditions are fulfilled (convicts...) or by the willingness of the person. A system architecture where the position is computed in an external processing facility must have the person's acknowledgement to 'track' him without its willingness. On the contrary, the computation by the person directly allows to have an architecture where the person controls his position information before sending it to other people.

The second question depends more on the selection of the tools used to locate the person. For the system architecture, the important aspect is the distinction between sensors that are placed on the person and sensors that are part of an external infrastructure. There is also a category of tools that need both: tools placed on the person and external infrastructure (such as GNSS that requires receiver and satellites). The sensors placed on the person offer the advantage to be independent of the environment. Each time an external sensor is used, external infrastructure is required, which can become very expensive for a 'everywhere' positioning requirement. Satellite infrastructure offers certainly the most Global coverage. Anyway this choice is of course driven by the application and the user requirement.

The third question depends on the second one. It depends also on the availability of a communication tool associated with the navigation system. The display of the information can be made at the person itself or to a specific person or institution (police or ambulance in case of emergency).

Beyond the first and third question, there is the question of communication link. If the position must be displayed in another place than where it has been computed, there is a need for a communication link that must also fulfil the user requirement (continuity, availability). This specific aspect of the system (the combination of communication and navigation) has not been evaluated in the present thesis.

2.1.4 Environment

The possible environments are selected and sorted considering the direct possible impact on the localisation techniques and system architecture. The first distinction is between indoor and outdoor navigation.

The terminology indoor considers the situations in which the pedestrian is walking in a building, in a subway or into a tunnel; i.e. without a direct view of the sky. This first distinction is in fact guided by the GNSS localisation technology, which is available only when the user has a direct line of sight with the positioning satellites. But, regarding GNSS techniques, this first distinction is not complete. As explained in the previous section, GNSS positioning can also be problematic in outdoor environment because of obstruction caused by trees, topography or buildings.

This consideration is at the source of the second distinction. It is based on the potential availability of the GNSS signal. A classical categorisation starts from the more favourable environment to the most constraining one.

- Rural environment. It is a clear sky environment without important obstruction. The reception of the GNSS signal can be considered as ideal.

- Mountain environment. The topography generates some obstructions that can shadow a part of the sky. The pedestrian has to walk (or climb) a long distance to change the obstruction.

- Urban environment. Obstructions are generated by buildings. They can vary with the height and the density of buildings. The obstructions are changing fast when the pedestrian moves in a city and reaches intersection or changes street and orientation.

- Forest environment. The trees are attenuating the penetration of GNSS signals. Today receivers have a better tracking capability in this environment. However, the acquisition of the signal of the satellites is still difficult.

For most of the applications, the pedestrian will change environment. The system must function in different environments. For some special application, only one environment can be considered. For example, indoor environment for the automated guide in a museum.

This paragraph closes the presentation of the four approaches of the pedestrian navigation. Any related system can be described by following one of the four approaches or by combining several of them.

2.2 Classical navigation techniques

In this section the two main navigation techniques are presented:

- INS: Inertial Navigation System

- DR: Dead Reckoning

The algorithms, the errors sources and the error propagation are explained. The application of these techniques for pedestrian navigation is also discussed.

2.2.1 Inertial Navigation System

As mentioned in the introductory chapter, integrated INS/GPS is the main instrument in the classical navigation domain to compute the position and/or the trajectory of a plane, boat, u-boat or terrestrial vehicle. The utilisation of this technique for pedestrian navigation has to be considered because it works with satisfaction in a lot of different vehicles and is, a priori, suitable to compute a person's position. Inertial systems are often categorized in two groups [Lawre98]: gimbals and strapdown INS. The gimballed systems are heavy and large. Hence, they will not be considered for pedestrian navigation. Advances in sensors development [Barbo01b] in terms of size, precision and cost, as well as advances in computation capabilities of processor let think that a strapdown MIMU can be applied for pedestrian navigation.

The classical process of strapdown INS is now briefly presented. An INS is composed of three gyroscopes and three accelerometers. All the sensors are mounted orthogonally. They are sensing respectively the angular rate and the acceleration in one of the three directions (see Fig.2.1).

The strapdown INS mechanisation consists first in computing the attitude of the system. The definition of the attitude is the orientation in space of the INS axes (body frame x,y,z) with respect to the reference frame (see Fig.2.2) which can be:
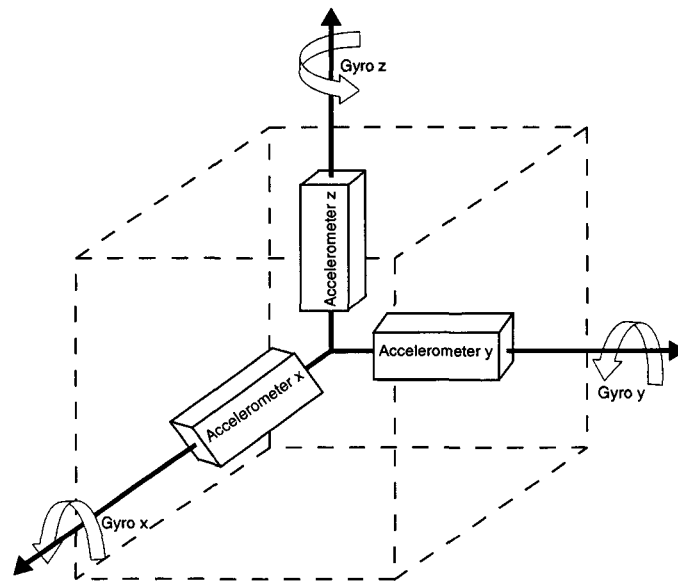
Figure 2.1: A classical strapdown INS containing three gyroscopes and three accelerometers

- the Inertial frame; this frame is not rotating with respect to the fixed stars. Gyroscope and accelerometers are measuring physical rotation or acceleration in this frame. For example, a gyroscope placed on the Earth will sense its rotation. However this frame is not practical for localisation and, consequently, navigation.

- the Earth frame; the axes of this frame are fixed with respect to the Earth. The origin is the centre of the Earth. The first axis is the polar axis; the second goes through the intersection of the equator plane and the Greenwich meridian. This frame is usually parameterised with the geographic coordinates: latitude, longitude and height. It is used for global systems such as GPS.

- the Navigation frame (ENU or NED); it is a local geographic frame. The origin is at a chosen point and the axes are defined along the North, the East and the local vertical. This frame is very practical for navigation. However, the use of this frame for large areas will introduce errors. Then, the origin must be shifted regularly in function of the travelled distance. It allows also keeping a coherent physical interpretation of the parameter that are usually East, North, and Up. (see Fig.2.2)
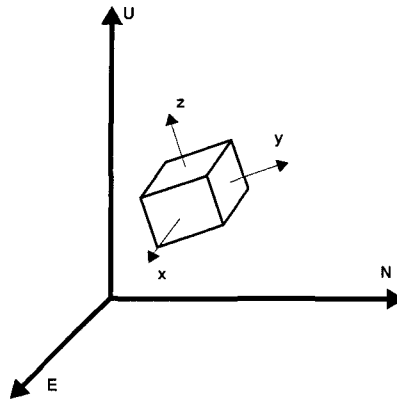
Figure 2.2: Body frame (x,y,z) and navigation frame (E,N,U)

The attitude is numerically represented by a 3x3 attitude matrix **R** that is an orthogonal endomorphism [Gabag97a, Shust93, Markl78]. Different parameterisations of the attitude are possible. But all possible sets of parameters can be extracted from the **R** matrix. The attitude is generally measured by gyroscopes. However, an array of at least three GPS antennae, can also provide these parameters [Cohen95, Gabag97b]. The next list presents the most used parameters.

- Quaternions have advantages from a numerical and computational point of view [Shust93].

- Euler angles (ϕ, θ, ψ) are the most significant parameters. They represent three successive rotations about the axes.

- Direction cosines represent the unit axis vector of the body frame projected along the navigation axes.

- One axis and one rotation (x, y, z, Ω) where the attitude is considered as a single rotation about an axis defined by the x,y,z vector.

The measurements of the gyroscopes $(\omega_x, \omega_y, \omega_z)$ are combined with the previous attitude to provide the changes in the parameters of the attitude.

For example, in the case of a Euler's parameterisation[1]:

---

[1]the equation and the Euler parameterisation depend on the sequence of the chosen axis about which the rotation are successively performed.

$$\begin{aligned}
\dot{\phi} &= (\omega_y \sin\phi + \omega_z \cos\phi)\tan\theta + \omega_x \\
\dot{\theta} &= \omega_y \cos\phi - \omega_z \sin\phi \\
\dot{\psi} &= (\omega_y \sin\phi + \omega_z \cos\phi)\sec(\theta)
\end{aligned} \tag{2.1}$$

The determination of the first attitude is called initial alignment. When using precise gyro, it is possible to use the gyro to point the North (the technique is called gyrocompassing). Sensing the earth gravity with the accelerometers can align the pitch and roll angle. However, this procedure requires sensitive instruments and is not possible with low cost sensors. Hence, the initial alignment must be provided by an external source. Once the attitude is known the mechanisation shown in Fig.2.3 is performed. The measured acceleration (a_x, a_y, a_z) is projected from the body frame (x,y,z) into the local frame (E, N, U) using the attitude matrix $\mathbf{R}$ [Wei90]. Then they are integrated numerically twice to obtain the change in velocity and the displacement. Finally both are added to the previous position to obtain the present ones. The initial position should be provided by an external mean.
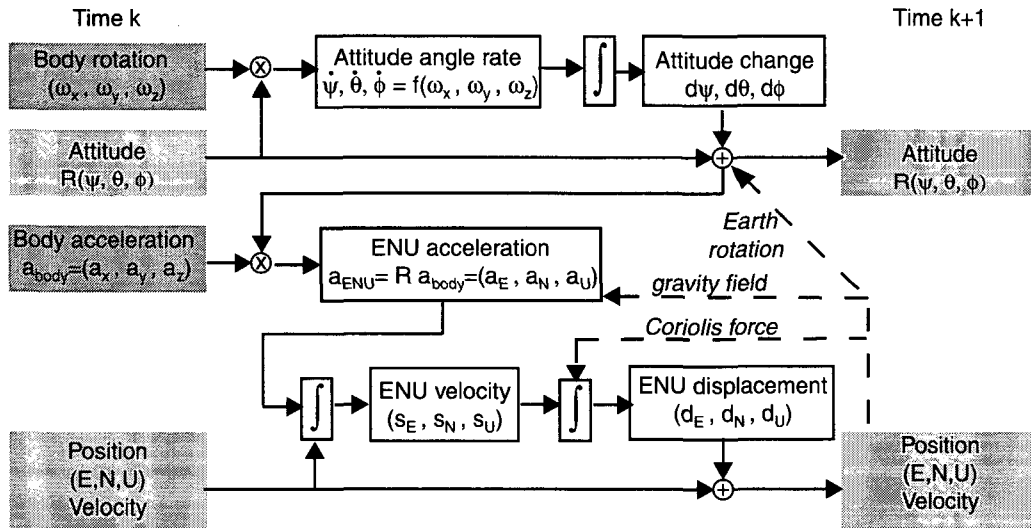
Figure 2.3: The INS mechanisation

In complement to the Fig.2.3, it must be mentioned that other physical effects have to be taken in account (illustrated with the slashed line on Fig.2.3).

- the Corriolis force: this force is generated by the conjunction of the earth rotation and the velocity of the vehicle.

- the gravity field: this field is not constant on the surface of the earth and influences the measurement of the accelerometers.

- earth rotation: it is considered as constant (for the proposed application) but is measured by the gyroscopes. The implementation of this phenomenon in the algorithm is strictly and meticulously explained in Britting [Britt71].

2.2.2   INS errors in pedestrian navigation

During the INS mechanisation process, errors find their sources mainly in the lack of determination of the parameters of the sensors. By definition, and explained in a schematic way, each sensor transforms a physical input to an electrical signal (Fig.2.4). The voltage v_e of the signal is measured and transformed into a numerical value corresponding to a known unit, say $^o/s$ for gyroscope or m/s^2 for an accelerometer. The mathematical formulation of the transformation is:

$$unit = \lambda_1 \cdot v_e + b_1 \text{ or } unit = \lambda_2 \cdot (v_e + b_2) \tag{2.2}$$

where

λ_1 or λ_2 is the scale factor
b_1 or b_2 is the bias

Figure 2.4: Sensor: from physical input to numerical output

Any error on λ, b or v_e conducts to an error in $\omega_{x,y,z}$ or $a_{x,y,z}$ and then to an error in the position. As the INS mechanisation works as a closed loop process, errors accumulate themselves quickly and create a drift (see Fig.2.5). Different procedures allow to determine and partially eliminate errors on b and/or λ. Two of them are now presented.

- ZUP : Zero velocity UPdate. The principle is to stop the vehicle to have a known output. Accelerometers and gyroscopes have to output zeros (after eliminating the earth rotation and the gravity). The difference between what the sensor should output and what they actually output is the bias.

- Integration of GPS. INS/GPS integration is as old as GPS. Early, the advantages of the integration between both systems have been investigated [Schwa83]. From a schematic point of view, the position given by the GPS is compared with the INS position. The difference is due to:

  - GPS residuals, due to errors in the orbits and in the clocks of the satellites, to multipath, to atmospheric effects and to receiver internal errors.

  - INS residuals, due to errors of bias, scale factor, initial alignment and initial position.
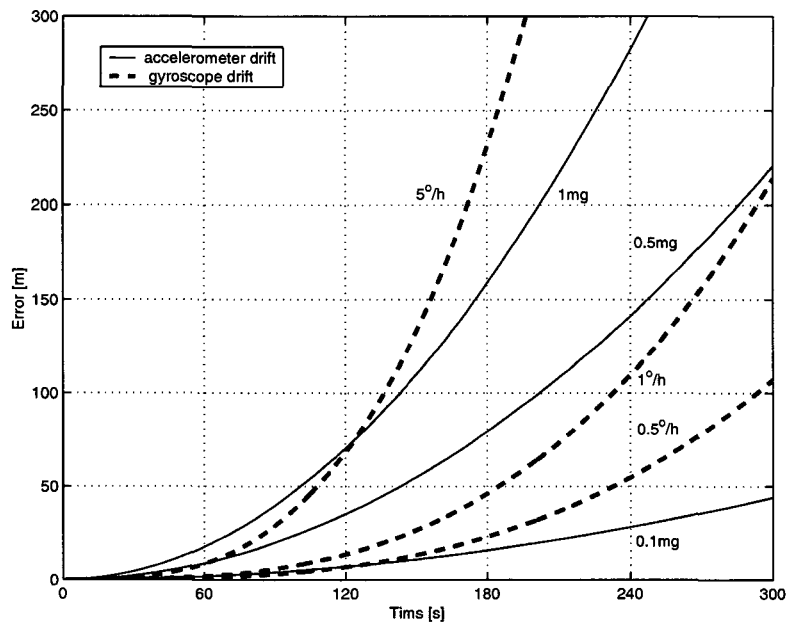
Figure 2.5: Position error induced by the sensors errors

The distribution of the difference in position among the parameters is generally done by using a Kalman Filter [Skalo99, Grewa00]. The correction of the parameters $d\mathbf{x}$ is computed as:

$$d\mathbf{x} = \mathbf{K} \cdot \tilde{\mathbf{v}} \qquad (2.3)$$

23

where **K** is the gain matrix (see Appendix A) and $\tilde{v}$ is the difference between the GPS measurement (pseudolite, phase, phase rate or position) and a function of the considered parameters (position, velocity, attitude, bias, scale factors, misalignment, non-orthogonality, ...). Some models include more than fifty parameters.

To use these techniques in pedestrian navigation is not suitable for different reasons exposed in the following.

- All the sensors (3 gyroscopes and 3 accelerometers) must be carried by the person. It means that the size must be small enough to be wearable. As mentioned in the previous chapter, the consequence is that the random processes that drive the errors on the parameters of the sensors (bias, scale factor) are more noisy and their stability becomes worse. The error propagation in the INS mechanisation involves a quick loss of precision when no GPS signals are available. As illustrated in Fig.2.5 the error induced by a non-corrected drift of the accelerometer or of the gyroscope can rise quickly.

  Tests with precise INS (less than 0.01 $^o/h$ for the gyro and 50 μg for the accelerometer) carried in a backpack have been conducted and give interesting results [Soehr00, Gille00]. The second author obtains in real time an accuracy better than 1 meter per travelled kilometre without GPS but with ZUP performed every 2 minutes. During the ZUP procedure, it is asked to the walker to put the backpack down to avoid any movement. This solution matches only for special projects and not for a generalised use. Indeed the weight (5-10 kg) and the size (a full backpack) are not small enough to be carried all the day even by a healthy person. Integration of GPS with MEMS is now further investigated [Wolf97, Marse98b, Mao00, Ander01] and yield interesting results.

- The full computation of the INS mechanisation requires non negligible resources from the processor. The sampling rate of classical INS is generally greater than 50Hz. Because of power consumption, more power-sparing algorithms must be proposed.

- Initial self-alignment is not possible with the low cost sensors. The procedure of alignment is only possible when the person does not carry the sensors.

- INS/GPS integration asks that the GPS and the INS are mounted on a stiff platform which the human body is not. However, small variation in the distance between INS and GPS are acceptable considering the required precision.
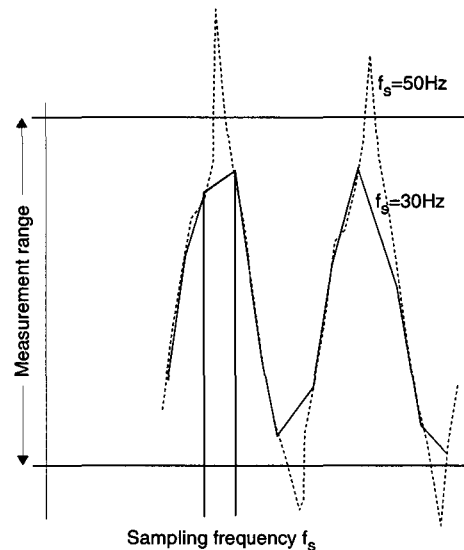
Figure 2.6: Measurement band and sampling frequency limitation

- The movement of a person is not as smooth as the movement of a vehicle, boat or aircraft. The jerk is high. A shock occurs at each step and provokes errors (as sudden changes of bias) in the low cost sensors. These shocks create another two requirements. The sampling frequency must be high enough to detect the peak and the measurement band of the sensor must be large enough to measure it. Increasing the measurement band will diminish the resolution and the precision. Increasing the sampling rate increases the computation process and then the energy consumption. (See Fig.2.6)

Those considerations combined with the requirements of precision, ergonomics and cost exposed in the section 2.3.1. force to find another approach for pedestrian navigation than the classical INS mechanisation with GPS integration.

At this point, it must be mentioned that research at the Charles Stark Draper Laboratory in Cambridge, Massachusetts, specialised in MEMS, uses

the classical INS mechanisation for pedestrian navigation using low size sensors. They use the fact that during the gait cycle there is a moment when no force is involved and then the acceleration must be nil. They develop a concept of personal inertial navigation systems aided by zero velocity update of the accelerometers at each footfall. They show that the technique is sufficient to determine the location of a pedestrian within a large building complex after hours of operation. In addition to the accelerometer, updates of the gyro via zero attitude rate techniques enhance position accuracy, and provide an attitude reference [Elwel99]

2.2.3 Dead Reckoning

Car navigation is a demonstrative example to illustrate the dead-reckoning techniques for terrestrial navigation [Harri90, Frenc96, Zhao97]. Even if car navigation can also be performed with an inertial system [Abous93, Marse98a]. First of all the 3D positioning is split in a 2D - horizontal - and a 1D -vertical- computation of position. These 2 aspects are computed separately. For the 2D, two elements must be measured: the distance and the orientation. In car navigation, an odometer (or wheel sensor) furnishes the first element and a gyroscope the second. It is sometimes replaced with (or completed by) a magnetic compass. In addition some make use of a differential odometer for the computation of the orientation. The DR algorithm is:

$$N_k = N_{k-1} + distance \cdot \cos(\phi_k) \qquad (2.4)$$

$$E_k = E_{k-1} + distance \cdot \sin(\phi_k) \qquad (2.5)$$

$$\phi_k = \phi_{k-1} + (\lambda \cdot \omega + b) * dt \qquad (2.6)$$

$$distance = odo_{count} \cdot 2\pi \cdot r \cdot \cos(slope) \qquad (2.7)$$

where

E_k, N_k	are the East and North position at time k
ϕ_k	is the azimuth at time k
odo_{count}	is the number of turns of wheel counted by the odometer between time $k-1$ and time k
ω	is the angular rate measured by the gyroscope
dt	is the time difference between time k and $k-1$
λ, b	are the scale factor and the bias of the gyroscope
r	is the radius of the wheel
$slope$	is the slope of the road (interaction between vertical positioning and horizontal one).

The height can be measured in different ways: barometer or inclinometer. If the height, and then the slope, is not measured, then the cos(*slope*) is considered as a scale factor on the distance in the same manner as the radius of the wheel.
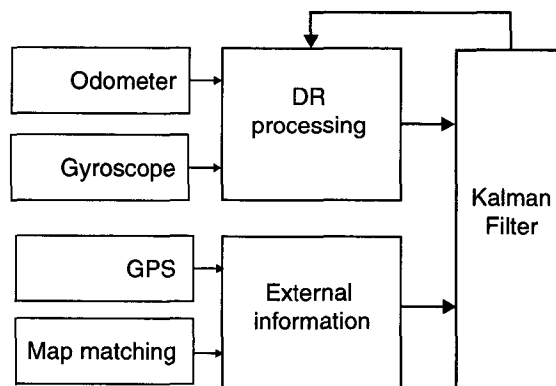
Figure 2.7: Methodology adopted in most car navigation systems

The errors due to the odometer count or provided by the parameters of the gyroscopes have a similar effect than in the classical INS mechanisation. The DR algorithm needs external information to correct the errors. In car navigation, GPS and map matching provide the external sources of information. Kalman filter is also used to combine all the measurements and to filter the trajectory. A schematic presentation of car navigation algorithm is presented in Fig.2.7. Some systems do not consider the map matching for the Kalman Filter. This process is performed only with the odometer, gyroscope and GPS data. Then the output of the filter is compared with the map, and the map matching algorithm is performed.

2.3 Adopted system for pedestrian navigation

The first part of this chapter has been dedicated to the presentation of several concepts, tools and techniques. Depending on the application, all of them can be applied to or used by a pedestrian navigation system. The selection of the system will then be driven by the specific requirement of the targeted application. This section aims at presenting the foreseen application, at giving the requirements and at presenting the selected system (tools and techniques).

2.3.1 Requirements

The requirement depends on the targeted application. For the purpose of this work the main requirements are listed below. The targeted application is the localisation of weak person (disable, elderly, subject to hart attack) to offer them efficient emergency services in case of need.

Accuracy and availability

The precision required for the system is 15 meters (1σ). It allows finding quite easily the person in case of emergency. The availability of the position information must be as high as possible.

Type of system

The chosen option is to have a personal device with the computation to determine the position made on the person and not in a service center. This gives more flexibility to the system to match requirements of other applications.

Communication

To have the alarm transmitted to the emergency centre, a communication link must exist. However, this aspect has not been developed in the frame of this work.

2.3.2 System architecture

To answer to these requirements, the choice to use a GNSS sensors has been made because of its global coverage. Other advantages of this technique are the possible augmentation of the satellite constellation (Galileo) and the technological development in the receivers to enhance the performances of GNSS positioning in difficult environment (urban canyon, trees canopy, indoor). Because of the availability requirement it was necessary to complement the GNSS device with another system that allows furnishing location information where less than three satellites are visible. Next section explains the choice of these complementary sensors.

As communication is also needed for such a system, the technique of localisation via mobile telephony network has been also investigated. This

technique is not yet available with the required precision, so this solution has not been considered further.

Choice of complement sensors

To complement the GNSS receiver, the Dead Reckoning approach has been selected because of its availability that complements perfectly the disadvantages of GNSS techniques. For the distance measurement, an accelerometer has been chosen because of its capability to count the number of steps and to offer the possibility to determine speed. This will be explained in details in the next Chapter. For the orientation determination, the gyroscope solution has been investigated in details. However, the magnetic compass has also been taken into account, as shown in the Chapter 4.

Placement of the sensor

While the selection of the used sensors is important in the pedestrian navigation, the critical part is their placement on the person [Boute97b]. As the body is not a rigid structure that moves smoothly, the acceleration and orientation response depends on the sensor placement with respect to the body. This response can be completely different if they are placed on the limbs (arm, legs), on the trunk (back or thorax) or on the head. The medical studies on the walk (biomechanics), on the energy expenditure (linked to the activity monitoring) gives very useful information about the response of the accelerometers. It helps to choose the placement of the sensors.

- In [Farri87] and [Smidt71], it is demonstrated that the movement measured at the centre of mass of the body is representative of the total body movement. Sensors have to be placed as close as possible to the center of mass if the interest focus on the body movement, which is different than the person position.

- [Lapor79] and [Webst82] have investigated different placement to see on which members the accelerometers record the greatest activity during walk. They show that a sensor placed on the legs gives the best acceleration response.

- For the computation of the energy expenditure by the means of accelerometry, the best placement of the sensor is the one that gives the best correlation between the acceleration measured and the energy

spent as well as the best repeatability of the results for a same subject. In [Washb88], it is shown that the best choice was to place the accelerometer at the waist or on the chest. [Balog88] states that the placement on the waist gives the best correlation.

- The influence of the placement on the error in the measurement of the accelerometer have been described in [Redmo85] and [Kitaz95].

- The spectral response of the accelerometer measuring the movement during walk depends also on the placement on the sensors [Anton85]. In this study, it is indicated that the walk generates information, in the frequency domain, until 15 Hz. This means that, considering the Niquist theory, a sampling frequency of 30 Hz is sufficient to measure the activity.

- Investigations have also been made on the placement of other sensors such as inclinometer in [Tanak94] or on the placement of 6 accelerometers [Ladin91].

Selected system

The studied system utilises sensors fastened to the thorax. This choice allows the system to use the same sensors also for an other system developed by the CSEM (Centre Suisse d'Electronique et de Microtechnique, Neuchâtel): the Fall Detection Sensor System (FDSS). The GPS receiver and the power supply are carried in a backpack while the GPS antenna is placed on the shoulder. The first accelerometer is placed vertically (along the thorax), the second one is mounted perpendicular to the first and oriented along the walk direction (anterio-posterior). The gyro measures the angular rate about the axis of the first accelerometer.

Another solution, adopted by Ladetto [Ladet99], consists in placing the sensor near the gravitational centre of the body, which means at the bottom of the person's back. Comparison of results depending on the placement of the sensors are presented in Fig.2.8. The differences of the sensors outputs will drive the implementation of slightly different algorithms. Some aspects of the effect of the sensors placement have been described by Bouten [Boute97b].

The person wears also a portable pen-computer to log all the raw data for post-processing investigation purpose. Sometimes, a second person carries the pen-computer to avoid any external disturbance of the walk of the first person.
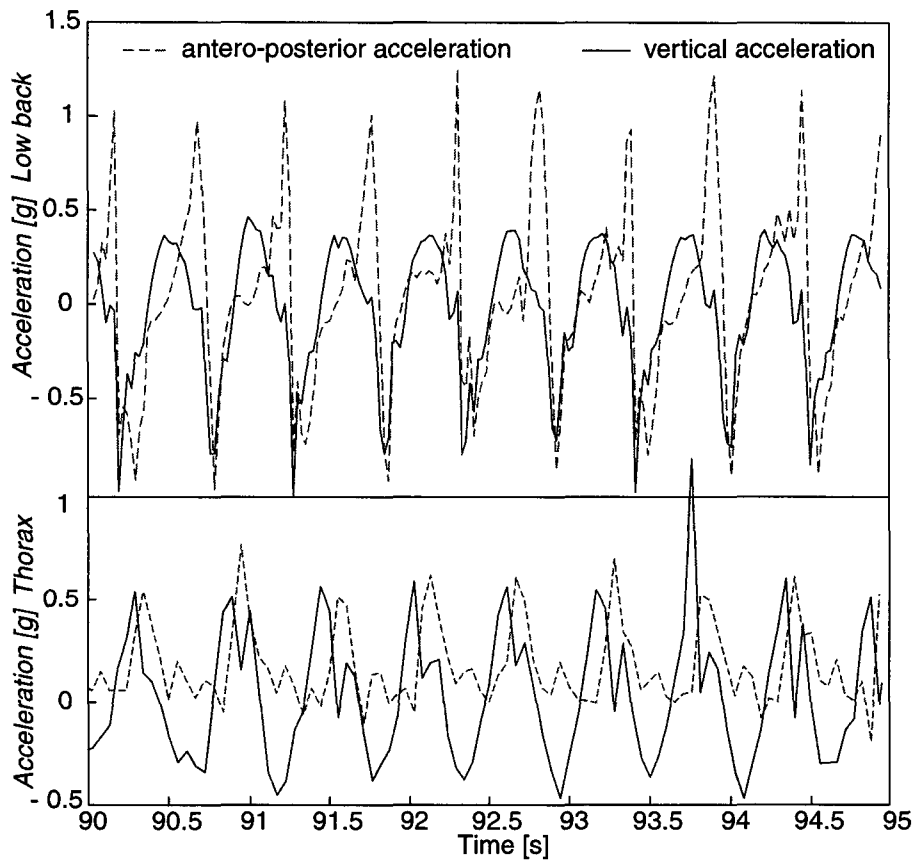
Figure 2.8: Accelerometers response (vertical and anterio-posterior) for two different placements: the person's back (upper part), the thorax (bottom part).

All the developments presented in this thesis are based on this system architecture.

2.3.3 Activity monitoring

A GNSS receiver and INS sensors are the instruments to perform the different functions of the pedestrian navigation. However, another branch of medical studies is needed to improve the system. Indeed, it is necessary to know the activity of the person to run the correct algorithm at the right moment. A typical example is when a person is climbing stairs, the received signal from the accelerometer and the gyroscope are different. If this difference is not detected then the algorithm for *walking* instead of *climbing stairs* will be applied.

So the activity monitoring is the first step of the process. In the system architecture, an algorithm is providing to the system the information whether the person is walking or not. For demo purpose simple activity monitoring algorithms have been implemented (see Chapter 5). However, more improved techniques can be considered. For example, accelerometers can be used to analyse the activity of the person [Makik95, Velti96, Najaf99] or the context awareness [Rande00]. Inclinometers [Tanak94] or gyroscopes are also used for this purpose. The algorithms are generally based on pattern recognition [Fisch97]. More recently some techniques based on neural network have been implemented [Amini99].

2.4 Other research activities

Other research groups are investigating the pedestrian navigation domain. The following list indicates some of them:

- The company Point Research has proposed a commercial product based on GPS, accelerometer and magnetic compass [Judd97].

- The University of Tampere in Finland is integrating GPS and MEMS in small devices for pedestrian navigation [Kappi01, Leppa01, Colli01].

- The Draper Laboratory has developed algorithms based on the classical inertial navigation techniques [Elwel99].

- The company Telematica has developed a device based on GPS, accelerometer and compass [Legat00].

- The University of Brunel is developing a GPS-magnetic compass device for blind navigation [Jiraw00, Garaj01].

- The University of Nottingham uses a GPS-INS system for pedestrian. This system is complemented with an augmented reality visualisation system [Rober01]. They are also developing a system for blind persons [Dodso99].

- Golding has also developed a system based on wearable sensors [Goldi99].

- The company Applanix has performed some test with an INS/GPS platform generally used for vehicle navigation [Gille00].

After this Chapter describing the scope of pedestrian navigation and the choice made for this thesis, the next chapter will present the way in which the distance is computed considering data coming from accelerometers and from the GNSS receiver.

Chapter 3

Distance determination

This Chapter focuses on the determination of the distance travelled by a pedestrian. The adopted method is based on a dead-reckoning approach that has similarities with the method used for car navigation. Two different methods are presented. The first one is based on the use of a pedometer and a GPS receiver. Only the number of steps and their occurrences are considered and combined with the GPS measurements. The second method is more sophisticated approach based on medical studies related to the mechanism of walking, to the person's energy expenditure and to the human's activity monitoring. It combines accelerations measured along two axis and the GPS measurements. This second approach needs the establishment of new models. These models use individual parameters that must be determined for each person. The way to determine the models and to calibrate these parameters are also described and discussed.

3.1 1st Method: Pedometer and GPS

The first solution to determine the distance travelled by a pedestrian comes from the analogy that exists between car and pedestrian navigation: the number of steps replaces the turn of wheel counter; the step length substitutes the radius of the wheel. The solution proposed and explained below is based on the use of a pedometer and the determination of the step length by GPS. A pedometer is an accelerometer combined with a step determination algorithm. The second part of the section proposes different strategies for the step detection. The third part develops algorithms for the determination of the length of the steps.

34

3.1.1 Methodology

Fig.3.1 illustrates the methodology to compute the travelled distance. The two boxes at the left represent the two sensors (the GPS receiver and the accelerometer). The first stage is an activity analysis based on the accelerometer output to deduce whether the person is walking or not [Najaf99]. If he is walking, an algorithm finds out the step occurrence or frequency from the accelerometer signal. The GPS sensor gives a position computed through a carrier smoothed code algorithm. When the GPS position is available (at least three satellites are observed for a two dimensional positioning) the difference between two successive positions gives the GPS-distance that is used for the determination of the step length. Finally, the step length is included into the people navigation process in a similar way that of the radius of wheels in a car navigation algorithm.
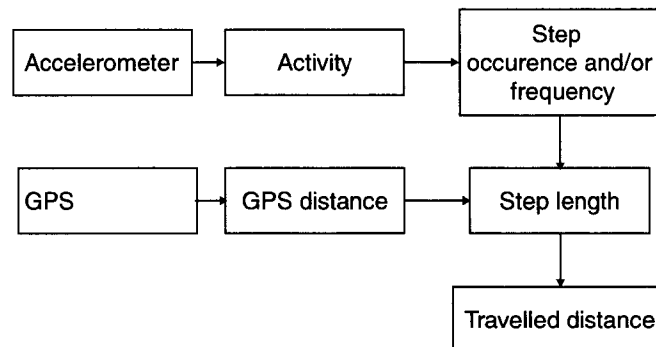
Figure 3.1: Methodology for the step length determination by GPS

The main goal of computing the step length is obviously to use it in Dead-Reckoning mode, i.e. when no GPS data are available.

3.1.2 Step: occurrence, frequency

A pedometer is actually an *intelligent* accelerometer, i.e. an accelerometer with a step detection algorithm. The signal is processed to extract the step occurrence or the step frequency. The following paragraphs focus on this process. Four different techniques are now presented.

Fig.3.2 illustrates the horizontal x-axis (a) and the vertical z-axis (b) response of the accelerometers. The acceleration is measured along two axes. In the presented methodology, a vertical sensor is sufficient. The strongest

horizontal acceleration occurs just after the vertical peaks. The step pattern changes according to the ground surface, the type of shoes or the person's style of walk. Asymmetry between the right and left foot can also appear. The placement of the sensors on the body has an immediate influence on the signature too. To obtain a maximal value for the peaks, the accelerometer must be placed on the foot of the walker. While optimal for step detection, it is not ideal for other purposes as presented in the second methodology and in the next chapter.
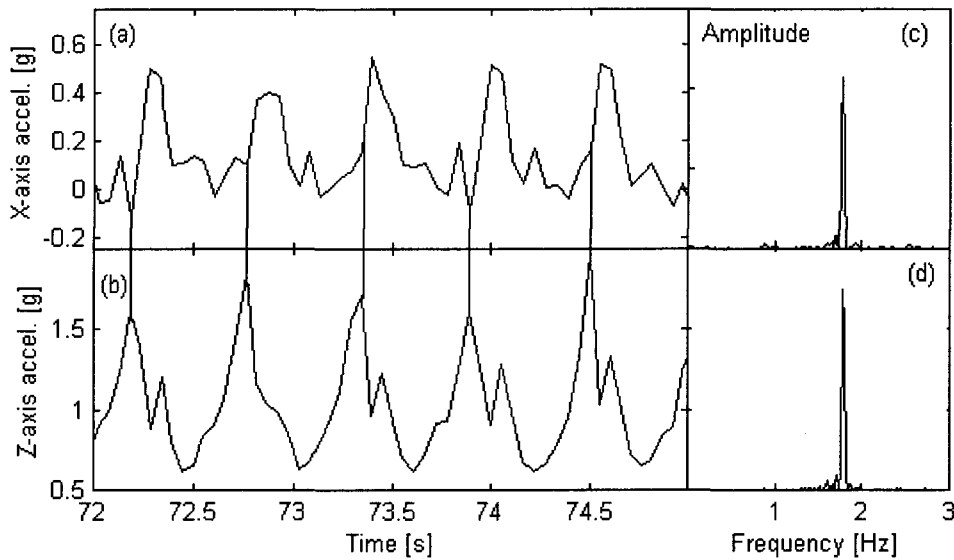
Figure 3.2: Accelerometer signal in time and frequency domain

Technique 1: Frequency extraction with Fourier Transform

A Fourier analysis of x-axis (3.2c) or z-axis (3.2d) accelerometer raw data provides the step frequency. Obviously, the results are identical for both axes. Once the frequency is obtained, the step count during an elapsed time dt is easily computed as:

$$\#_{step} = dt \cdot frequency \tag{3.1}$$

The on-line computation of frequency with a Fourier transform can be performed but is a computationally heavy technique. The solutions presented hereafter are more straightforward.

Technique 2: peak detection

The time analysis of the z-axis response allows the determination of the step occurrence. Each group of two peaks corresponds to a step. Their amplitude is not a constant due to the low sampling rate (20 Hz). The peak detection algorithm is based on the following conditions.

1. A certain time must elapse between two steps.

2. The amplitude of the peak must be higher than a defined level.

3. The value of the acceleration at time $k - 1$ and $k + 1$ must be smaller than the value at time k.

The first condition overcomes the problem of detecting the double peak that occurs often in the acceleration pattern of the step. The double peak of the vertical acceleration has no clear explanation. The heel and the sole touching the ground in a short sequence can create this pattern. However a rebound of the accelerometer just after the step or the resonance of the sensor after the first shock could also explain this double-peak pattern. Once the step is detected, the detection process is stopped during the defined time (point 1). The determination of the elapsed time is driven by the frequency of the steps:

$$time = 0.4/frequency \qquad (3.2)$$

The second condition is related to the activity determination process. The peak must reach a certain value to consider it as a step and not as a movement of the body of the person while he is performing another activity (sitting or lying). This condition can become tricky in certain circumstances as with elderly persons. This detection of the activity *walk* can also be based on the step detection algorithm. Indeed, if two steps occur within 1 to 2 seconds then the person walks. However this type of activity monitoring reaches its limits when a person is going up- or downstairs. In this case more sophisticated algorithms have to be used. The third condition is obvious. The maximal acceleration value must be greater than the previous and the next one.

Fig.3.3 illustrates a z-axis accelerometer response with the step occurrences. The time differences between step occurrences gives the step frequency.

In the presented step detection algorithm, the minimal level of the peak value (2$^{\mathrm{nd}}$ condition) is the most difficult parameter to fix. The reasons are:
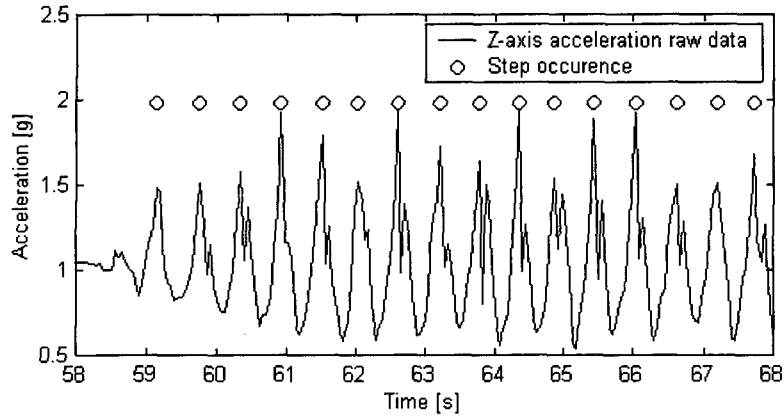
Figure 3.3: Step occurrence determined with a vertical accelerometer

- the bias: the change of the bias of the accelerometer outputs can reach 0.3 g (especially for a low cost accelerometer). It influences directly the value of the peak and then the minimal level.

- the verticality: the change of the orientation of the vertical sensors provokes a variation of the acceleration value. It is due to the change of the angle between the axis and the Earth's gravity field. Its effect is similar to a change of the bias.

To avoid these two problems, the use of a two-axis accelerometer (as proposed in the beginning of the paragraph) constitutes a solution. The modulus of the acceleration is then considered:

$$a_{tot} = \sqrt{a_x^2 + a_z^2} - 1 \quad \text{in } [g] \tag{3.3}$$

The Earth's gravity field is immediately subtracted to maintain the numerical value close to zero and without this bias of $1g$. This subtraction will play a role in the next section where other values will be computed from the a_{tot}. It is assumed that no significant roll (lateral incline) of the accelerometers occurs. To avoid the problem of the bias, the computation of the mean acceleration value over 2 to 3 seconds is done regularly and compared to the previous mean. The level value is computed as a function of this averaged value. The scheme for passing from one to two axes can be continued for the passage from two to three axes. With a three-axis sensor the orientation of the sensors does not have any influence if the total acceleration is considered.

Then it becomes possible to detect peaks independently of the orientation of the sensor.

The choice of a 1, 2 or 3-axis accelerometer depends on the application and on the design of the device. Is the product worn on the chest? If yes, then a 2-axis is sufficient. Is the device put in the pocket? If yes, then a 3-axis is more appropriate because the orientation of the device is completely free.

Technique 3: Zero-crossing

The research group of the University of Tampere proposed another solution for step detection [Kappi01]. It is called the zero-crossing. It consists in counting a step each time the total acceleration crosses the zero value in an ascending way. The total acceleration is obtained by a 3-axis accelerometer. This technique works well and is very simple to implement. However it assumes that the activity "walk" is detected previously, as it is explained in section 2.3.3.

Technique 4: Kalman filtering

The fourth technique consists of an algorithm incorporating an on-line recursive filter (Kalman filter). The measurement model contains four parameters: mean acceleration (C), amplitude (A), frequency (F) and phase shift (D). The vertical axis acceleration (a_z) is modelled as:

$$a_z - v = C + A \cdot sin(2\pi \cdot F \cdot t + D) \qquad (3.4)$$

where t is the time and v is the error.

An identification stage allows the determination of the type of random processes associated with these parameters [Brown97]. Gauss-Markov processes of different orders have been adopted in the kinematic model. The effect of this filter is illustrated in Fig.3.4. It is essentially the same as applying a low-pass filter. However, the advantage of this technique is the immediate availability of three interesting parameters, namely, the frequency F, the amplitude A and the mean C, carried by the state vector. It allows to have an estimation of the accuracy of the determination of these parameters.

The basic concept of the four techniques is clearly different. Tab.3.1 illustrates the differences and the advantages of each technique. Elements taken in consideration are:
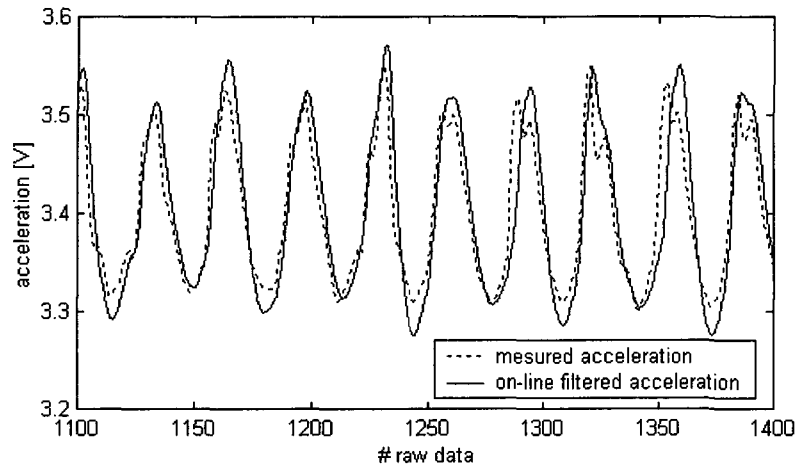
Figure 3.4: Recursive filtering applied to Z-axis accelerometer raw data

- the parameter that the method outputs

- the computation requirement

- the robustness, i.e. the capacity to avoid errors (miss a step)

Technique	parameter	computation requirement	robustness
1	frequency	high	good
2	occurrence (mean)	low	low
3	occurence (delayed)	very low	low
4	mean, frequency, (amplitude)	medium	good

Table 3.1: Differences and advantages of the four step detection methods

The first technique is not adapted. The FFT-transform must be applied only when the person is walking, then an activity algorithm has to be used in parallel. The FFT requests an analysis on a predefined time interval that contains at least two steps (around one second). It induces a time delay in the step detection. Moreover, in this technique, the FFT requires a great number of numerical operations which is not the case of the following techniques.

40

The second and third techniques are simple and give good results. The risk to miss a step is present. Even if the consequences of a missed step are not important in term of accuracy of the position, it has an impact in the step length calibration process (see next paragraph).

The fourth technique is computationally heavy for step detection. But it gives interesting results, such as mean and amplitude, which will be used in the next section.

The second technique is finally retained for this first method. In comparison to the third technique, the second offers a better robustness. Indeed, the acceleration curves can also cross zero when the person make other activities than walking. The threshold value of the second technique plays also a role for activity monitoring and offer a better robustness, although the risk to miss a step or to account another movement for a step remains.

3.1.3 Step length measurement by GPS

Once a step is detected, it is necessary to measure its length. This section presents theoretical developments to compute the step length and its accuracy as well as results of different tests.

Step length computation

The step length computation is obvious. Having a distance *dist* measured by GPS and a count n of the number of steps. The averaged step length $\overline{step}$ can be obviously determined as:

$$\overline{step} = \frac{dist}{n} \tag{3.5}$$

Now the real question is to determine the accuracy of the step length determination. This is done first with a theoretical development and then by test.

Theoretical computation of the accuracy of the step length

The aim of this paragraph is to compute the accuracy of the step length measured by GPS by a classical error propagation method. The scenario consists of a pedestrian walking north over a distance *dist*, says 30m, at a

speed of 1.5 m/s. The distance is then computed as the difference between the coordinates of the first P_1 and last points P_2.

The distance between the two points P_1 and P_2 is computed as a function of dE and dN that are, respectively, the East and North difference of coordinate between the two points:

$$dist_{GPS} = f(dE, dN) \tag{3.6}$$

Extending the function f, we have:

$$dist_{GPS} = \sqrt{(E_{P_2} - E_{P_1})^2 + (N_{P_2} - N_{P_1})^2} = \sqrt{dE^2 + dN^2} \tag{3.7}$$

The next paragraphs will now explain how to compute the accuracy of the determination of the point P_1, by GPS.

The GPS accuracy (SA off) of the first point depends upon the satellite constellation (number and position). Indeed, without entering into details, the GPS position is computed as a function of the pseudo-range between satellite n and receiver. This pseudo-range ρ_n is the result of a peak measurement of the cross-correlation function between a code modulated on the carrier wave and the same code generated in the receiver. The index n denotes that the measurement is made with satellite n.

$$\rho_n - v_{\rho_n} = range_{sat_n - receiver_P} + c \cdot dt \tag{3.8}$$

The parameters are:

$$\mathbf{x}_P = \begin{bmatrix} E_P & N_P & U_P & dt_P \end{bmatrix}^T \tag{3.9}$$

where index p means that the person is at position P.

After linearising the equation (3.8), we obtain the following design matrix:

$$\mathbf{H} = \begin{bmatrix} cos(el_1) \cdot sin(az_1) & cos(el_1) \cdot cos(az_1) & sin(el_1) & 1 \\ cos(el_2) \cdot sin(az_2) & cos(el_2) \cdot cos(az_2) & sin(el_2) & 1 \\ \vdots & \vdots & \vdots & \vdots \\ cos(el_n) \cdot sin(az_n) & cos(el_n) \cdot cos(az_n) & sin(el_n) & 1 \end{bmatrix} \tag{3.10}$$

where

n is the number of the satellites

az_n and el_n are the azimuth and elevation angles of satellite n

The cofactor matrix of vector $\mathbf{x}_P$, that contains position E_P, N_P, and U_P and receiver clock error dt_P, is computed as:

$$\mathbf{Q}_{\mathbf{x}_P\mathbf{x}_P} = (\mathbf{H}^T\mathbf{P}\mathbf{H})^{-1} \tag{3.11}$$

where $\mathbf{P} = \mathbf{I}_{n \times n}$ at first approximation. Sometimes, satellites pseudo-ranges are weighted as a function of the elevation angle of the satellites because pseudo-ranges of satellites with low elevation are noisier than pseudo-ranges of ones with high elevations. The non-diagonal elements of the matrix $\mathbf{Q}_{\mathbf{x}_P\mathbf{x}_P}$ are generally non-zero, which mean that a correlation ρ_{EN} exists between the East and North coordinate.

The following covariance matrix encompasses the variance of the element of vector $\mathbf{x}_P$ in its diagonal:

$$\mathbf{C}_{\mathbf{x}_P\mathbf{x}_P} = \mathbf{Q}_{\mathbf{x}_P\mathbf{x}_P} \cdot \sigma_o^2 \tag{3.12}$$

where σ_o is the standard deviation of a pseudo-range. With SA off we consider [Stran97]

$$\sigma_o = 5m \tag{3.13}$$

The horizontal dilution of precision (HDOP) is an indicator of the quality of the GPS constellation. It is computed as:

$$HDOP = sqrt\frac{\sigma_E^2 + \sigma_N^2}{\sigma_o^2} \tag{3.14}$$

The accuracy of two successive computations of the GNSS position is identical only if a short time elapses between both measurements. This assumption can be made because the satellite constellation is considered to be the same over a short period of time. It means that, in the present situation:

$$\mathbf{Q}_{\mathbf{x}_{P_1}\mathbf{x}_{P_1}} = \mathbf{Q}_{\mathbf{x}_{P_2}\mathbf{x}_{P_2}} \tag{3.15}$$

Coming back to equation (3.7), we consider the following differential matrix $\mathbf{D}$ to pass from $E_{P_2} - E_{P_1}$ to dE and from $N_{P_2} - N_{P_1}$ to dN:

$$\mathbf{D} = \begin{bmatrix} -1 & 0 & 0 & 0 & 1 & 0 & 0 & 0 \\ 0 & -1 & 0 & 0 & 0 & 1 & 0 & 0 \end{bmatrix} \tag{3.16}$$

that multiplies the vector:

$$\mathbf{x} = \begin{bmatrix} \mathbf{x}_{P_1} & \mathbf{x}_{P_2} \end{bmatrix}^T \tag{3.17}$$

to obtain:

$$\mathbf{d} = \begin{bmatrix} dE & dN \end{bmatrix}^T = \mathbf{D} \cdot \mathbf{x} \tag{3.18}$$

To compute $\mathbf{Q_{dd}}$, the cofactor matrix of vector $\mathbf{d}$, the cofactor matrix $\mathbf{Q_{xx}}$ of the vector $\mathbf{x}$, must be first considered.

The cofactor matrix of the vector $\mathbf{x}$ takes into account the accuracy of the points $\mathbf{x}_{P_1}$ and $\mathbf{x}_{P_2}$, contained in the cofactor matrix $\mathbf{Q}_{x_P x_P}$ and the correlation ρ between the points P_1 and P_2:

$$\mathbf{Q_{xx}} = \begin{bmatrix} \mathbf{Q}_{x_P x_P} & \rho \cdot \mathbf{Q}_{x_P x_P} \\ \rho \cdot \mathbf{Q}_{x_P x_P} & \mathbf{Q}_{x_P x_P} \end{bmatrix} \tag{3.19}$$

The determination of the correlation ρ is now explained. In terms of error, a correlation exists between the errors of two successive points even if the person is moving. If the travelled distance is not big, then the correlation is assumed to be the same as the GPS time-correlation computed on a same point. The correlation can be high if the carrier smooth code technique [Hatch82] is used in the algorithm of the receiver. Usually, the manufacturer does not make this information available. To determine the time correlation for the Canadian Marconi receiver (Allstar), the positions were collected on a static point over 100 minutes and the East and North error have then been computed. The autocorrelation is determined for projections of the errors in four different directions (East, North, both diagonals $\Phi = 45^0$ and $\Phi = 135^o$) to have an indication for different walk orientations. Indeed, for a walker marching in the East direction, the correlation between the North errors do not play an important role.

Then an inverted exponential curve (see equation 3.20) is adjusted to determine the correlation length α. Fig.3.5 shows the four autocorrelation functions and three adjusted exponential curves. One curve is adjusted with the East autocorrelation value, one with the North and the bold one is adjusted with both East and North. It appears clearly that the filter used by

CMC correlates more the East than the North component. The reasons for this effect are not clear and cannot be explained without going further into the receiver algorithms and architecture. The same applies for the oscillating behaviour of the North correlation.

Then an "averaged" correlation function has been computed. This last curve (bold) is used to predict the correlation between two positions given a known elapsed time (noted *time*). The function is:

$$correlation: \quad \rho = e^{\frac{-time}{\alpha}} \tag{3.20}$$

where α is called the correlation length. It corresponds to the time when the correlation value is equal to $e^{-1} = 0.37$.

From the test with the Canadian Marconi receiver, the correlation length α is fixed to 220s.
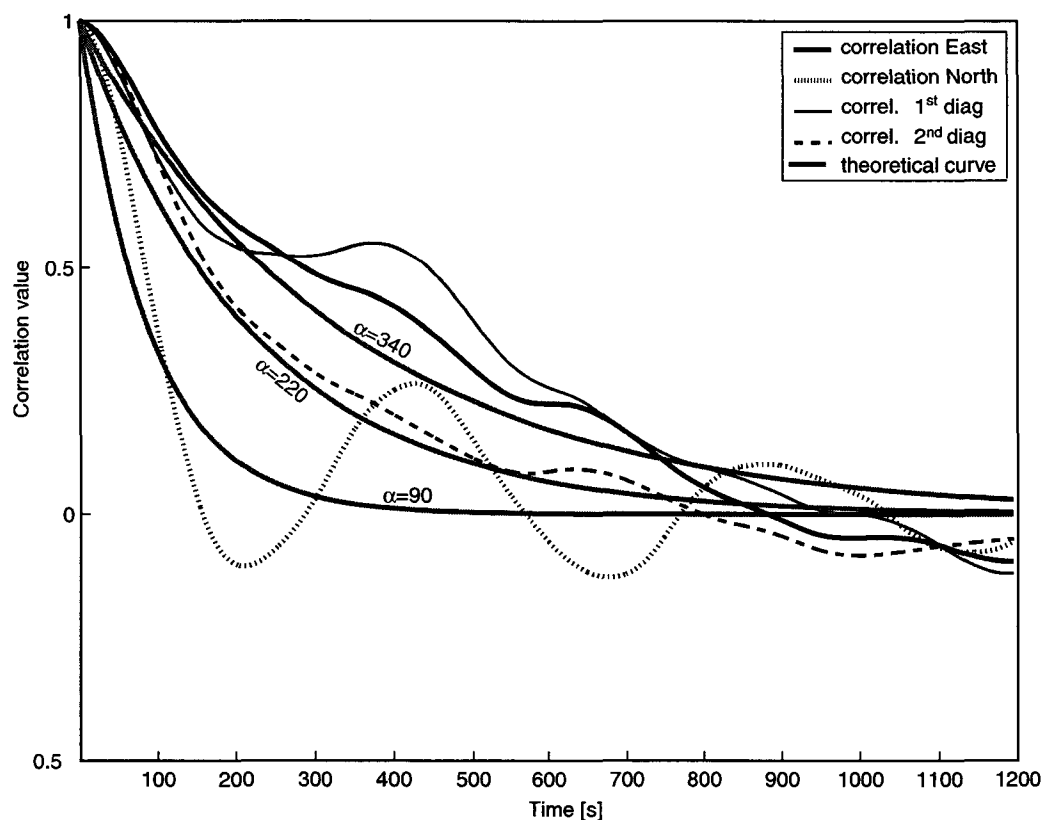
Figure 3.5: Autocorrelation curves computed with 100 minutes of data at 2 Hz for an Allstar Canadian Marconi receiver

At this point the cofactor matrix of the distances dE and dN, included in vector $\mathbf{d}$, can be finally computed as:

$$\mathbf{Q_{dd}} = \mathbf{D} \cdot \mathbf{Q_{xx}} \cdot \mathbf{D}^T \qquad (3.21)$$

To pass from the parameter dE and dN to the desired distance $dist_{GPS}$, the equation (3.6) must be used. This equation must be linearised to compute the accuracy σ_{dist} of the distance $dist_{GPS}$. The linearisation occurs with a first order Taylor's series around the dE and dN value to obtain:

$$ddist_{GPS} = \frac{\partial f}{\partial dE} \cdot ddE + \frac{\partial f}{\partial dN} \cdot ddN = \mathbf{F}^T \cdot \begin{bmatrix} ddE \\ ddN \end{bmatrix} \qquad (3.22)$$

with

$$\mathbf{F}^T = \begin{bmatrix} \frac{dE}{\sqrt{dE^2 + dN^2}} & \frac{dN}{\sqrt{dE^2 + dN^2}} \end{bmatrix} \qquad (3.23)$$

Finally the variance of the distance is computed as:

$$\sigma_{dist}^2 = \mathbf{F}^T \cdot \mathbf{Q_{dd}} \cdot \mathbf{F} \cdot \sigma_o^2 \qquad (3.24)$$

The accuracy of the averaged step length is then computed as:

$$\sigma_{\overline{step}} = \sigma_{dist}/n \qquad (3.25)$$

where n is the number of steps, which is a non-stochastic (deterministic) value.

Finally, the accuracy of the average speed is also computed for information:

$$\sigma_{\overline{speed}} = \sigma_{dist}/time \qquad (3.26)$$

where $time$ is the time elapsed while the walker goes from the first point P_1 to the last point P_2 considered for the $dist$ computation.

Tab.3.2 gives the standard deviation of distance and speed for three different distances which will be used in the next paragraph dedicated to the results of tests (HDOP=2).

To evaluate the influence of the satellite geometry on the accuracy, the Fig.3.6 shows the standard deviation of the distance for different HDOP (see equation 3.14).
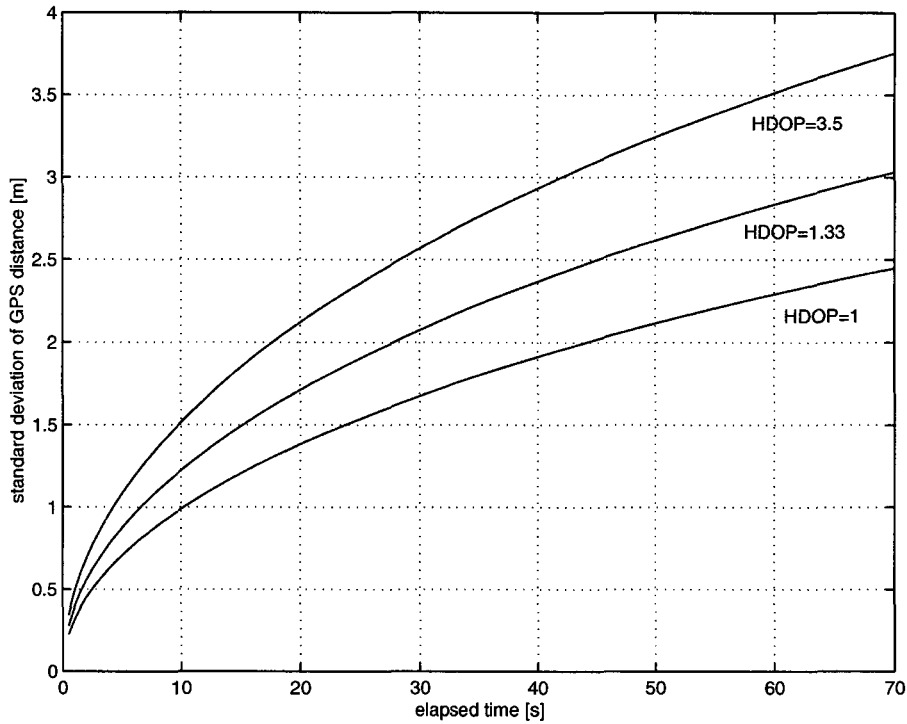
Figure 3.6: Standard deviation of the distance measured by GPS in function of the elapsed time.

Test to validate the theoretical accuracy

The test takes place on a 30 meter straight path without any obstruction for the reception of the satellite signals. A person walks several times along the path carrying the GPS sensor (Allstar, Canadian Marconi), the antenna, the accelerometers (an integrated tri-axial accelerometer sensor system with a measurement range of ±2g, based on the Spac2g product, CSEM, CH) and the data logger. The inertial microsensor system is a component of the FDSS device (Fall Detection Sensory System, CSEM, CH), capable of monitoring the human's activity. One of the main problems of data acquisition is the time synchronisation. Accelerometer and GPS are connected through two serial communication ports to a common data logger. Working with a single data logger provides an immediate and simple realisation of the time synchronization.

number of steps	distance	time	correlation	σ_{dist}	$\sigma_{\overline{step}}$	$\sigma_{\overline{speed}}$
10	8m	5s	0.976	0.8m	8cm	14cm/s
37	30m	20s	0.91	1.4m	4cm	7cm/s
125	100m	67s	0.74	2.5m	2cm	4cm/s

Table 3.2: Theoretical accuracy of distance, averaged step length and averaged speed measured as computed by GPS

The placement of the sensors is the same as defined in section 2.3.2. The antenna was placed on the shoulder of the person. The signal obstruction by the person's head proved not to be an issue and the availability of the GPS satellites was sufficient. The other sensors are place on the thorax.

For each 30 meter path the person tries to maintain a constant walk. The GPS data provides the walk trajectory including its length. The standard deviation of all the distances computed with GPS is 7 meters (σ_{dist}). The number of steps (n) varies from 34 to 37 and is considered as a deterministic value. Under the assumption that the steps during the calibration run are completely correlated, the standard deviation of the step length determined in this way may be estimated as $\sigma_{dist}/n = 0.2m$. The maximum error obtained during the test is 0.4 meter. These results show that the step length determination cannot be performed over a short time. As long as GPS positions are available, the calibration of the length of the steps must be a continuous process and not a preliminary or periodic operation in the navigation algorithm.

These tests took place in January 2000, before Selective Availability was turned off (beginning of May 2000). With SA off, the standard deviation of the computed distance can be considerably reduced. Other tests performed on a 100m track give an indication for the accuracy of a distance measured by GPS. The estimated accuracy for a 100m distance is $\sigma_{dist} = 1.5m$. Thus, for 100m, the accuracy of the averaged step length measured by GPS is 1cm which corresponds to the theoretical result of 2cm (Tab.3.2).

3.1.4 Real-time step length calibration

As the length of steps is not a constant and can change with speed [Marga76], the step length parameter must be determined continuously during the walk to increase its precision. A Kalman filter (see Appendix A) is an appropriate tool for the on-line determination of the step length.

Kinematic model

Assuming that the step length does not vary much during the walk, we can apply a prediction algorithm from one step to the following one. This prediction has an uncertainty when the step length changes with the slope of the path [Terri99] and with the person's speed. Basically, the variations in the step length have systematic character in the short term, and random character in the long term. The change of the step length is assumed to be a first order Gauss-Markov process with a correlation time of 20 seconds. The standard deviation of the driving noise is fixed to $0.2\,m/\sqrt{Hz}$.

Observation model

A new observation is computed every ten steps. The step length is considered as constant within the 10 steps. The observation is the length of the GPS trajectory during the ten last steps divided by ten. It has a standard deviation of 0.2 meter (SA on) according to the previous test results. With SA off the standard deviation is 0.08 m. Therefore the update phase of the step length is achieved every ten steps, i.e. about 5 seconds for standard walking speed. Between the updates, the error propagation due to the uncertainty in the prediction increases the standard deviation. This permits the model to accept the change of the step length due to a change of the speed or in the slope.

Fig.3.7 illustrates two walk sequences separated by a short stop phase. The step length is initialised with an arbitrary value of 0.85m and a standard deviation of 0.2m. During the stop phase, the step length and its standard deviation are not updated. They become the initial information for the next walking sequence. The middle graph shows the observations (dotted line) and the filtered step length (solid line). During the first ten steps, just after the vertical dotted line, the step length has a value of 0.85m. After ten steps, a first step length measurement is performed and gives a value of 0.73m (dotted line). At the same time, this value is introduced in the Kalman Filter. It ouputs a value of 0.79m that will be considered as the step length for the next ten steps, waiting for a new input (external measurement of the step length). The standard deviation (lower graph) of the step length is decreasing to reach a value of 10 cm. On a longer path, the precision could reach a value smaller than 10 cm.
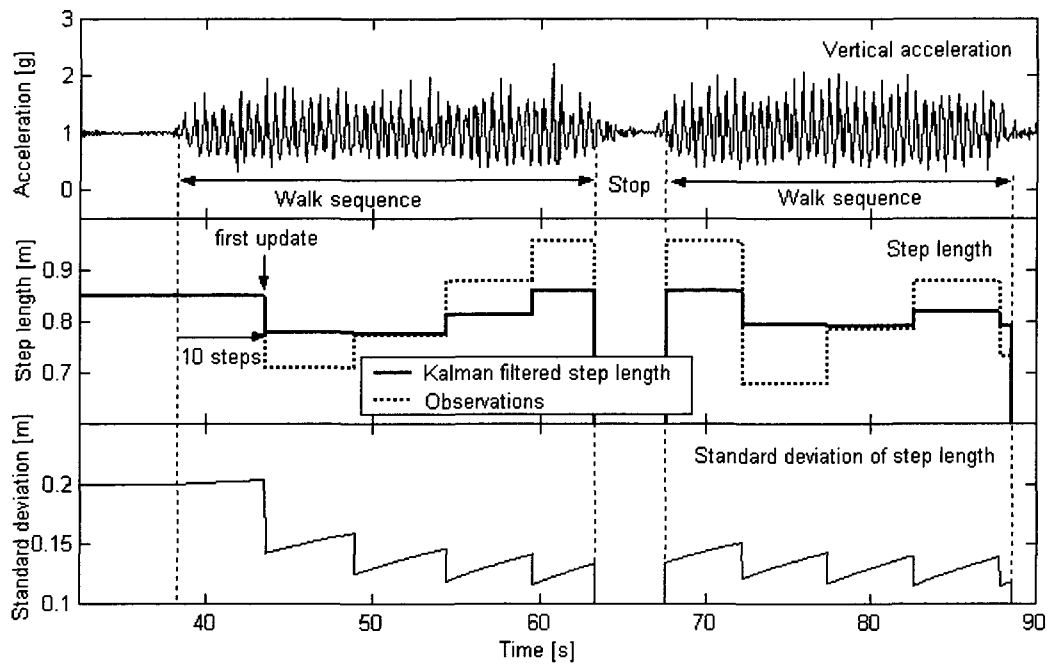
Figure 3.7: Kalman filtering to obtain step length

3.1.5 Discussion

This first solution, based on a simple pedometer combined with GNSS, is light from an implementation point of view. It does not yield robust results as the sudden change of step length can be detected only when GPS measurements are available, which is not often the case in urban environment (around 60% availability). However, this method remains interesting today because both simple pedometer and GPS are available on the market. The presented technique shows a simple way to integrate both devices, combining their outputs (step count and position) without any modification to the available devices.

3.2 2nd Method: Accelerometers and GPS

The first approach presented in the previous section has a main drawback: when no GPS signals are measurable then the step length is considered as a constant and sudden changes of the length cannot be detected until GPS measurements are available again. Then, to obtain an efficient Dead Reckoning algorithm, a relation between accelerometric signal and velocity must be found to allow the system to be sensitive to changes of the step length when information from GPS satellites is not available. To establish the good relation it is necessary to go into medical literature, in physiology and biomechanics. Medicals have been studying human's walk on more than one century [Carle1872], for different purposes (external work measurement, energy expenditure, activity monitoring, rehabilitation, virtual reality, ...) and with different tools (photography, video, accelerometry, treadmill, ...). The next paragraph focuses on different studies that are valuable for pedestrian navigation.

3.2.1 Accelerometry studies of the walk

The first medical domain that provides information for pedestrian navigation is physiology, more precisely the research concerning energy expenditure. In different publications ([Morri73, Monto83, Boute97a]) authors were interested in quantifying the energy expenditure of a person as a function of his activity. The activity of the human body is related to the external work of the body. The work is the force multiplied by the travelled distance [Cavag76]. Therefore the activity can be measured with force plateform [Brouh60] or with the help of accelerometers. Reswick establishes a

linear relation between the energy expenditure and the summation of the time-integrated absolute value of a vertical accelerometer output [Reswi78]. He uses a head-mounted accelerometer. Wong has developed an apparatus called Caltrac (www.caltrac.net) that logs acceleration parallel to the vertical axis of the body [Wong81]. The absolute value of the accelerometer output was integrated over the total test duration. The value was called *acceleration count*. The reproducibility was good (coefficient of correlation r=0.94) and the correlation between energy expenditure and acceleration count was interesting for medical studies (r=0.72). Then Ayen and Montoye have demonstrated that better results can be obtained by using three Caltrac mounted orthogonally (r=0.75 instead of r=0.65 for a single axis) [Ayen88]. The numerous publications in that domain bring other interesting results for pedestrian navigation purposes. Antonsson demonstrated in 1985 that 99% of the power spectral density of the acceleration deployed during walking take place below 15 Hz [Anton85]. This means that the information of the walk takes place between 0 and 15 Hz and that the frequencies higher than 15 Hz contains only noise. Three years before, Cappozzo showed that the spectral density of the acceleration of the upper body was comprised between 0.8 and 5 Hz [Cappo82].

In the same medical domain, a clear relation is drawn between the energy expenditure and the speed and incline which the person has travelled during the period [Marga76, Hagan80, Herre99]. The walking efficiency and the weight of the person are two other parameters. Some authors described tests using other sensors in addition to accelerometers to determine the energy expenditure. For example, Meijer uses a heart rate sensors [Meije89]. In the biomechanic domain, the works of Margaria and Cavagna are significant to find a relation between the step length and biomechanical parameters (length of legs, age, sex, etc) [Marga76, Cavag64].

Considering all the medical research mentioned above, it is clear that a model can be created to predict the speed as a function of the acceleration measured in one point of the body and in function of individual parameters.

The proposed relation is thus:

$$speed = f(body\ acceleration,\ individual\ parameters) \qquad (3.27)$$

The main idea remains that the speed, and therefore the distance, can be predicted with accelerometers outputs without a formal double integration. This means that the relation will not be deterministic because not based on an explicit physical law.

From a more mechanical point of view, one should consider that the human body cannot be reduced to a single kinematic point and, therefore, placing a sensor on a part of the body will force to account for the body as a moving complex and inhomogeneous structure with a lot of interactions. However, from a navigation point of view, the pedestrian is a single point, characterised with a position and a speed. All the medical studies consider the body in all its complexity and a large step must be made from medical literature to get the useful information for pedestrian navigation. The main problem, starting form a medical point of view of the pedestrian navigation, is to make the step from a (bio-)mechanical conception of the body to a navigation one, i.e. to reduce a complex structure to a single point. Reciprocally, starting form a navigation point of view, one cannot consider the human in the same manner as a boat or a car. In the navigation domain we consider the human body as a point which position and trajectory are of interest.

The model is then empirical. The next section focuses on the establishment of this model.

3.2.2 Determination of the characteristics of the body acceleration

To establish the model, tests have been made with different people. A three-axis accelerometer (Crossbow) with a 2g measurement band and a 10Hz bandwidth has been placed on the thorax of the person. The performance of these accelerometers are very similar to the performance of the CSEM accelerometers. The Crossbow has been chosen here because it contains in the same box also gyroscopes that will be useful for the orientation determination (Chapter 4). The person walks at various speeds over a determined distance (30m or 100m). The speed is considered as constant during the walk. The signals of the anterior-posterior accelerometer (close to horizontal) and of the close-to-vertical one have been stored and analysed. It is assumed that the signal from the lateral accelerometer is not significant for normal walk. The use of this third accelerometer is interesting for special movement (side-stepping) and for activity monitoring. It must be considered compulsory if the device may be worn in an unknown orientation. Then the three-axis are necessary to obtain the total vector of the acceleration. This is not the case in the frame of this thesis, where the sensors placement (thorax) allows to consider that the lateral inclination is close to zero.

The main difficulty in the establishment of a model is the lack of a clear relation between the acceleration measured on a part of the body to the

walking speed.

To define a model for speed prediction, it is necessary to find a **characteristic** of the measured accelerations that is well correlated with the velocity. A **characteristic** means a significant numerical value (sort of signature) that can be extracted directly from the signal.

To be efficient the characteristic must fit the following requirement.

Ergodic: The values of the characteristic computed from different samples of the signal generated by the same person going at the same speed in the same external conditions (shoes, soil, ...) is constant.

Stationary: The size of the computational time interval (2, 5, 10, 20 seconds) does not influence the value and, when the speed is constant, the moment when the computation is performed does not have any influence.

Fig.3.8 shows the vertical acceleration during a sudden change of speed. Analysing the data and taking the result of the medical studies into account, the following characteristics of the signal have been computed.

- VAR is the averaged quadratic acceleration amplitude $(a_i - \bar{a})$ which is computed relatively to a mean acceleration $(\bar{a})$. This value is different from the jerk which is the instantaneous change $(a_i - a_{i-1})$ over a time period. The square of the $a_i - \bar{a}$ avoids the problem of sign when a_i is smaller than $\bar{a}$.

$$VAR = \frac{\sum\limits_{i=k-n}^{k} (a_i - \bar{a})^2}{\Delta t} \qquad (3.28)$$

where

$$\bar{a} = \frac{\sum\limits_{i=k-n}^{k} a_i}{n+1}$$

Δt is the elapsed time between the samples $k - n$ and k

k is the epoch of the acceleration measurement a_k at the end of the time interval

n is the number of samples a_i during the interval Δt, which depends on the sampling rate.
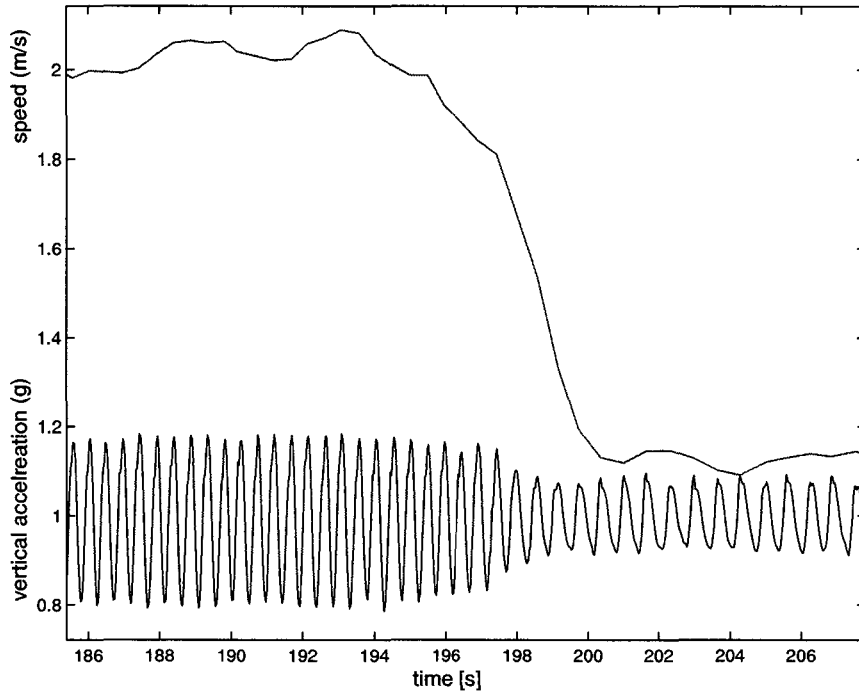
Figure 3.8: Sudden change of speed compared with the signal of a vertical accelerometer

- RMS is defined as the square root of VAR. The rationale of computing this value is to come back to a smaller degree of the acceleration (g instead of g^2).

$$RMS = \sqrt{VAR} \qquad (3.29)$$

- ABS is the average of the absolute value of the acceleration amplitude. In comparison with the characteristic VAR, the ABS represents another possibility to avoid the problem of sign.

$$ABS = \frac{\sum\limits_{i=k-n}^{k} |a_i - \bar{a}|}{\Delta t} \qquad (3.30)$$

- AMP is the mean amplitude of the peak (difference between the smallest $min(acc)$ and the highest $max(acc)$ acceleration value of 1 stride).

$$AMP = \frac{\sum\limits_{step=1}^{n} \left(max(acc)_{step} - min(acc)_{step}\right)}{\Delta t} \qquad (3.31)$$

- $FREQ$ is the step frequency. This value can be computed in different ways as presented in section 3.1.2.

The determination of those values have been computed on both accelerometers a_x and a_z and on the total acceleration a_{tot} as computed in equation (3.3). Instead of standardising the value by the time Δt it is also possible to do it by the number of steps. The results are very close considering at least 4 steps or 2 seconds. Further investigations about the time-interval are presented in section 3.3.5. A specific analysis of the choice of the Δt will be performed in section 3.3.5. Only one value of VAR will be computed over the Δt interval. This value will be used to compute a speed that will be the averaged speed of the walker over the period covered by the Δt. If the objective is to detect the change of speed as soon as possible, then the Δt must stay short. If the objective is to calibrate the model (3.27) then Δt can be longer.

Speed	Person	$FREQ$	RMS_x	ABS_x	AMP_x	RMS_z	ABS_z	AMP_z	RMS_{tot}	ABS_{tot}
0.6	1	0.981	0.983	0.976	0.851	0.980	0.981	0.782	0.985	0.990
to	2	0.954	0.990	0.980	0.765	0.990	0.990	0.760	0.994	0.994
2.2m/s	1+2	0.959	0.985	0.923	0.696	0.969	0.946	0.749	0.974	0.973
1.0	1	0.989	0.978	0.964	0.632	0.974	0.984	0.876	0.978	0.987
to	2	0.886	0.963	0.954	0.548	0.975	0.788	0.843	0.980	0.989
2.0m/s	1+2	0.925	0.971	0.956	0.582	0.971	0.870	0.838	0.976	0.984

Table 3.3: Correlation value between speed and characteristics of the signal

The correlation value between those parameters and the velocity have been computed. Table 3.3 furnishes results for two different persons and for two speed ranges. The two persons are between 25 and 30 years old with close biomechanical characteristics (size, weight, ...). The correlation has also been computed mixing the data of both persons (line 1+2). This combination gives an indication of the variability of the characteristics between different persons. If the Persons(1+2) correlation is near to the Person(1) and/or Person(2) correlations then the difference of the individual parameter of the two persons is little. This is of interest for fixing the variability of the individual parameters.

The RMS_{tot} and ABS_{tot} values give the best correlation value. To choose between a single axis accelerometer and the total acceleration provided by two accelerometers, other considerations need to be taken into account. Perrin et

al. show that the slope is a real limitation for a relation between speed and RMS [Perri00]. The pedestrian changes his walking bio-mechanical strategy to afford downhill or uphill. In particular, the person changes the incline of the body, which change the influence of the gravity field on the sensors.

Moreover the fixation of the sensors on the body can produce a change of the orientation. Choosing a RMS computed with only 1 axis exposes the system to systematic errors that can be partially compensated by taking the RMS computed with the total acceleration into account. For these reasons, it appears that the total acceleration is more adapted to compute the travelled distance of the pedestrian. At this point the use of a third accelerometer is clearly an advantage. However we choose to consider only two accelerometers assuming that no lateral incline occurs. The algorithms can be easily adapted for a 3-axis accelerometer system computing:

$$a_{tot} = \sqrt{a_x^2 + a_y^2 + a_z^2} - 1 \quad \text{in } [g] \tag{3.32}$$

As for the equation (3.3), the Earth's gravity is immediately subtracted.

Fig.3.9 illustrates the speed in function of frequency (a), amplitude of the z acceleration (b), RMS of the antero-posterior acceleration x-axis (c), RMS of the total acceleration vector (d). The values have been computed using the full set of data for each walk, i.e. Δt for computation of RMS and AMP is maximal.

The correlation numbers described in Tab.3.3 can be visualised in these four graphs through the capacity for a line to pass through all the dots or crosses. If the gaps between the dots or crosses and the 'best' fitting line are too big then the correlation value will be smaller (i.e. closer to zero) and it will be more difficult to build a linear model.

3.2.3 Establishment of the models

The relation (3.27) is now transformed in:

$$speed_{DR} = f(VAR, \; individual \; parameters) \tag{3.33}$$

or

$$speed_{DR} = f(RMS, \; individual \; parameters) \tag{3.34}$$

The definition and determination of the individual parameters is now the most important key for determining the distance travelled by the pedestrian
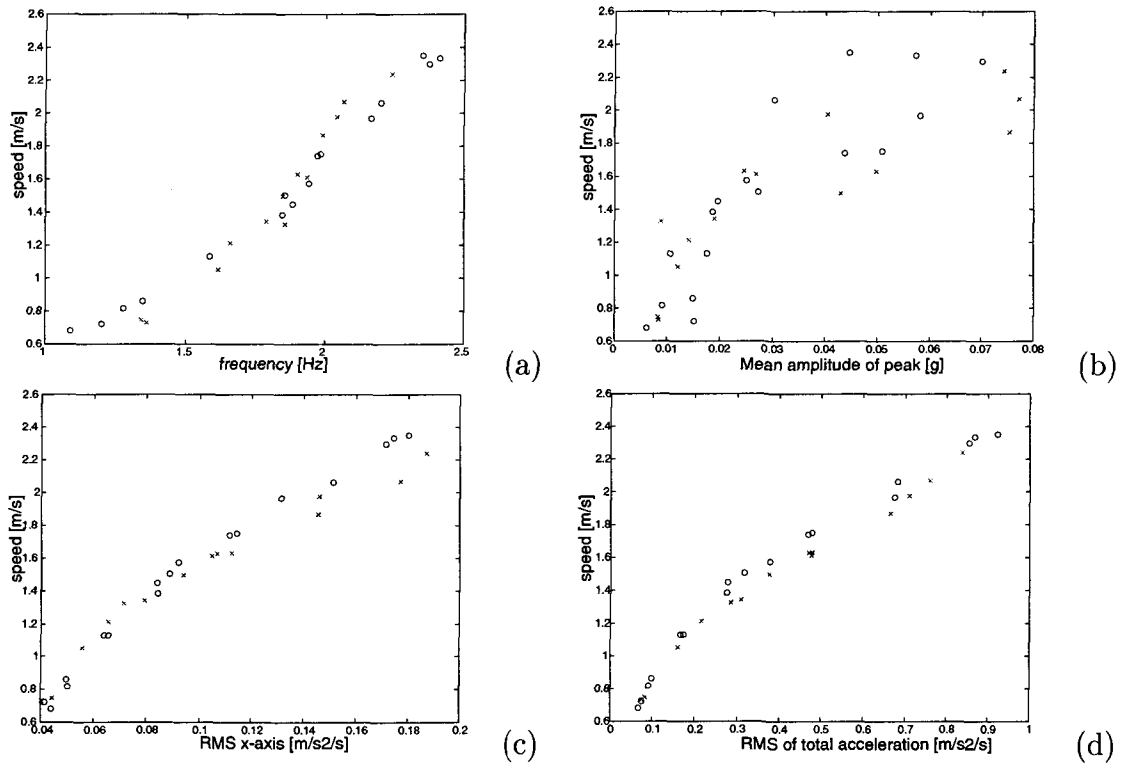
Figure 3.9: Speed in function of frequency (a), amplitude of vertical peak (b), RMS_x (c), RMS_{tot} (d) for two different persons (the first represented with the circles, the second with the crosses).

in dead-reckoning mode. The first relation proposed is directly inspired by the medical studies.

1st model:

The first model is:

$$speed_{DR} = A \cdot \sqrt{VAR} + B = A \cdot RMS + B \qquad (3.35)$$

where $\sqrt{VAR}$ is called the RMS.

To evaluate this model, tests have been done on an athletic track. The parameters A and B of the 1st model have been determined following the procedure described in section 3.3.1. The length of the track is 100m. Then the relation is applied to 100, 200 and 400 meter tests that have taken place on the same athletic track. The mean speed of each test is variable. The maximum error between the computed distance (by integrating the speed) and the ground truth is less than 4% of the travelled distance when the mean speed is over 1m/s. Tests with slower walking speed are inaccurate (relative error more than 36%). The conclusion is that the relation (3.35) is not adapted for low speed. Thus, an augmentation of the number of parameters or a change of the model is required to improve the relation.

2nd model:

The second model proposed is:

$$speed_{DR} = A * VAR^{C} + B \qquad (3.36)$$

Applying this formula shows better results in determining the speed. The maximum relative error on all the tests, including low speed, is about 5% of the travelled distance (instead of 36% in the model 1).

The main drawback is the number of parameters that have to be determined. As it will be shown in section 3.4, the so-called unconstrained calibration of the parameter can drive to problematic results with the 2nd model. The type of people and their average speed must be the driver to determine the model. Elders walk at lower speed than sportsmen!

3$^{\text{rd}}$ model

A third model is proposed. It is based on a physical deduction. When a person is not moving, his speed is 0 m/s and the variation of acceleration VAR must be also 0. That means in fact constraining the parameter B to be 0.

The third model is:

$$speed_{DR} = A * VAR^{C} \qquad (3.37)$$

As the model is not deterministic, other models could be looked at. Models using a logarithmic function instead of a power function have been tested. The results are close to those obtained by the three presented models. Other models including several characteristics have also been developed and analysed. For example, Ladetto developed a model with a characteristics similar to VAR and the step frequency [Ladet00a] to determine directly the step length (and not the velocity). As the correlation between both characteristics (VAR and $FREQ$) is strong, the improvement of the model is not obvious. Other analysis techniques can be used to define the best combination of characteristics that will describe the velocity (or the step length). They will be discussed in the Chapter 6.

Actually, the most important criteria for the choice of the model are on one hand the number of parameters, and on the other hand the numerical difficulty to calibrate and to use the chosen model.

3.2.4 Accelerometer error sources and consequences

The accuracy of the determination of the different characteristics of the acceleration is directly linked with the external error sources affecting the acceleration measurements. When fixing an accelerometer on the body, the signal contains the followings [Balog88, Boute97b]:

1. body movement

2. gravitational acceleration

3. mechanical resonance of the sensor [Redmo85]

4. acceleration due to the tissue under the accelerometer

5. external vibration, not produced by the body itself

6. jolting of the sensors on the body due to the looseness of the attachment

The first element (body movement) is the most relevant component of the signal. The second element is considered as a constant distributed among both accelerometers: mainly the vertical one, but also the anterio-posterior when the body is inclined. The element 3. to 6. are errors. They produce uncertainty in the computation of the characteristics and then in the velocity and in the travelled distance. The errors 3. and 4. are always the same during the walk. They are present during the calibration and operational phase, then the calibration process (presented in the next section) allows to eliminate them. The error of type 5. and 6. are gross errors that produce faults if they are not detected.

3.3 Calibration of the models of the 2nd method

In order to analyse and evaluate the different models in more detail, it is necessary to find an appropriate way to determine the A, B and/or C parameters. This phase is called the *calibration phase*. However, the analysis and evaluation of the model is not the only objective of the calibration presented in this section. It aims also at implementing a process that will furnish the distance component to the Dead Reckoning process.

Two different scenarios are proposed:

- a constrained calibration : it takes place before the sensor is used in normal conditions. It is an initialisation procedure during which the pedestrian must follow instructions. This calibration makes use of the accelerometers only.

- an unconstrained calibration: the pedestrian walks freely. This calibration can be applied during the normal use of the system under the condition that external measurements, provided by GPS, are available. It integrates also the DR approach for the distance determination with GPS.

The two scenarios are compatible and can be combined: first a constrained calibration will determine the parameters before small corrections, computed with the unconstrained calibration, will be applied to these parameters.

In this section, the constrained calibration will be discussed first. Then considerations are made on different aspects of the calibration such as: the

numerical computation and the number of measurements needed. The difficulty of the calibration of each model will drive the choice of the most appropriate model. Results of tests are then presented to demonstrate the accuracy of the calibration. The last paragraph of this section s dedicated to the computational interval of VAR (or RMS). The rationale of the analysis of this specific aspect is given in the corresponding section. In the next section, the integration of the model chosen in this section with GPS (i.e. the unconstrained calibration) is presented as well as simulation results and the limitation of the applicability of the models.

3.3.1 Constrained calibration

The constrained calibration consists in forcing the pedestrian to walk a predetermined distance, say 30m, at a constant speed and to repeat it at different speeds. Each travelling time must be measured to compute the $speed_i$. Then the parameters are computed by a least square adjustment [Gelb74, Maybe94].

1st model:

The observation model of the adjustment process is:

$$\begin{pmatrix} speed_1 \\ speed_2 \\ \vdots \\ speed_n \end{pmatrix} - \begin{pmatrix} v_1 \\ v_2 \\ \vdots \\ v_n \end{pmatrix} = f(A, B, VAR_i) \qquad (3.38)$$

The computations of $speed_i$ and VAR_i are based on the full data set of each walk, i.e. $Deltat$ is maximal. The equation is linear. In matrix notation we have:

$$\begin{pmatrix} speed_1 \\ speed_2 \\ \vdots \\ speed_n \end{pmatrix} - \begin{pmatrix} v_1 \\ v_2 \\ \vdots \\ v_n \end{pmatrix} = \begin{bmatrix} \sqrt{VAR_1} & 1 \\ \sqrt{VAR_2} & 1 \\ \vdots & \vdots \\ \sqrt{VAR_n} & 1 \end{bmatrix} \cdot \begin{bmatrix} A \\ B \end{bmatrix} \qquad (3.39)$$

which we write:

$$\mathbf{s} - \mathbf{v} = \mathbf{H} \cdot \mathbf{x} \qquad (3.40)$$

The estimated parameters $\hat{A}$ and $\hat{B}$ are included in the vector $\hat{x}$ and are computed as:

$$\hat{x} = (H^T P H)^{-1} \cdot H^T P s \tag{3.41}$$

where P is the weight matrix and is assumed to be an identity matrix:

$$P = I_{n \times n} \tag{3.42}$$

Thus, we consider that all the speed measurements have the same precision.

To avoid correlation between A and B, the intersection of the vertical axis (speed) with the horizontal one ($\sqrt{VAR}$) is changed. The $\sqrt{VAR}$ is shifted by $\frac{\sum_{i=k-n}^{k} \sqrt{VAR_i}}{n-1}$. This manipulation yields A and B uncorrelated, which is convenient for the unconstrained calibration presented below.

The model 1 can also be parameterised as follows:

$$\sqrt{VAR_i} - v_i = \frac{speed_i - B}{A} \tag{3.43}$$

Assuming $x_1 = 1/A$ and $x_2 = -B/A$ or $-B \cdot x_1$ we have:

$$\sqrt{VAR_i} - v_i = x_1 \cdot speed_i + x_2 \tag{3.44}$$

In this case, we consider the error on the computation of VAR, rather than on the measurement of the speed. The possible error sources that can affect VAR are presented in section 3.2.4. Both types of parameterisation generate very close results.

2$^{\text{nd}}$ model:

For the 2$^{\text{nd}}$ model the methodology is similar. Except that the relation is not linear. The linearisation is performed by developing equation (3.36) in a Taylor's series of the first order. The series is developed around the approached parameters $\mathring{A}$, $\mathring{B}$ and $\mathring{C}$ to obtain the following observation model:

$$\begin{pmatrix} speed_1 - \mathring{A} \cdot VAR_1^{\mathring{C}} - \mathring{B} \\ speed_2 - \mathring{A} \cdot VAR_2^{\mathring{C}} - \mathring{B} \\ \vdots \\ speed_n - \mathring{A} \cdot VAR_n^{\mathring{C}} - \mathring{B} \end{pmatrix} - \begin{pmatrix} v_1 \\ v_2 \\ \vdots \\ v_n \end{pmatrix} =$$

$$\begin{bmatrix} VAR_1^{\mathring{C}} & 1 & \mathring{A} \cdot VAR_1^{\mathring{C}} \cdot \ln(VAR_1) \\ VAR_2^{\mathring{C}} & 1 & \mathring{A} \cdot VAR_2^{\mathring{C}} \cdot \ln(VAR_2) \\ \vdots & \vdots & \vdots \\ VAR_n^{\mathring{C}} & 1 & \mathring{A} \cdot VAR_n^{\mathring{C}} \cdot \ln(VAR_n) \end{bmatrix} \cdot \begin{bmatrix} dA \\ dB \\ dC \end{bmatrix} \qquad (3.45)$$

which we write:

$$\mathring{\mathbf{v}} - \mathbf{v} = \mathbf{H} \cdot d\mathbf{x} \qquad (3.46)$$

The estimated increments of the parameters are computed as such:

$$d\hat{\mathbf{x}} = (\mathbf{H}^T \mathbf{P} \mathbf{H})^{-1} \cdot \mathbf{H}^T \mathbf{P} \mathring{\mathbf{v}} \qquad (3.47)$$

Finally we obtain the estimated parameters:

$$\hat{\mathbf{x}} = \mathring{\mathbf{x}} + d\hat{\mathbf{x}} \qquad (3.48)$$

where $\mathring{\mathbf{x}} = \begin{bmatrix} \mathring{A} & \mathring{B} & \mathring{C} \end{bmatrix}^T$, $\mathring{\mathbf{x}}$ can be computed with three $speed_i$ values, taking the slower, the higher and the median speed.

The cofactor matrix $\mathbf{Q_{xx}} = (\mathbf{H}^T \mathbf{P} \mathbf{H})$ lets appear strong correlations between the parameters. This is not ideal in the perspective of the unconstrained calibration. The strong correlation means that a change of the value of a parameter can be compensated by a change of another parameter without changing the outputs. It means that the parameters are not independent. If a change has to be applied to the parameters to improve the distance determination, it is difficult to determine to which parameter the increment must be applied. The $\mathbf{Q_{xx}}$ is close to singular and the inversion of the matrix during the computation of the estimated parameter (3.47) can create numerical problems.

3$^{\text{rd}}$ model

The third model is very close to the second one. The observation model after linearisation is:

$$\begin{pmatrix} speed_1 - \mathring{A} \cdot VAR_1 \\ speed_2 - \mathring{A} \cdot VAR_2 \\ \vdots \\ speed_n - \mathring{A} \cdot VAR_n \end{pmatrix} - \begin{pmatrix} v_1 \\ v_2 \\ \vdots \\ v_n \end{pmatrix} =$$

$$\begin{bmatrix} VAR_1^{\mathring{C}} & \mathring{A} \cdot VAR_1^{\mathring{C}} \cdot \ln(VAR_1) \\ VAR_2^{\mathring{C}} & \mathring{A} \cdot VAR_2^{\mathring{C}} \cdot \ln(VAR_2) \\ \vdots & \vdots \\ VAR_n^{\mathring{C}} & \mathring{A} \cdot VAR_n^{\mathring{C}} \cdot \ln(VAR_n) \end{bmatrix} \cdot \begin{bmatrix} dA \\ dB \end{bmatrix} \qquad (3.49)$$

Strong correlation appears also between the two parameters, as for the second model.

To achieve a good calibration, for all the models, the travelled speeds $speed_i$ must cover a spectrum as large as possible, i.e. from very slow to fast walk. Using the first model, very slow speed must not be taken into account because of the non-linearity of the model for low velocity.

3.3.2 Numerical calibration of the three models

Fig.3.10 illustrates the adjustment of the three models on the data sets obtained form tests performed by two different persons.

The a posteriori standard deviation of each adjustment is computed as:

$$\sigma_o = \sqrt{\frac{\mathbf{v}^T \mathbf{P} \mathbf{v}}{n - u}} \qquad (3.50)$$

where n is the number of epochs and u is the number of parameters.

Tab.3.4 shows the a posteriori standard deviation value in m/s for each data set and model.

Speed range	Person	Model 1	Model 2	Model 3
0.6 to	1	0.122	0.040	0.047
2.3 m/s	2	0.079	0.045	0.048
1.0 to	1	0.058	0.034	0.036
2.0 m/s	2	0.032	0.027	0.042

Table 3.4: A posteriori value of the root mean square

This a posteriori value is an approximation of the precision of the observation, i.e. the velocity. Considering a pedestrian walking at a normal velocity, we can consider that the DR velocity can be determined with a precision of
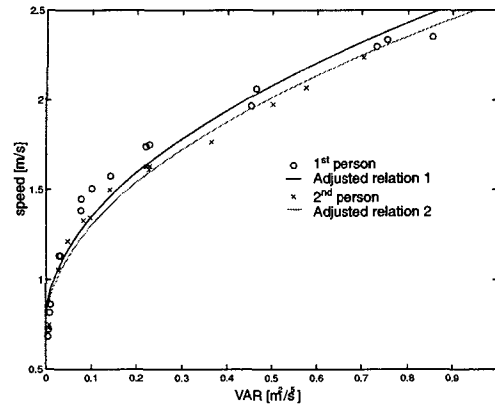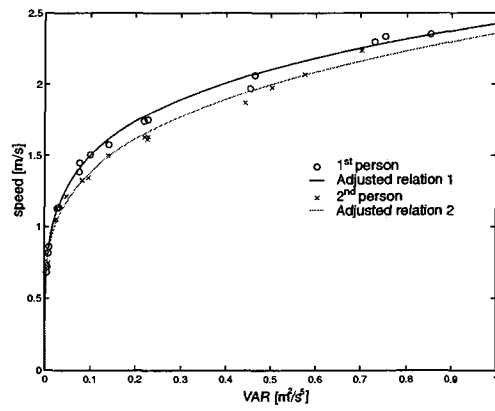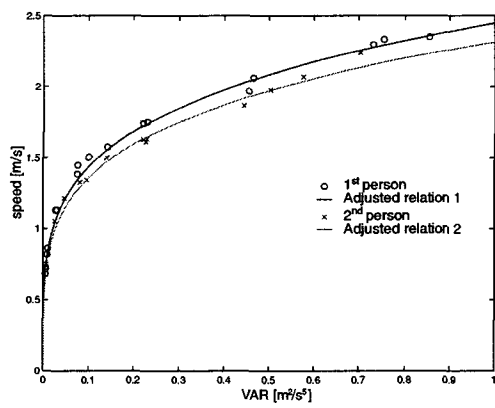
(model 1)

(model 2)

(model 3)

Figure 3.10: Adjustment of the three models for speed determination based on measurements of accelerations

66

3 to 4 cm/s. The condition is that there is no major change of the external conditions (see section 3.4).

3.3.3 Optimal number of tests for calibration

The accuracy of the estimated parameters is a function of the number of observations and of their repartition inside the velocity spectrum. Fig.3.11 and Fig.3.12 illustrate the evolution of the accuracy of the determined parameters in function of the number of walks achieved during the constrained calibration phase. The first figure accounts for a calibration with speed varying from 0.8 to 2 m/s. In the second figure, the speed range is larger and goes from 0.5 m/s to 2.2 m/s.

The dilution of precision (DOP) is computed as the root of the trace of the cofactor matrix. The smaller is the DOP, the better is the performance.

$$DOP = sqrttrace(\mathbf{Q_{xx}}) = sqrttrace((\mathbf{H}^T\mathbf{PH})^{-1}) \qquad (3.51)$$

To compute $\mathbf{H}$, and then $\mathbf{Q_{xx}}$, the chosen velocity is distributed at equal intervals within the velocity range.

A comparison between Fig.3.11 and Fig.3.12 shows clearly that the accuracy of the calibration is better if the speed range increases.

If the speed range goes lower than 0.6m/s (this number can change from a person to another one) then the DOP of the model 2 decreases fast, as well as the correlation between the three parameters A, B and C. The extension of the speed range has not a great influence on the DOP of model 3, but it reduces also the correlation between the two parameters (from 0.95 to 0.8).

The figures show that the parameters are better determined if the number of tests increases. The "ideal" number of test can be determined between 6 and 8. A separate analysis is also performed for each element of the diagonal of the cofactor matrix. It is not represented here because it yields the same type of curves and then drives to the same conclusion.

The comparison of the performance between the three models is not appropriate with the value DOP because the parameters do not have the same nature (exponent or constant) and their number is changing: two parameters for the first and third models and three parameters for the second model.

In conclusion, for constrained calibration, the chosen speed must form a spectrum as large as possible. Concerning the choice of the model, even if the first one does not react correctly for the slower speed, the second and third
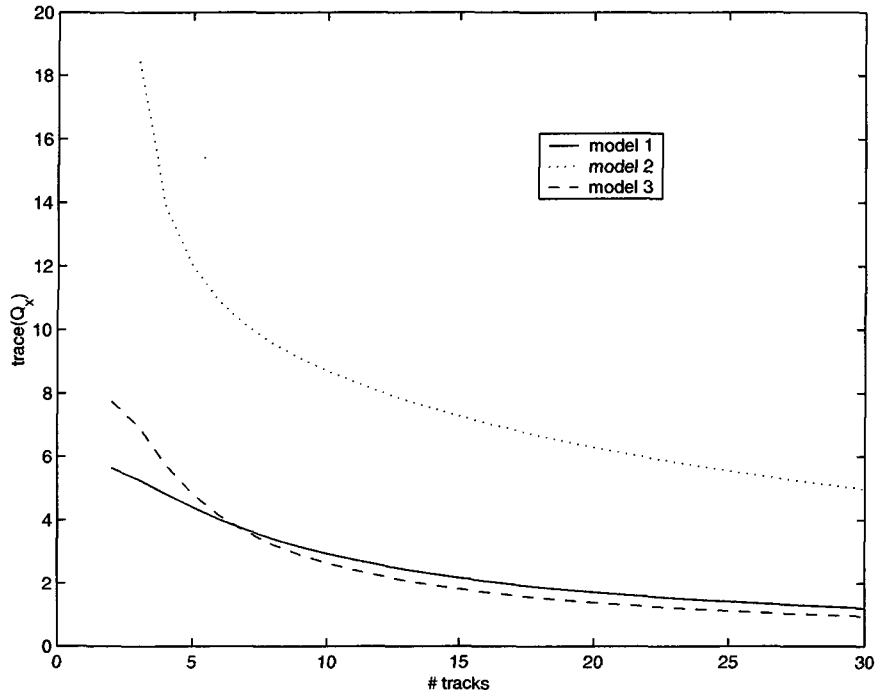
Figure 3.11: Trace of the cofactor matrix Q_{xx} for each model in function of the number of tests. Velocity varying from 0.8 to 2 m/s.

ones can become numerically unstable and then can yield a wrong solution. Therefore, the first model will be used in the following sections and chapters.

3.3.4 Test on a 100 meter track

A test has been accomplished following these instructions.

1. The estimation of the parameters of the first model is done with 7 walks of 100m (speed varying from 1.1 to 1.9 m/s).

2. Additional walks on 100m (speed varying from 1.2 to 1.9 m/s) are performed in the same conditions as for the estimation (same days, on the same ground surface).

The true speed is computed by measuring the time spent by the walker to achieve the 100m. Tab.3.5 shows the results.

True speed m/s	$\sqrt{VAR}$	Predicted speed m/s	Error cm/s
1.479	0.457	1.408	-7.1
1.537	0.498	1.495	-4.2
1.588	0.555	1.616	2.8
1.116	0.337	1.154	3.8
1.095	0.316	1.109	1.4
1.695	0.603	1.717	2.3
1.877	0.683	1.887	1.0
1.465	0.485	1.468	0.3
1.653	0.585	1.680	2.7
1.157	0.355	1.192	3.5
1.509	0.514	1.528	1.9
1.775	0.663	1.844	6.9
1.908	0.691	1.903	-0.4
1.242	0.385	1.256	1.4
1.503	0.503	1.505	0.2
1.832	0.657	1.831	-0.1
1.462	0.473	1.442	-1.9

Table 3.5: Results of the calibration (7 first lines) and of the walks. The travelled distance is 100m
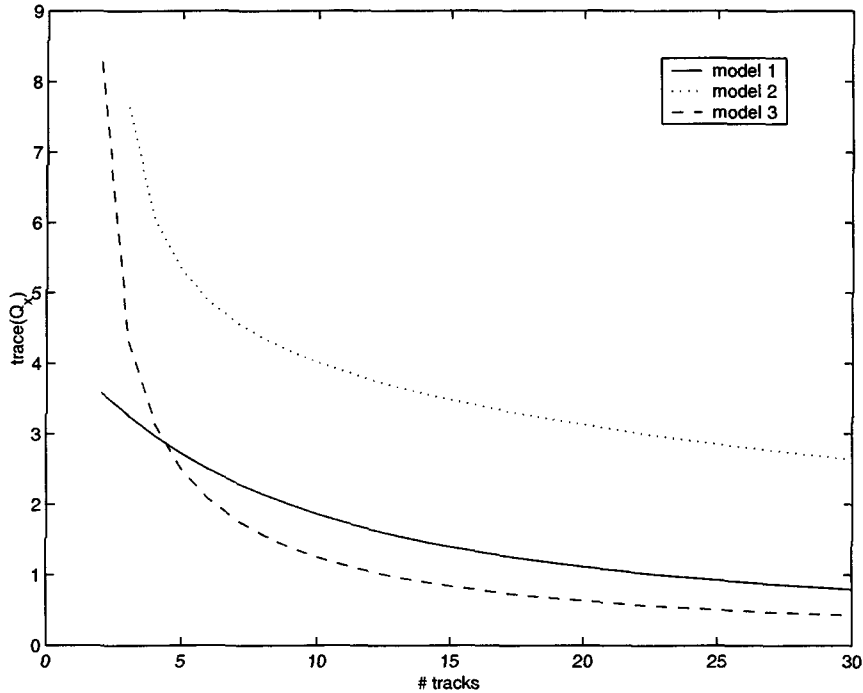
Figure 3.12: Trace of the cofactor matrix Q_{xx} for each model in function of the number of tests. Velocity varying from 0.5 to 2.2 m/s.

The maximal error on speed is 7 cm/s. There is no correlation (r = 0.08) between error and speed. The mean error is equal to 1 cm/s and indicates that there is no bias in the model. Thus there is no bias and no systematic effect on speed. The errors can be considered as white noise. It means that the model 1 can be adopted for the speed computation. For this test the standard deviation of the predicted speed applying model 1 is $\sqrt{\sum error^2/n - 1} = 3.3 cm/s$.

Fig.3.13 illustrates the velocity determined once per second with a Δt interval of 2 seconds (interval in which the data are considered to compute RMS). The data have been collected during a walk on a 400m field track. The speed changes were sudden an numerous. The Δt interval is here not anymore the full walk (which would have given only the average speed) but is limited to 2 seconds to obtain all the changes of speed. The rationale of the 2 seconds is explained in the next section.

The determination of the distance, based on the velocity computed by the first model that has been calibrated with the 100m tests, is 406m. It represents a relative error in the distance of 1.5%.
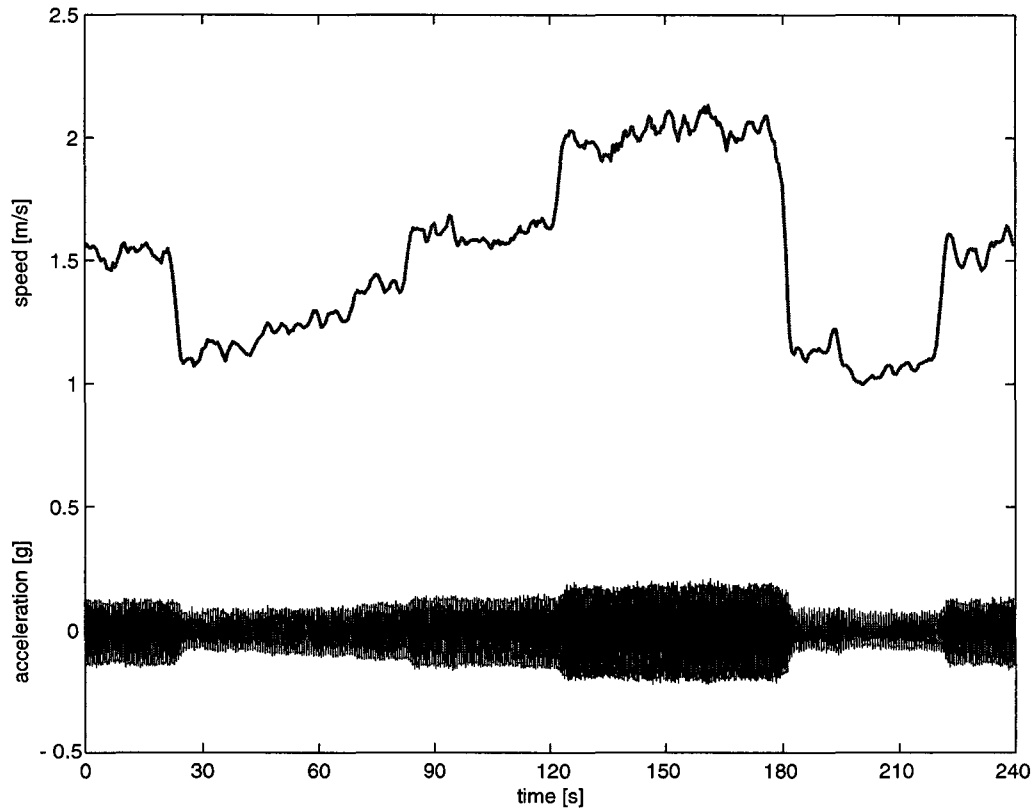
Figure 3.13: Speed computation during a 400m path with frequent speed changes

3.3.5 Computational interval of VAR

The characteristic VAR of the total acceleration must be computed over a certain interval Δt. This interval can be determined in term of seconds or in term of quantity of steps. This section focuses on the determination of the ideal time- or step-interval for the real-time computation of VAR. This interval is defined as the best compromise between the filtering capacity of the speed (by choosing a large interval) and the reaction within a short delay to sudden changes of speed (by choosing a short interval). For example a short time-interval (2 steps or 1 second) can allow the model to react rapidly

to a true speed change. Moreover it will give a noisy speed because the VAR is computed with only few data.
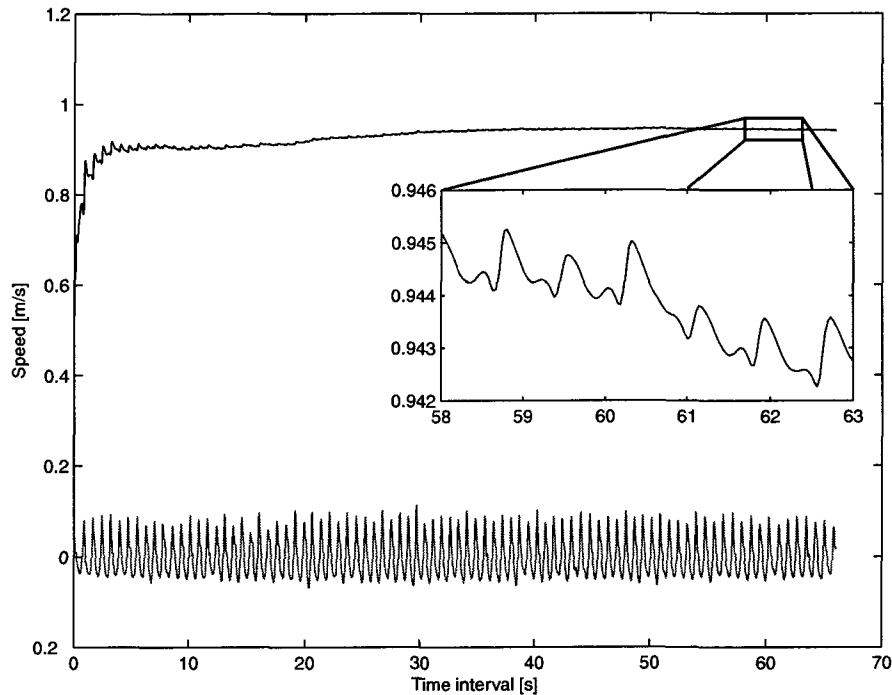
Figure 3.14: Speed computation in function of the time-interval

In this section, the velocity is computed at the same rate as the data sampling, using the first model which is calibrated as presented in section 3.3.1. With a sampling frequency of 30Hz, there are 30 different speeds computed per second. As it will be explained in Chapter 5, the final DR algorithm computes the distance only once per interval and then jumps to the next interval.

The first point is to examine the influence of the time-interval on the speed computation for a distance walked at a quasi-constant speed. The distance is computed through model 1, equation (3.35).

Fig.3.14 illustrates the speed computation. A speed is computed at each collected sample (30 Hz) taking into consideration the last 30 collected a_i samples (1 second). The effect of the steps on the characteristic VAR is clearly visible with a short time interval. Indeed, as illustrated in the inside box of Fig.3.14, the influence of the steps is always present.

72
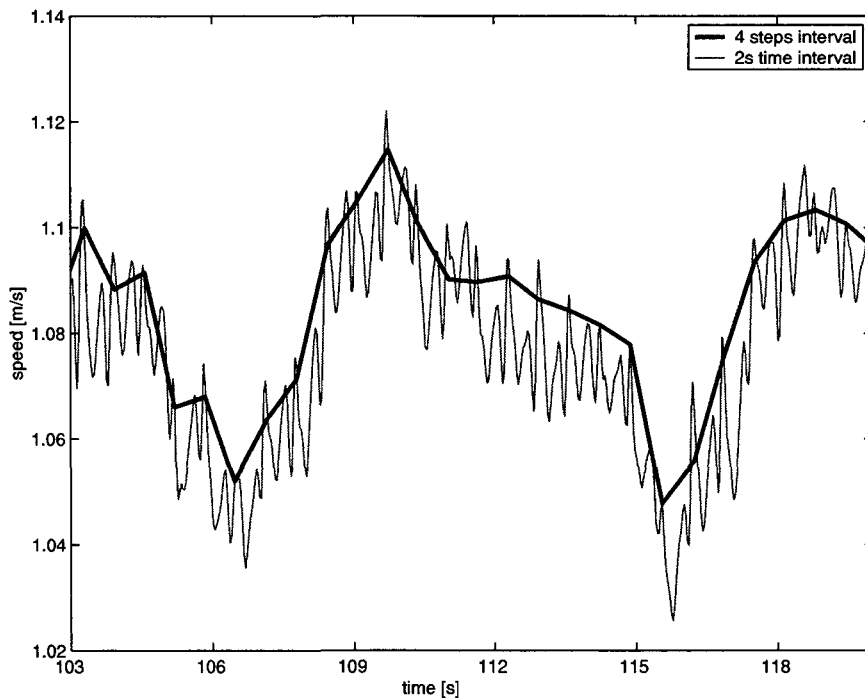
Figure 3.15: Speed computation with a 2 second time-interval and an interval of 4 steps

If the interval is not counted in time but in steps, then it can be expected that the determined speed will be more constant. A comparison between step-interval (4 steps) and time-interval (2 seconds) is made in Fig.3.15, where the velocity computed with a step based interval is always in the upper part of the one computed with a time based interval. For the step-based interval, the velocity is computed at each step taking all the a_i samples collected during the last 4 steps. For the time based interval, the velocity is computed at each sample a_i, considering all the a_i samples collected during the last 2 seconds. Actually, when using a step based interval, i.e. an interval going from a maximal peak to the next one we have the maximal VAR value. Changing a little bit the interval will conduct to a diminution of the VAR value and then of the determined speed.

Fig.3.16 shows the velocity computed at each step occurrence, with a computational interval of 2 steps. The result is very noisy and is subject to errors if the steps are not well detected. The lower peak at the beginning of
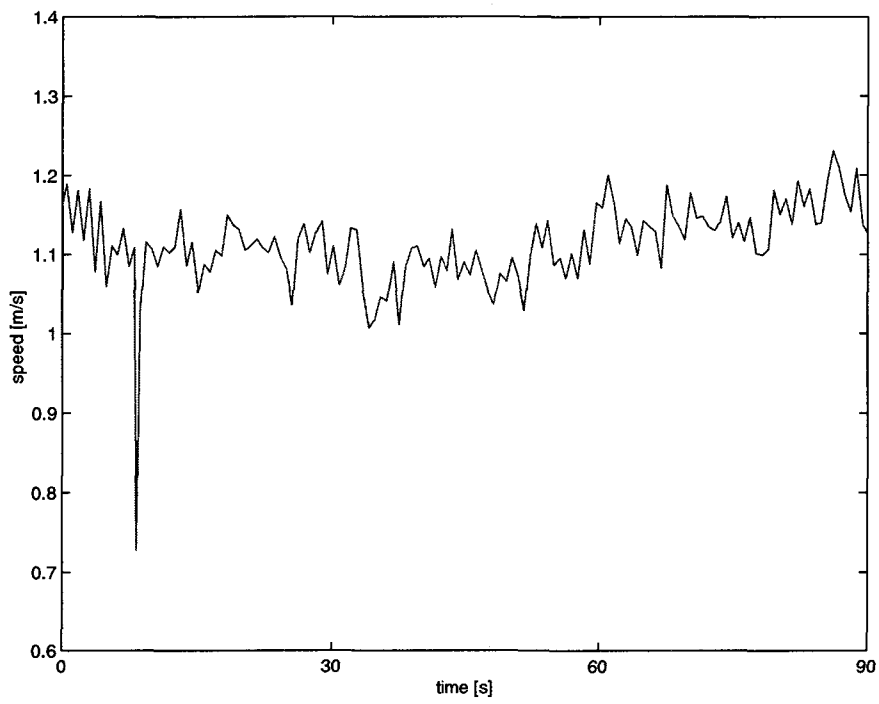
Figure 3.16: Speed computation with a 2 steps interval

the samples (around 8 seconds) is typical of the type of errors.

Fig.3.17 compares different velocities computed with different time intervals (1 second, 2 seconds and 10 seconds). The velocity is computed at each sample a_i (30 times per second). The filtering capacity of the long time-interval is obvious.
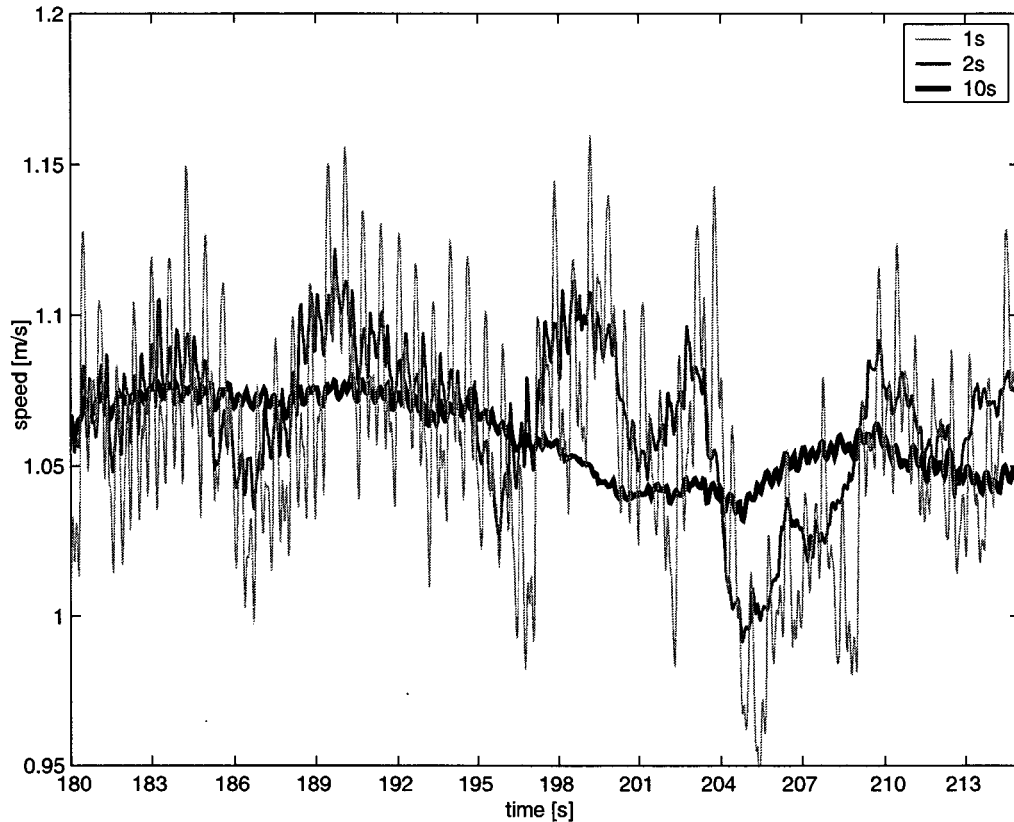
Figure 3.17: Speed computation with a 1, 2 and 10 seconds time interval

Finally the chosen interval for the distance algorithm is a compromise between filtering and reaction. It is fixed to 2 seconds.

3.4 Integration of 2nd method with GPS

Until this point in the second method, the computation of the distance is based only on the accelerometers signal: a purely DR approach. In this section, the integration of this distance determination method with GPS is presented.

3.4.1 Unconstrained calibration

This second type of calibration is called unconstrained because no special action is asked to the pedestrian. The calibration occurs when the person is performing usual activities. The constrained calibration yields good results. However the parameters must be controlled and adapted when external conditions change. By external conditions we consider:

- slope

- lateral orientation of the sensor

- ground surface

- shoes

Some of these elements can be measured and taken into account in the models. For example, a barometer can provide information about the slope. Aminian develops a technique based on neural network to estimate speed and slope out of an signal coming from an accelerometer worn by a runner [Herre99]. The results show an accuracy of 12 cm/s for the speed and 1 degree for the slope. However the implementation of the algorithm in a real-time system is heavy. The establishment of the neural network for a single person requires lots of tests made under different conditions of speed and slope.

The lateral orientation of the sensor is the incline of the sensor about the antero-posterior axis. Ideally this incline is $0°$ and the gravity field is fully sensed by the two accelerometers. Any change of the lateral inclination will reduce the gravity field and a change will occur in the computation of VAR for an identical speed. A gyroscope could measure this lateral incline. However its determination cannot be precise with low cost sensors. A third accelerometer can bring another solution: the orientation of the sensors has then no influence for the computation of VAR.

The two last external conditions are not measurable in real time. Then an unpredictable change of the model can occur.

Kalman filter design for the calibration

The main idea of the unconstrained calibration is to refine the parameters of the chosen model during the walk with the help of GPS measurements. This is done by a Kalman filter. Let us begin with a simple statement considering a pedestrian walking on a straight line and applying the first model for speed

determination (3.35). The GPS speed $speed_{GPS}$ is compared with the DR speed $speed_{DR}$. Ideally we have:

$$speed_{GPS} = speed_{DR} = \check{A}\sqrt{VAR} + \check{B} \tag{3.52}$$

Introducing the increments dA and dB of the parameters and a residual on the GPS speed $v_{speed_{GPS}}$, equation (3.52) becomes:

$$speed_{GPS} - v_{speed_{GPS}} = (A + dA)\sqrt{VAR} + (B + dB) =$$
$$speed_{DR} + dA\sqrt{VAR} + dB \tag{3.53}$$

then we have the observation $z = speed_{GPS} - speed_{DR}$

$$z - v_{speed_{GPS}} = speed_{GPS} - speed_{DR} - v_{speed_{GPS}} = dA\sqrt{VAR} + dB =$$
$$\left[\sqrt{VAR} \ \ 1 \right] \cdot \left[\begin{array}{c} dA \\ dB \end{array} \right] \tag{3.54}$$

The equation (3.54) is the observation model of the KF. The stochastic part of this model is the accuracy of the instantaneous GPS speed $speed_{GPS}$ that can be fixed to 20 cm/s [NATO91] for a GPS receiver using the carrier smooth code algorithm [Hatch82] to measure velocity. Most of the receivers obtain an approximation of the carrier by considering the doppler shift.

The kinematic model for the parameter dA and dB is simple. The functional part says that

$$\left\{ \begin{array}{rcl} \dot{dA} & = & 0 + u \\ \dot{dB} & = & 0 + u \end{array} \right. \tag{3.55}$$

where

u is a white noise with a spectral density of quu that has a numerical value of 0.01.

dA and dB are then considered as random walks, i.e. integration of a white noise. Another possibility is to consider both parameters as a Gauss-Markov process [Brown97].

The outputs of this filter are the new estimated parameters $\hat{A}$ and $\hat{B}$ that will be used to compute with equation (3.35) the DR speeds $\tilde{speed}_{DR}$ until the next update.

RMS **filtering**

Another parallel process can also be performed to filter the *RMS* value to make it less noisy for the speed computation. A standard low pass filter can be applied, however a Kalman filter is the alternative proposed here. To filter a signal with a Kalman filter, the signal is considered as an external measurement and the signal error must be modelled with a random process. For *RMS* a Gauss-Markov process has been chosen with a correlation time of $\alpha = 1/2s$. We have then:

$$d\dot{R}MS = \exp^{-\alpha t} \cdot dRMS + G \cdot u \tag{3.56}$$

where the numerical value of q_{uu} is set to 0.01.

The observation model has a simple functional part:

$$\mathbf{H} = [1] \tag{3.57}$$

The stochastic part of the observation model is the covariance matrix of the *RMS*:

$$\mathbf{Q}_{\ell\ell} = 0.03^2 [m^2/s^3] \tag{3.58}$$

this corresponds to a standard deviation of the velocity of $5cm/s$.

No reset of the *dRMS* is performed, that means that the predicted *dRMS* is not 0.

Fig.3.18 illustrates the filtering of the *RMS* signal itself by a Kalman Filter.

Merged Kalman Filter

Finally the next Kalman Filter merges the individual parameter KF and the *RMS* KF. It is a combination of the two filters (3.55) and (3.56). The kinematic model is:

$$\dot{\mathbf{x}} = \mathbf{F} \cdot \mathbf{x} + \mathbf{G} \cdot u = \begin{bmatrix} 0 & 0 & 0 \\ 0 & 0 & 0 \\ 0 & 0 & -\alpha \end{bmatrix} \cdot \mathbf{x} + \begin{bmatrix} 0 \\ 0 \\ 1 \end{bmatrix} \cdot u \tag{3.59}$$
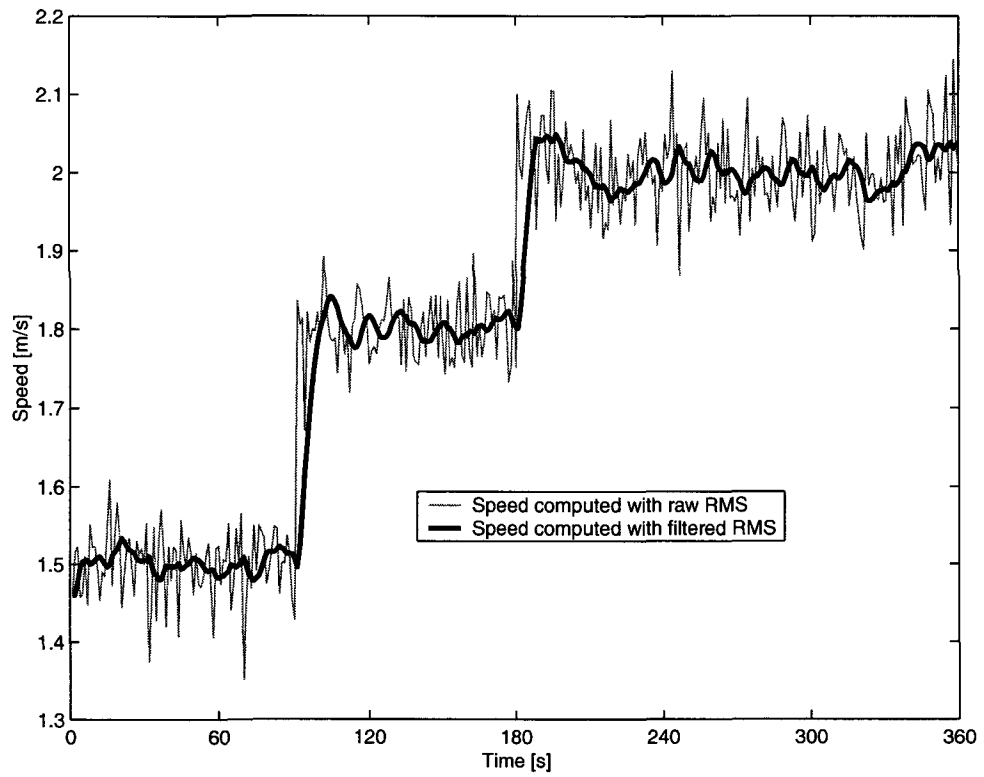
Figure 3.18: Simulation of a pedestrian walk with a change of external conditions and a real speed change. The *RMS* is filtered through a Kalman Filter

The observation model is then:

$$z - v = \begin{bmatrix} RMS & 1 & A \\ 0 & 0 & 1 \end{bmatrix} \cdot \begin{bmatrix} dA \\ dB \\ dRMS \end{bmatrix} \tag{3.60}$$

The outputs of this filter are the new estimated parameters $\hat{A}$, $\hat{B}$ and $\hat{RMS}$ that will be used to compute with equation (3.35) the DR speed.

3.4.2 Simulation

These filters are now illustrated through simulation. Fig.3.19 and Fig.3.20 illustrate the result of a simulation of a walk applying first the A and B filter presented in (3.55) and then the merged filter (A, B and RMS) proposed in equation (3.59). The GPS speed measurements are available during the entire path. The updates are performed each time a GPS velocity is observed, i.e. once per second. Two special events are simulated.

The first one (after 90 second) is a change of the external conditions (ground surface or slope) without modification of the true speed. It creates an error in the DR speed computation $speed_{DR}$. This error is due to the fact that the RMS value changes because of the modification of external condition, while the estimated A and B parameter are staying constant. Thus, the $speed_{DR}$ computation process continues to use the wrong, not corrected, individual parameter. To avoid an error when the external conditions change, the individual parameters A and B have to change also to allow the equation (3.35) to issue the same velocity. The GPS measurements $speed_{GPS}$ will allow to calibrate again, in real time, the individual parameter, thanks to the proposed Kalman Filter.

The second event is a real change of speed (from $1.5m/s$ to $1.7m/s$). It occurs at time 180s. Here, the individual parameter can remain constant because there is no change of the external condition. The $speed_{DR}$ computation process reacts then perfectly because A and B remains correct and the RMS changes due to the change of the true speed produce the needed effect in equation (3.35).

As shown in both figures, the GPS speed measurements allow to correct the A and B parameters after the first event. During the second event, the GPS+DR speed follows immediately the true speed because of the change of the RMS induced by the true change of velocity. As the GPS speed $speed_{GPS}$ changes also there is no effect of the filter in the first figure. However, due to
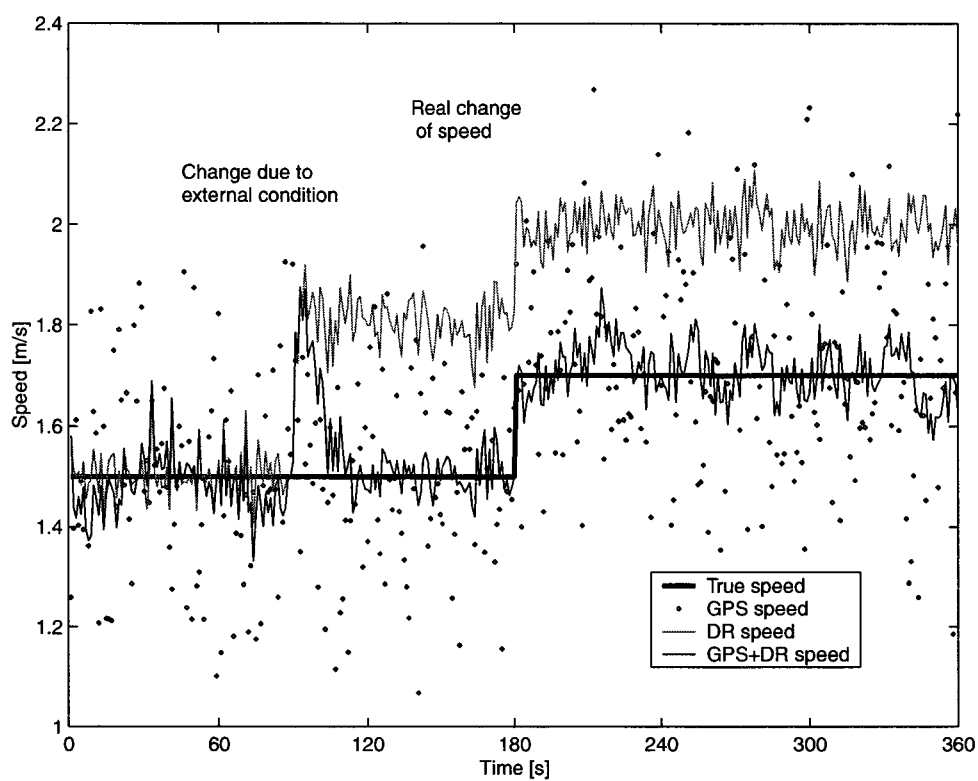
Figure 3.19: Simulation of a pedestrian walk with a change of external conditions and a real speed change. The individual parameters A and B are filtered through a Kalman Filter

the *RMS* filtering, the second figures shows that the *RMS* filter produced some unwanted effects in this case.
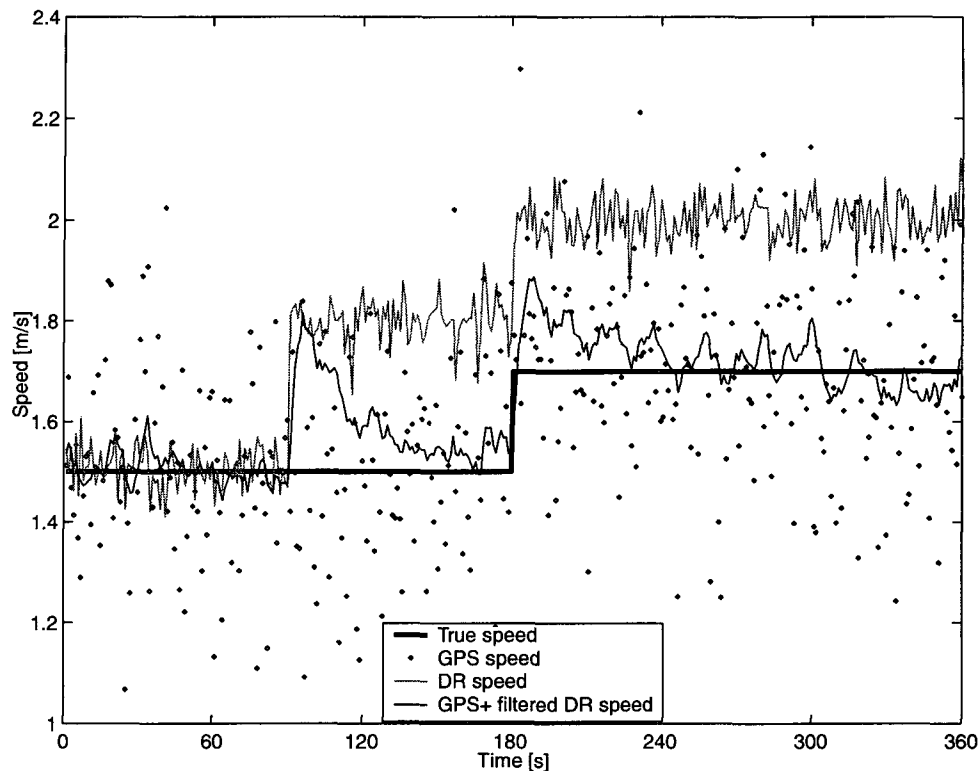
Figure 3.20: Simulation of a pedestrian walk with a change of external conditions and a real speed change. The individual parameters A and B as well as the *RMS* are filtered through a Kalman Filter

This simulation shows a way to calibrate the individual parameters when GPS is available. The choice to filter or not the *RMS* has not a critical influence on the final result (the walker's speed). The filtering of the *RMS* is decreasing the capacity of the filter to correct the parameters. However, in case the parameters are not changing and the speed remains constant, the filtering of the *RMS* allows to create a smoother estimation of the speed. Finally, the filtering of the *RMS* has not been retained because it brings more computational effort and the advantages are not obvious.

It is also possible to filter the GPS velocity *speed$_{GPS}$* in a separate filter before using it as external measurement for the distance Kalman Filter

(3.54). The redundancy of filter at each stage of the process is useless as the KF proposed here have the same function. So this solution has not been investigated further.

A centralised Kalman filter will be presented Chapter 5, using the filter developed in this chapter. At the same time, real data will be used to validate the simulation result presented in this chapter.

3.4.3 Limitations of the distance determination models

The present chapter shows tests and algorithms that have been developed for a walking person. The limitations of those algorithms are various and must be mentioned.

1. Limitation with the slope:

   Ladetto and Perrin demonstrated clearly the limitation of such a speed (or step length) determination model when the slope is greater than 7% [Ladet00a, Perri00].

2. Limitation with the speed (run)

   As mentioned briefly during the present chapter all the tests have been conducted with a walking person. The maximal velocity can go up to 3 m/s , depending on the person. Athletes specialised in walking competition, can travel a distance of 20 km in less than 80 minutes i.e. with an average speed of more than 4m/s!) Similar algorithms can be applied for the run but the biomechanical changes between the walk and the run induce the necessity to adapt the parameters. Moreover a fine activity monitoring can detect when the person is walking or running and then switch to the appropriated model. No model for running have been developed during the thesis, but information can be found in [Herre99]. They show that the considerations taken into account to develop the model for the walk are also valid for the run.

3. Limitation with special movement.

   A pedestrian does not just walk with a quasi-constant speed. He can accomplish a lot of special movements as side-stepping, jumping, going backward etc. The algorithms presented above do not account for those sorts of movements. Special algorithms based on pattern recognition must be applied to detect those unpredictable movements.

3.5 Conclusion

This chapter demonstrates that a good velocity and distance determination can be obtained by the signal of two accelerometers placed on the trunk of the body of a walking person. Ladetto shows also that other algorithms can be implemented to find similar results [Ladet00b] when accelerometers are placed on the back of the pedestrian. The model used is empirical and contains individual parameters i.e. parameters that change from a person to another one and with the different ground structure or other aspects. The calibration of these individual parameters is the crucial phase. It can be done off-line or on-line. The off-line calibration, named constraint calibration, shows that the determination of the parameter allows to compute the distance with a relative accuracy of less than 2% of the travelled distance. For comparison, the first method using classical pedometer allows to reach a precision of about 4cm for the step length determination in a continuous mode, which means a relative error of about 5%. For the on-line parameter determination, GPS velocity measurements are introduced in a Kalman Filter. It allows to adjust the distance determination model to any change of the external conditions. This technique has been demonstrated by simulation in this Chapter. It will be used with real data in the Chapter 5, when the process will be included in a centralised Kalman Filter.

Chapter 4

Orientation determination

This chapter presents the way to obtain the orientation of the walk which is, after the distance, the second component of the DR strategy adopted for pedestrian navigation. The first part focuses on the gyroscope technology and associated error sources. Considerations are made on the effects created by placing an angular rate sensor on the body. The effects of the inclination of the sensor and of the body movement are discussed in details. Filtering of the raw data and azimuth computation are finally discussed. Then the combination of gyroscope and GPS is presented. Finally, the use of the magnetic compass for pedestrian navigation is discussed and an algorithm that integrates GPS, gyroscope and compass is proposed.

4.1 Gyroscopes technologies

Gyroscopes are used in many applications to sense the angular rate of rotation or the angle turned by a vehicle or a platform. Before speaking about the usage of the gyro, it is useful to make a brief and general classification of the gyro types. Titterton and Lawrence give more details for interested readers [Titte97, Lawre98].

The first category are the mechanical - also called conventional - gyroscopes. They are composed with a spinning mass. They have the propriety to define a direction in space, which remains fixed in the inertial reference frame (star-fixed). This type of gyroscopes is generally used in gimbals systems to maintain the orientation of a platform. The most precise conventional gyros can reach a precision of less than $0.001^o/h$. The performance varies with size and design. Small conventional gyros that can be carried by a person, are not appropriate for pedestrian navigation.

The vibratory gyroscopes form the second category. The principles of this technology are based on the Coriolis acceleration.
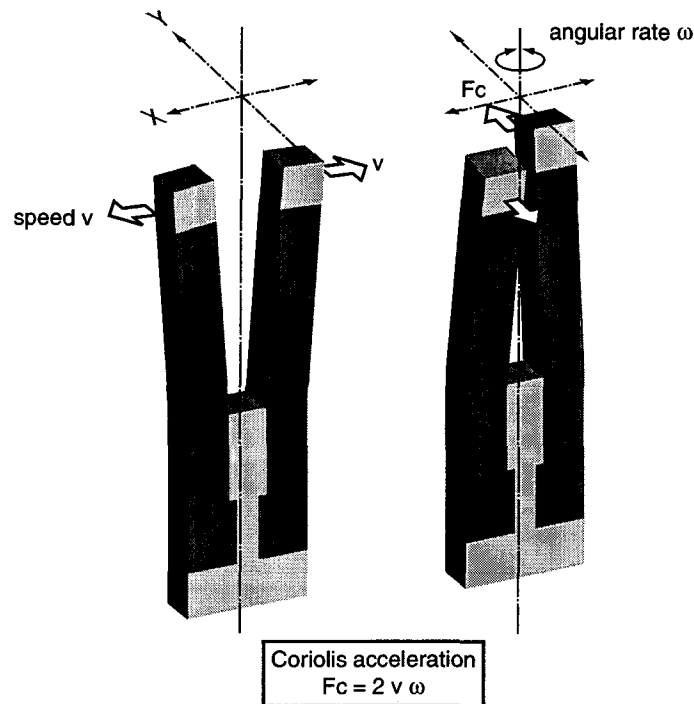
Figure 4.1: A vibrating fork gyroscope based on Coriolis acceleration.

The design of this type of gyroscope is various (single bar, fork, cylinder, hemispherical, ...) but the principles are the same. To illustrate it the tuning fork is now explained (Fig.4.1). An anti-phase vibration is applied intentionally to both piezoelectric bar in one plane. The vibration engenders a sinusoidal varying velocity v. If a rotation ω is applied along an axis that is orthogonal to the velocity plane, then a Coriolis acceleration is induced. The acceleration is orthogonal to both vibration and rotation and modifies the motion of the vibrating element. Electrical circuits are able to sense this modification that is proportional to the rotation. The most common design incorporates a quartz resonator with piezoelectric circuits. The smallest bias that can be obtained with such sensors are about $0.1^\circ/h$. However, typical performances are near 5 to 10 $^\circ/h$. The smallest sensors have bias of 0.1 to 1 $^\circ/s$. The vibrating gyroscopes are less accurate than conventional ones but the miniaturisation capabilities are better. Error modelling of this type of sensors has been investigated in [Marse96, Marse97]

Optical gyroscopes form the third category presented here. There are two

different technologies: fiber optic gyroscopes (FOG) and laser gyroscopes (RLG). The fundamental principle is the same for both technologies: the Sagnac effect [Sagna13a, Sagna13b]. When two light beams travel in a close circuit (circular ring for fiber optic gyro) in opposite direction, the length of the two paths is similar when no rotation occurs. However the lengths are different if the ring is rotated about an axis perpendicular to the plane containing the ring. The Fig.4.2 illustrates this difference that is measured with interferometer, i.e. a phase shift of one bean relatively to the second one. In this figure, both Ω and ω represent the angular rate. L is the increment in the path length. This path difference can then be measured with an interferometer. The difference between laser and fiber optic is the following: in FOG the light beam transits in the fiber and in RLG the light propagates in the air and is reflected by mirrors. The spectrum of performance of optical gyroscopes is wide. The performance of optical gyroscopes is inversely proportional with the size [Barbo01a]. With biases going from less than 0.001 $^o/h$ [Dunn01, FGS98] to tens of degrees, the performance of optical gyroscopes is similar to the conventional gyroscope. However, they offer advantages such as: digital output, high rate capabilities, instant start up.... The size and the price of the sensor conditions the utilisation of this technology in pedestrian navigation domain.

Finally the choice of the technology depends also on market considerations. The vibrating gyroscopes offer the best solution in terms of size and price. As it will be demonstrated below, their accuracy is sufficient for pedestrian navigation. However, the optical technology has a fast evolution [King98] and can offer in the future a good alternative for pedestrian navigation.

4.2 Gyroscope error sources

Lawrence cites different error sources for the gyro [Lawre98]:

- Bias: output of the sensor when input is 0.

- Asymmetry of the scale factor: the scale factor is different for positive and negative inputs

- Non-linearity: the relation between input and output is not linear but has second or third order terms.

- Composite error: small errors in the relation input-output mainly due to hysteresis and resolution.

87
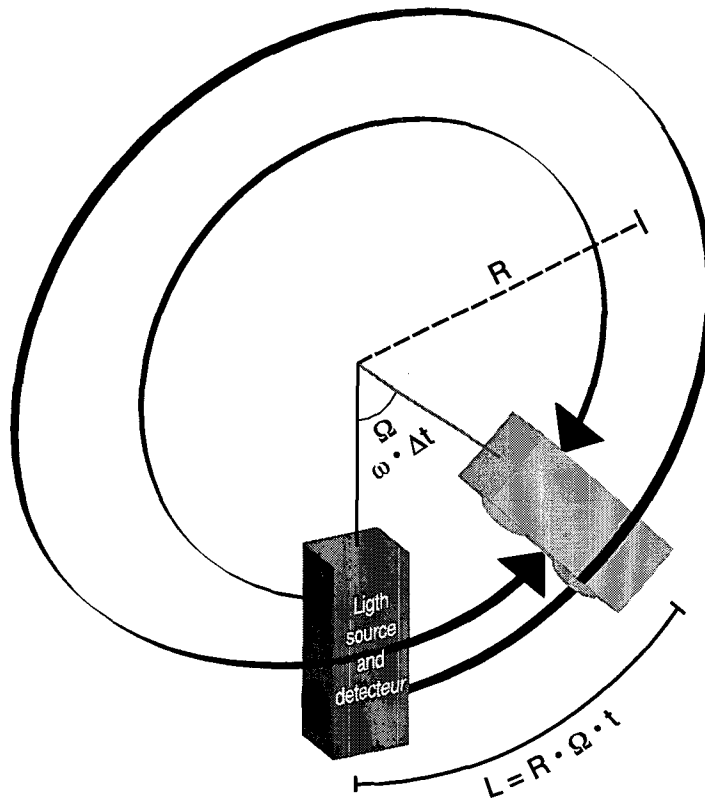
Figure 4.2: The principle of an optical gyroscope (FOG).

- Hysteresis: difference between the output generated by an increasing input and by a decreasing input.

- Day-to-day uncertainty: variation of bias and scale factor between two turns on of the sensor.

- Acceleration sensitivity: a gyroscope is sensitive to acceleration (just like an accelerometer is sensitive to the angular rate!)

- Anisoelasticity: sensitivity of the gyroscope to g^2 (especially for a mechanical gyro)

For the purpose of pedestrian navigation, low cost gyroscopes are used. The main error sources that have to be determined and eliminated are the changes in the bias due to shocks or other sources (anisoelasticity) and the changes in the scale factor mainly due to temperature. Fig.4.3 shows a representation of both bias and scale factor. In this figure, the horizontal

axis represents the physical input that is transformed by the sensor to a numerical output (vertical axis). On this figure other small errors can be seen (component error).
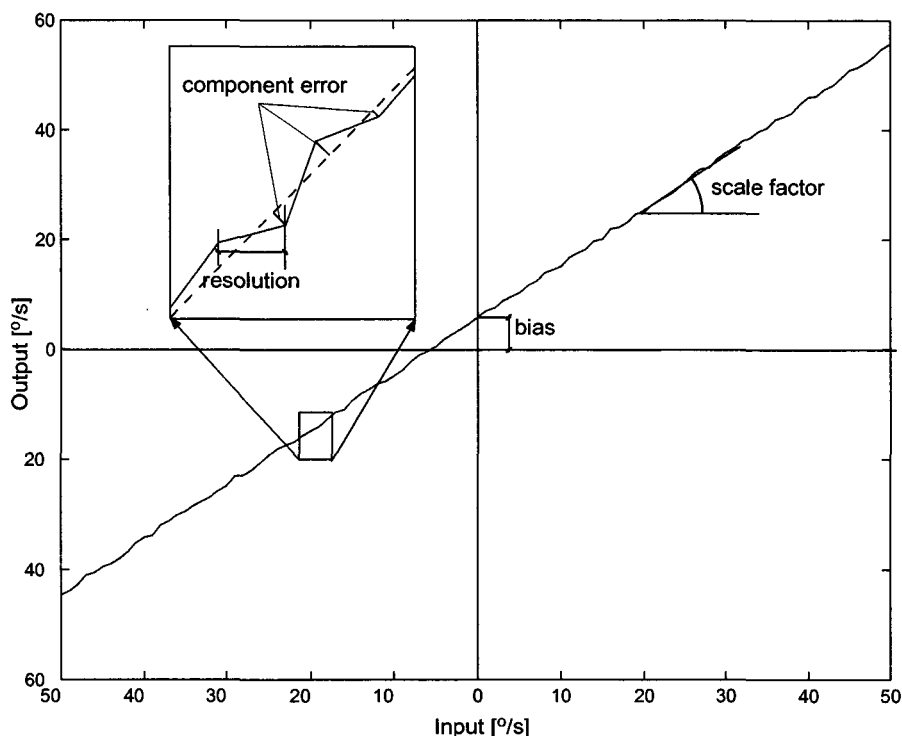
Figure 4.3: Bias and scale factor: the two main error sources.

The Fig.4.4 shows the position error induced by the bias of the gyro for a 2 dimensional approach. The error is computed as follow:

$$\begin{aligned}
\phi_k &= \phi_{k-1} + bias \cdot dt_{k-1}^k \\
E_k &= E_{k-1} + speed \cdot \cos(\phi_k) \\
N_k &= N_{k-1} + speed \cdot \sin(\phi_k) \\
error_k &= \sqrt{(E_k - speed * dt_0^k)^2 + (N_k)^2}
\end{aligned}$$

(4.1)

considering $\phi_0 = 0^o$, $E_0 = 0$, $N_0 = 0$ and $k = 1...n$.

This figure is different from Fig.2.5 because only the horizontal orientation is considered and not the full attitude.

For pedestrian navigation application, considering the chosen system (with only one gyroscope), other error sources or effects have to be considered. This is the purpose of the next section.
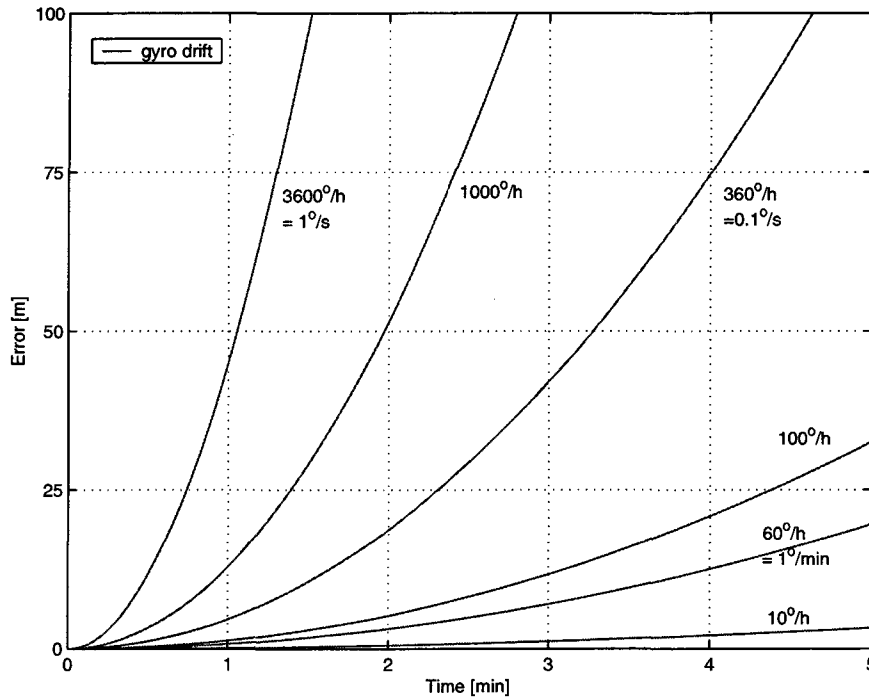
Figure 4.4: Drift in position due to an error in the bias of the gyroscope considering a speed of 1.5 m/s

4.3 Placing a gyro on a body

Assuming the system architecture presented in the Chapter 2, the gyroscope is fastened to the chest. In this section, considerations are presented in relation with the effect of the incline of the sensors and of the movement of the body during the walk. Then an error analysis is made for an unpredictable change of incline of the sensor.

4.3.1 Inclination of the sensor

The ideal situation is that the gyroscope stays vertical. Then it senses only the full change of azimuth. However even with a non-walking person this condition is difficult to fulfill. The question is then: what is the induced error of the non-vertical orientation of the sensor and how can it be eliminated or

reduced? In this section only the incline of the sensor is considered. Effects of the movement of the body is discussed in the next section (4.3.2).
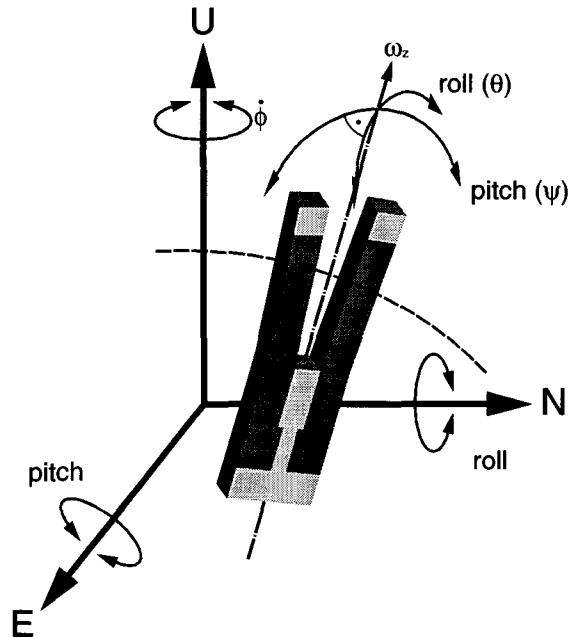
Figure 4.5: Possible inclination angle of the gyroscope

If the sensor is perfectly vertical and without error then the gyro senses the change of azimuth as:

$$\breve{\omega}_z = \dot{\phi} \tag{4.2}$$

where, as illustrated in Fig.4.5, $\dot{\phi}$ is the change of azimuth and ω_z is the output of the gyro (bias and scale factor are here intentionally omitted).

In general, when three gyroscopes are used, the relation between the angles and the output of the gyroscope is:

$$\Omega = \mathbf{C} \cdot \dot{\mathbf{C}} \tag{4.3}$$

where Ω is the vector containing the angles measured by the gyroscope:

$$\Omega = \begin{pmatrix} \omega_x \\ \omega_y \\ \omega_z \end{pmatrix} \tag{4.4}$$

C is the attitude matrix and $\dot{\mathbf{C}}$ contains the rate of change of the attitude angles. In the case of Euler's angles, we have:

$$\dot{\mathbf{C}} = \begin{pmatrix} \dot{\psi} \\ \dot{\theta} \\ \dot{\phi} \end{pmatrix} \tag{4.5}$$

When the sensor is inclined about the y-axis with an angle θ, the the change of azimuth $\dot{\phi}$ will be sensed by the gyro as the following:

$$\begin{pmatrix} \omega_x \\ \omega_y \\ \omega_z \end{pmatrix} = \mathbf{C}_2 \cdot \begin{pmatrix} 0 \\ 0 \\ \dot{\phi} \end{pmatrix} \tag{4.6}$$

where

$$\mathbf{C}_2 = \begin{pmatrix} \cos(\theta) & 0 & -\sin(\theta) \\ 0 & 1 & 0 \\ \sin(\theta) & 0 & \cos(\theta) \end{pmatrix} \tag{4.7}$$

and ω_x, ω_y are the response that would have been received from a gyroscope placed along the x- and y-axis; they are virtual gyroscopes in this specific case where only one gyroscope is used.

The equation (4.6) can also be written as:

$$\begin{cases} \omega_x = -\sin(\theta) \cdot \dot{\phi} \\ \omega_y = 0 \\ \omega_z = \cos(\theta) \cdot \dot{\phi} \end{cases} \tag{4.8}$$

The $\mathbf{C}_2$ matrix represents the rotation θ about the y-axis, called pitch. Euler's angles are chosen as parameters because of their clear mechanical and physical representation.

As $\cos(\theta) \leq 1$ the gyro does not sense the full azimuth change and a virtual gyro placed along the x-axis would also perceive it. An approximation for small angles allows to set down: $\cos(\theta) = 1$ and $\sin(\theta) = \theta$. A more detailed discussion is made below.

Now another inclination is considered. The gyroscope rotates about the x-axis with an angular rate of $\dot{\psi}$, called roll. An azimuth change will then be sensed by the gyroscope as follows:

$$\begin{pmatrix} \omega_x \\ \omega_y \\ \omega_z \end{pmatrix} = \mathbf{C}_1 \cdot \begin{pmatrix} 0 \\ 0 \\ \dot{\phi} \end{pmatrix} \tag{4.9}$$

where

$$\mathbf{C}_1 = \begin{pmatrix} 1 & 0 & 0 \\ 0 & \cos(\psi) & \sin(\psi) \\ 0 & -\sin(\psi) & \cos(\psi) \end{pmatrix} \tag{4.10}$$

then

$$\begin{cases} \omega_x = 0 \\ \omega_y = \sin(\psi) \cdot \dot{\phi} \\ \omega_z = \cos(\psi) \cdot \dot{\phi} \end{cases} \tag{4.11}$$

The combination of both rotation will give:

$$\begin{pmatrix} \omega_x \\ \omega_y \\ \omega_z \end{pmatrix} = \mathbf{C}_1 \cdot \mathbf{C}_2 \cdot \begin{pmatrix} 0 \\ 0 \\ \dot{\phi} \end{pmatrix} = \mathbf{C}_{tot} \cdot \begin{pmatrix} 0 \\ 0 \\ \dot{\phi} \end{pmatrix} \tag{4.12}$$

or

$$\begin{pmatrix} \omega_x \\ \omega_y \\ \omega_z \end{pmatrix} = \mathbf{C}_2 \cdot \mathbf{C}_1 \cdot \begin{pmatrix} 0 \\ 0 \\ \dot{\phi} \end{pmatrix} = \mathbf{C}_{tot} \cdot \begin{pmatrix} 0 \\ 0 \\ \dot{\phi} \end{pmatrix} \tag{4.13}$$

For example, for equation (4.12) we have:

$$\mathbf{C}_1 \cdot \mathbf{C}_2 = \begin{pmatrix} \cos(\theta) & 0 & -\sin(\theta) \\ \sin(\psi)\sin(\theta) & \cos(\psi) & \sin(\psi)\cos(\theta) \\ \cos(\psi)\sin(\theta) & -\sin(\psi) & \cos(\psi)\cos(\theta) \end{pmatrix} \tag{4.14}$$

Then

$$\begin{cases} \omega_x = -\sin(\theta) \cdot \dot{\phi} \\ \omega_y = \sin(\psi)\cos(\theta) \cdot \dot{\phi} \\ \omega_z = \cos(\psi)\cos(\theta) \cdot \dot{\phi} \end{cases} \tag{4.15}$$

The difference between equation (4.12) and (4.13) is the sequences of the rotations. If the rotation about the x-axis is first considered then formula (4.13) is applicable. Any incline of the sensor can be represented by equation (4.12) or (4.13). Numerically the $\mathbf{C}_{tot}$ is the same but the angles θ and ψ are slightly different.

Considering known pitch and roll angles of 5° we get

$$\omega_z = \cos^2(5^o) \cdot \dot{\phi} = 0.992 \cdot \dot{\phi} = \lambda \cdot \dot{\phi} \qquad (4.16)$$

The effect of pitch and roll angles on the sensor is then a scale factor. It is similar to the internal scale factor of the sensor. On-line adjustment, as it will be presented below, will also correct this effect induced by the lack of verticality of the gyroscope.
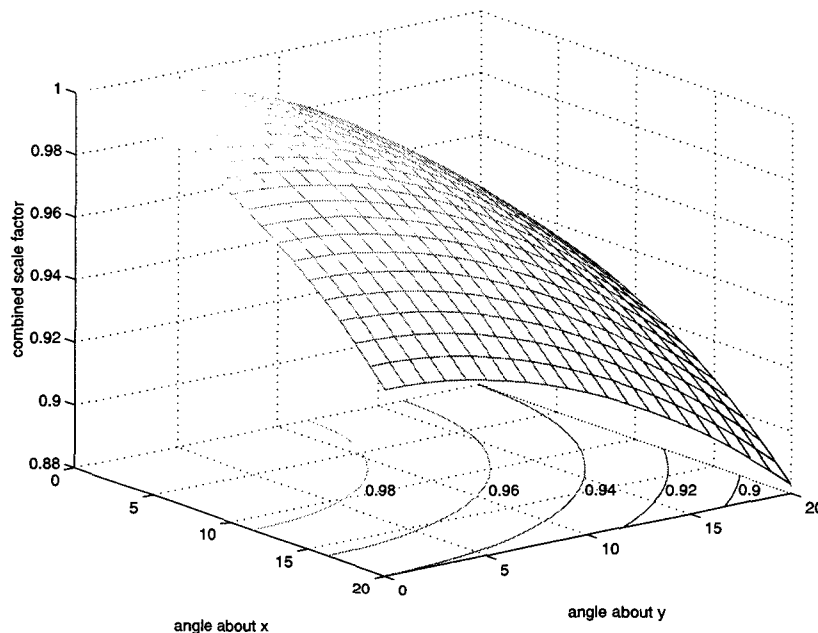
Figure 4.6: Scale factor generated by inclination about x- and y-axis

Fig.4.6 illustrates the scale factor λ for different inclination angles varying from 0 to 20 ^{o} for both x- and y-axis.

4.3.2 Movement of the body

The incline of the sensors is a phenomena that is mixed during the walk with the oscillation of the upper part of the body, especially the chest. To quantify the amplitude of the oscillation three orthogonal gyroscopes (included in the Crossbow DMU-VG product) have been placed on the chest of a person walking on a straight path. The z-axis was placed approximately along the

94

vertical and the x-axis along the walking direction. Fig.4.7 and Fig.4.8 show respectively the raw signal and the integrated angle issued from each gyroscope . The bias of the gyro has been computed as the mean of all the data and the internal scale factor fixed to 1. The full attitude has not been computed here because of the small amplitude of the angles. The initial angles are considered to be zero.
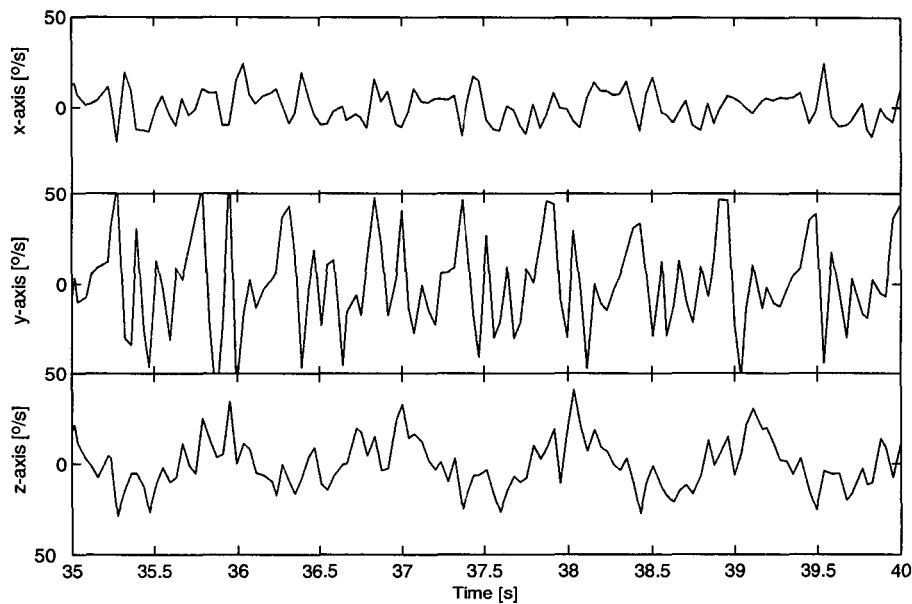
Figure 4.7: Raw signal of the three orthogonal gyroscopes

The amplitude of the oscillation about the x- and y-axis is smaller than 3°. The walking speed of the person during the collection of those data was 1.6 m/s. For higher speed (1.9 m/s) the amplitude increases, especially on the y-axis and can reach 4°. The maximal influence of the oscillation on the measurement is then $\cos^2(3^o)=0.997$ that is 3 $^o/_{oo}$.

This oscillation periodicity is one step about the y-axis and two steps about the x- and z-axis. The signal is closely symmetric, i.e. the shape of the signal is similar for left and right steps. Asymmetry between left and right steps depends on the person and can be more important for elderly people walking with a stick or for injured persons. However the time integration of ω_x or ω_y over two steps returns an angle change of about $0^o \pm u$ where u is a white noise. Thus, an average inclination of the sensor can be considered and taken into account as a single parameter. Then, the oscillation itself, due to the steps, can be neglected.
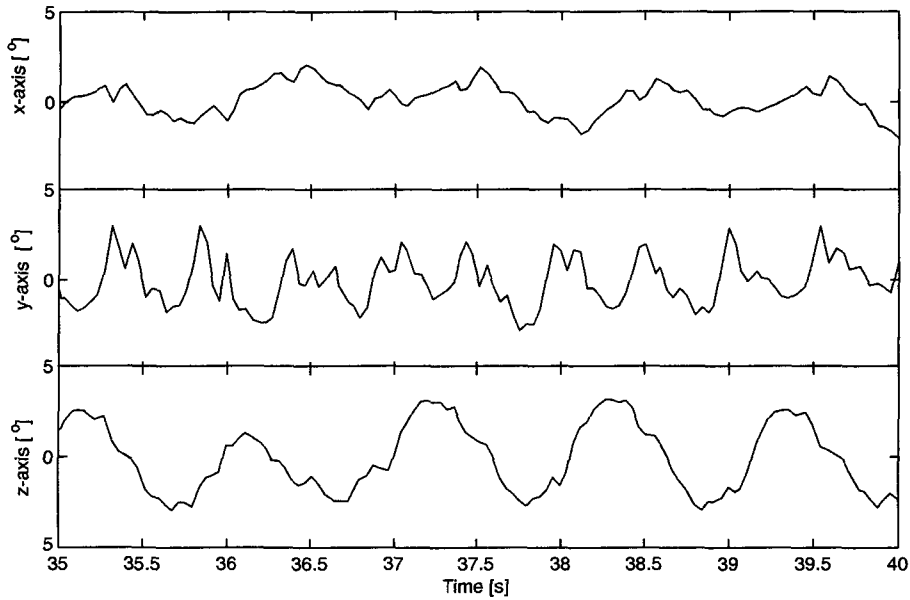
Figure 4.8: Oscillation angle computed from the signal of the three gyroscopes

4.3.3 Unpredictable errors in the inclination

From the last two sections, it appears that the oscillation due to body movement has no major influence for the orientation and that the average inclination of the sensor can be handled by the adjustment of the scale factor. The difficulty comes from an undetected change of the average inclination, when no adjustment is possible. This type of changes can occur by an abrupt movement of the person or by a modification of the fixation system. To analyse the effects of this change of inclination on the output of the gyroscope, it is necessary to make an error propagation analysis. Then, the equation (4.15) has been linearised to obtain:

$$d\omega_z = \frac{\partial(\cos(\theta) \cdot \cos(\psi) \cdot \dot{\phi})}{\partial(\theta)} \cdot d\theta + \frac{\partial(\cos\theta \cdot \cos(\psi) \cdot \dot{\phi})}{\partial(\psi)} \cdot d\psi \qquad (4.17)$$

$$d\omega_z = -\sin(\theta) \cdot \cos(\psi) \cdot \dot{\phi} \cdot d\theta - cos(\theta) \cdot \sin(\psi) \cdot \dot{\phi} \cdot d\psi \qquad (4.18)$$

Equation (4.3) offers another way to obtain the error on the vertical gyroscope induced by the inclination change. The effect of inclination can be

considered as similar to the effect of an attitude error, i.e. an error in $\mathbf{C}_{tot}$. The difference between the true attitude $\mathbf{C}_{tot_{true}}$ and the $\mathbf{C}_{tot}$ is:

$$\mathbf{C}_{tot_{true}} = B \cdot \mathbf{C}_{tot} \tag{4.19}$$

where $\mathbf{B}$ must be close to the identity matrix $\mathbf{I}$. Then, we have:

$$\mathbf{B} = \mathbf{I} - \Psi \tag{4.20}$$

where Ψ contains the small inclination angle:

$$\Psi = \begin{bmatrix} 0 & 0 & d\theta \\ 0 & 0 & -d\psi \\ d\theta & -d\psi & 0 \end{bmatrix} \tag{4.21}$$

In an ideal situation we will get:

$$\Omega_{true} = \mathbf{C}_{tot_{true}} \cdot \dot{\mathbf{C}} \tag{4.22}$$

where $\dot{\mathbf{C}}$ contains only the rotation $\dot{\phi}$.

Introducing equation (4.19) in equation (4.22), we have:

$$\Omega_{true} = \mathbf{B} \cdot \mathbf{C}_{tot} \cdot \dot{\mathbf{C}} \tag{4.23}$$

Replacing $\mathbf{B}$ by equation (4.20), we obtain:

$$\Omega_{true} = \Omega - \Psi \cdot \mathbf{C}_{tot} \cdot \dot{\mathbf{C}} \tag{4.24}$$

Finally the error in the angular rate measured by the gyroscopes, $d\Omega$ is defined as:

$$d\Omega = \Omega_{true} - \Omega \tag{4.25}$$

which means that:

$$d\Omega = \Psi \cdot \mathbf{C}_{tot} \cdot \dot{\mathbf{C}} \tag{4.26}$$

By computing this equation we have:

$$d\omega_z = (\sin(\theta) \cdot d\theta + \sin(\psi)\cos(\theta)d\psi) \cdot \dot{\phi} \tag{4.27}$$

97

Let us consider that an uncalibrated change of 5° occurs. The error $d\theta$ and $d\psi$ have values of 5° (θ and ψ values are arbitrarily set to 5°). The error on ω_z is: $d\omega_z = 0.015 \cdot \dot{\phi}$. The propagation of this error in the position is computed considering an average speed of 1.5 m/s with constant turns of 10 $^o/s$. $d\omega_z = 0.015 \cdot 10 = 0.15^o/s = 540^o/h$. The effect of such an error on position can be visualised using the Fig.4.4: an error of 50m after 3 minutes.

If the pedestrian does not turn ($\dot{\phi} = 0$), then an error in the inclination of the sensor ($d\omega_z$) does not produce any error in orientation and, then, in position.

4.4 Signal extraction

The gyroscope outputs are a mix of:

- real turn

- oscillation due to the body and

- sensors errors.

The next three paragraphs of this section investigate the way to obtain the real turn from the output.

Investigations have been done to determine if the gyroscope can provide a suitable orientation to the DR algorithm. Critical situations are defined as fast and very slow turns. Fast turns are critical because of the measurement band of the sensor. Usually, gyroscopes used for car navigation have a band of 100 to 200 $^o/s$. In pedestrian navigation, a quick turn can produce a rotation greater than the measurement band. Nevertheless, for a same type of gyro, increasing the band will decrease the resolution of the sensor and then the accuracy. A trade-off has been made between the resolution and the measurement band. The slow turns are also critical because the signal is completely hidden by the oscillations.

4.4.1 Wavelet analysis

The analysis of the signal and the separation between the turn and the oscillation has been done by applying the wavelet transformation [Chui92, Olivi91]. This technique allows to represent general functions in term of simple and

fixed blocks, at different time and at different scale. These blocks are called wavelets. They are generated from a mother wavelet by scaling and translation operations. The type of wavelet transformation process is generally characterised with the name of the mother function (Meyer, Haar ...).

The wavelet transform is an appropriate tool to analyse signals for which the frequencies change with time. A gyroscope placed on a walking person produces such a signal. The frequency of the oscillation depends on the velocity and then changes with time. Furthermore turns produce special events from time to time that modify the frequency characteristics of the signal. The raw signal has been logged during a walk containing short and long turns. It is decomposed with a symlets wavelet (sym8) that is suitable for this type of signals. The use of a Meyer wavelet is also adapted [Matla98, Olivi91]. The decomposition is done up to level 5. Fig.4.9 illustrates the raw signal at its approximation level. The detail levels are not shown. The wavelet analysis shows that this type of gyroscope can provide the information on turns, despite the oscillations.

The raw signal shows clearly the effect of the oscillation of the trunk during the walk. The approximate signal has no pattern of steps and reproduces the effective turn.

The wavelet analysis allows to pass from a bio-mechanical consideration of the walker (with all the oscillations) to a navigation consideration of the pedestrian (single point) having a non-oscillating orientation.

4.4.2 Low pass filter

The raw data can also be filtered through a low pass filter to eliminate the high frequency noise and to diminish the effect of trunk oscillation. It is desirable to keep the filter length short; otherwise it causes a delay for the real-time computation.

Design of the filter

The filter must have a finite impulse response (FIR filter) to avoid scaling the data. The used algorithm, proposed by the Matlab®toolbox, uses the Parks-MacLellan optimal equiripples filter. Fig.4.10 gives, in frequency (first column) and time domain (second column), the raw signal (first row), the filter (seond row) and the filtered signal (third row).
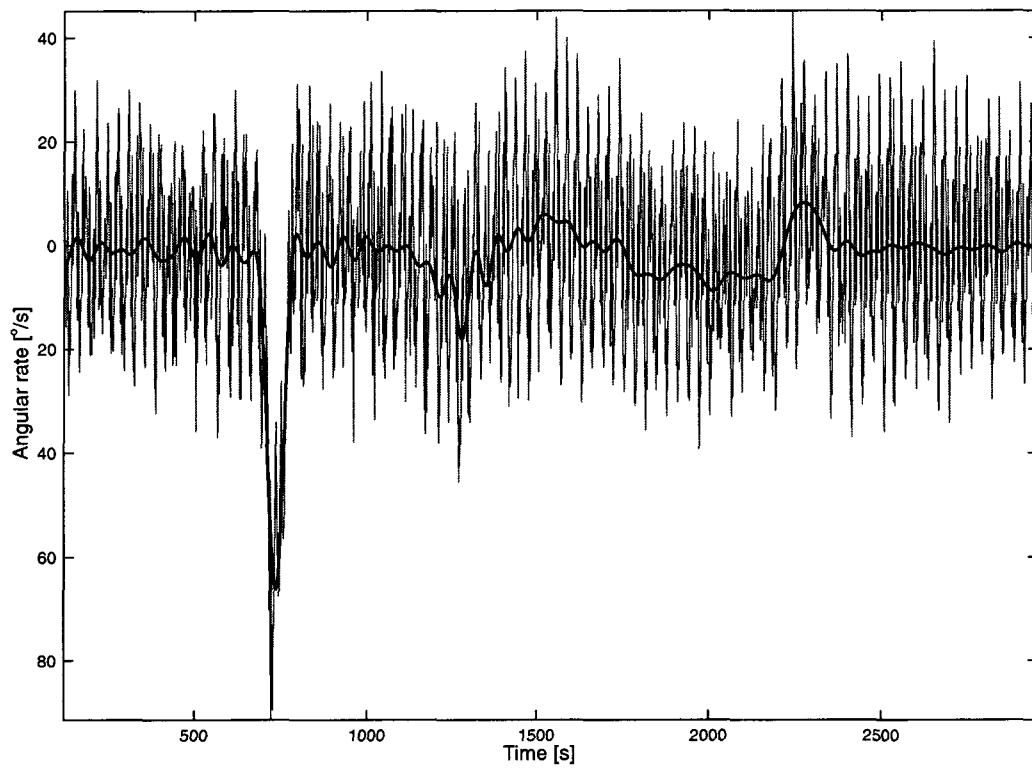
Figure 4.9: Gyro output signal (grey) and approximation (bold) at level 5 (symlets, 8).
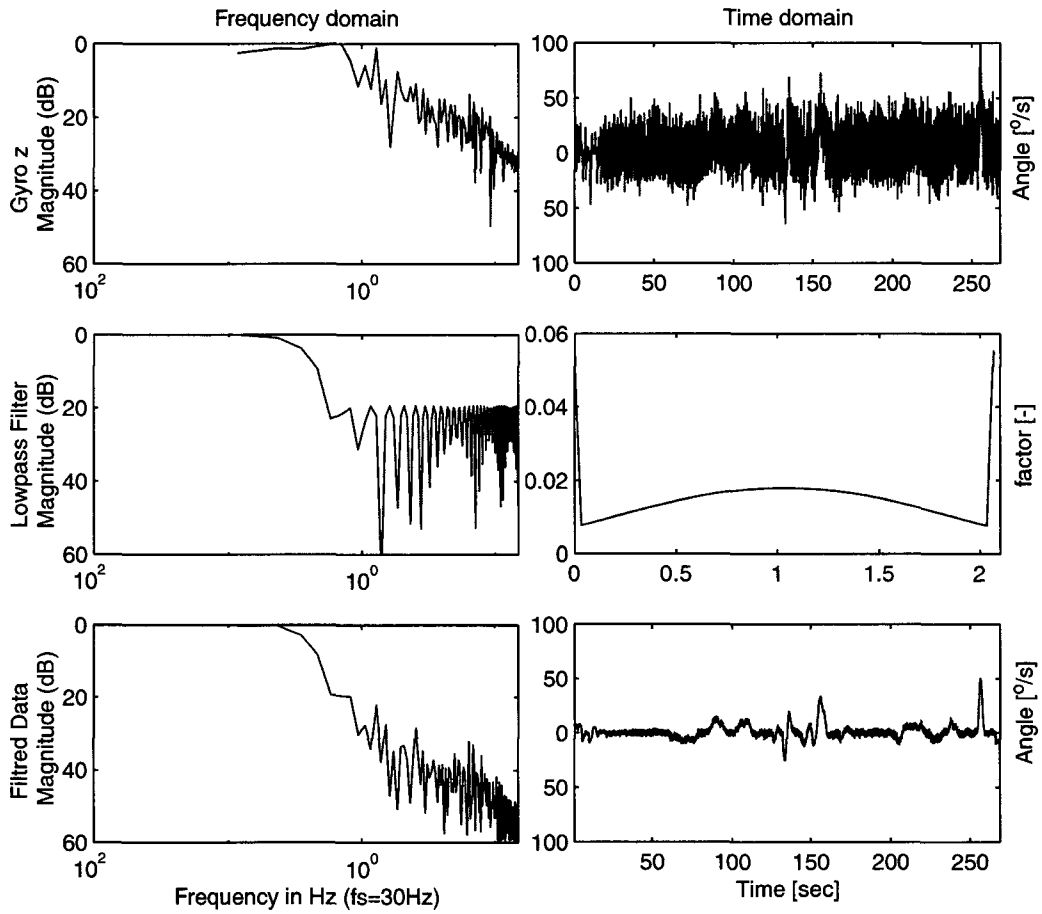
Figure 4.10: Filtering the raw signal. The left column shows the raw signal (up), the filter impulse response (middle) and the filtered signal in the frequency domain. The right column shows the same elements but in the time domain

101

The transition band of the filter must be large to keep a small time delay to the filter. In the chosen filter the delay is 1 second. The transition band of the filter is included between 0.1 Hz and 0.45 Hz.

Result

Several trials show that the azimuth computed with the filtered data is not significantly better that the one computed directly with the raw data. The filtered signal provides similar results than the unfiltered one (see Fig.4.11).

However, the filtering process provides a better instantaneous azimuth of the walk that can be easily compared with another azimuth provided by another sensor.
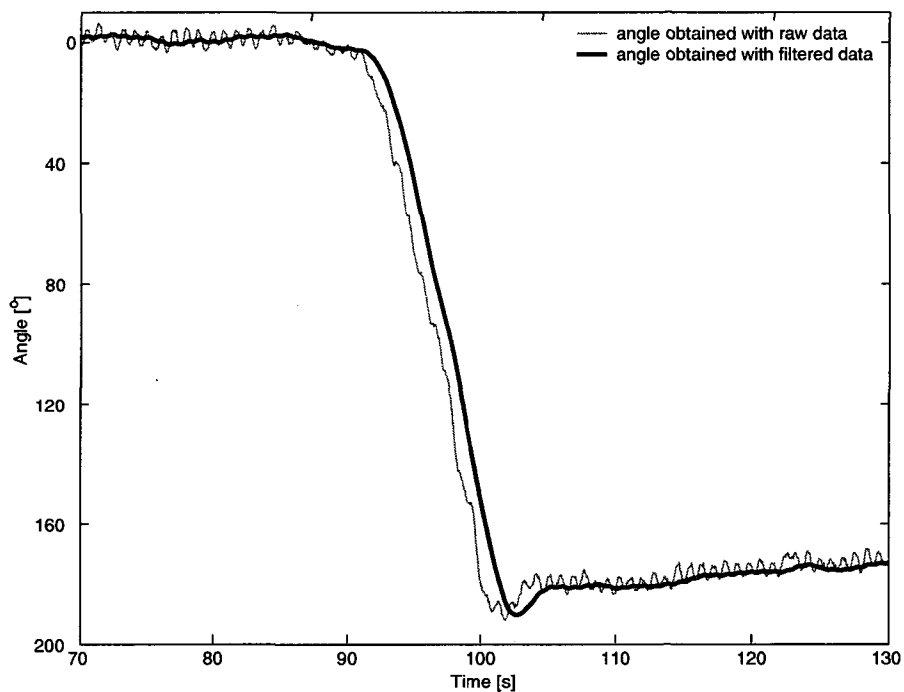
Figure 4.11: Comparison of a 180° turn computed with raw (light) and low-pass filtered (bold) angular rate data

4.4.3 Kalman filter

Instead of filtering the raw signal, it is also possible to filter the azimuth computed with the raw angular rate data. This can be done by a Kalman filter that plays the role of a low pass filter with some advantages as explained in the Appendix A. The Kalman filter can be applied to the raw data or to the azimuth, adding a degree in the process noise (second-order Gauss-Markov instead of a first order). This solution is adopted when the azimuth computed with the gyro ϕ_{gyro} is compared with the azimuth from another device as it will be the case in section 4.7.

Fig.4.12 illustrates the result of such a filter which is very similar in terms of frequency and delay to the results of the low-pass filter.
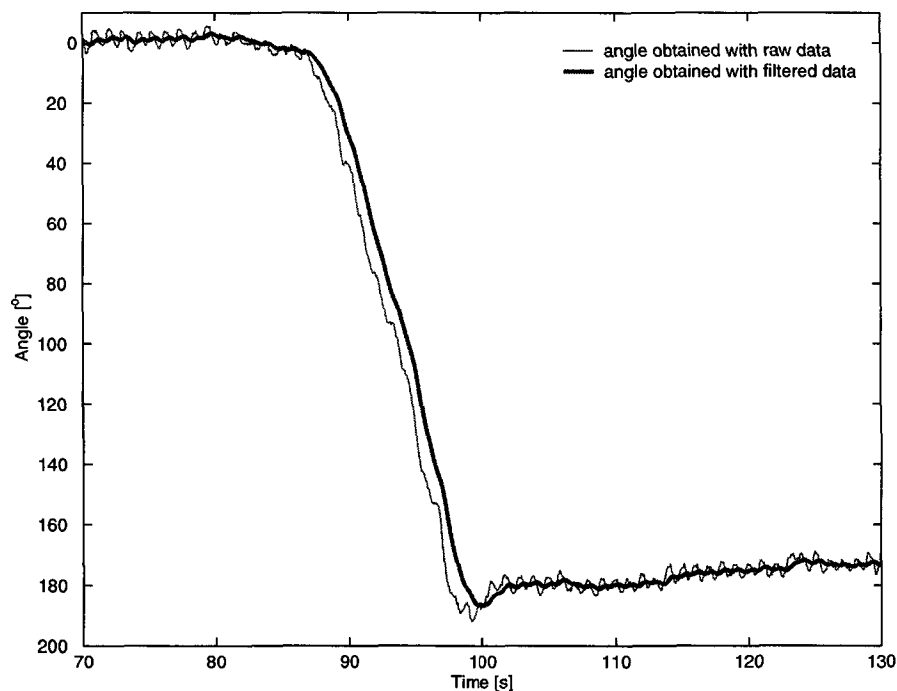
Figure 4.12: Comparison of a 180^0 turn computed with raw (light) and Kalman filtered (bold) angular rate data

The kinematic model of the filter has the following form:

$$\begin{bmatrix} \dot{\phi} \\ \ddot{\phi} \end{bmatrix} = \begin{bmatrix} 0 & 0 \\ 0 & -\alpha \end{bmatrix} \cdot \begin{bmatrix} \phi \\ \dot{\phi} \end{bmatrix} + \mathbf{G} \cdot u \qquad (4.28)$$

where α is the correlation length of the random process (second order Gauss-Markov) driving the error in the azimuth angle.

For reasons explained in the section 4.7, the Kalman filter approach has been finally chosen to filter the gyroscope outputs. Briefly, this technique allows to smooth the data to improve further the results. The wavelet transformation has been used as an analysis tool. A specific investigation has not been performed to implement this technique for the operational system in a real-time mode.

4.5 Orientation computation

Finally to get the azimuth from the gyroscope the following equation is applied.

$$\phi_k = \phi_{k-1} + (\lambda\omega + b)dt \qquad (4.29)$$

where

ϕ_k	orientation at time k
ω	angular rate provided by the sensor (filtered or not)
$\lambda = \lambda_1 \cdot \lambda_2$	scale factor
	λ_1 internal scale factor
	λ_2 inclination scale factor
b	bias
dt	time interval between k-1 and k

Thus an initial orientation must be provided to the system by an external source. The initial orientation will be considered as a parameter of the Kalman Filter presented in the following chapter.

As explained previously, the azimuth computed from the gyro, that is the DR azimuth, is very sensitive to errors in the bias and in the scale factor. Therefore the DR azimuth must be compared and adjusted from time to time with an azimuth coming from another source to keep an acceptable accuracy of the whole system. The two next sections expose the integration of the DR azimuth with GPS (section 4.7) and with a magnetic compass (section 4.8).

4.6 Azimuth measured by GPS

As mentioned in the introduction, GPS is able to provide an unbiased azimuth when the pedestrian, and hence the receiver, is moving. This section will focus on the way to obtain a GPS azimuth and to determine its accuracy. A filtering and smoothing process of the GPS azimuth is also presented. These processes aim at combining the GPS azimuth with the gyro azimuth.

4.6.1 Precision of a GPS azimuth

A GPS azimuth can be obtained in two different ways:

1. using the GPS speed vector, itself computed through the GPS Doppler (or phase rate) measurement

2. computing the difference of two successive positions.

If positions are computed through a carrier smoothed code, which is the case in most GPS receivers, the precision of both methods is equal. Indeed the carrier phase used in the smoothing algorithm is built with the Doppler (or phase rate) measurement.

Using the second method, the precision of the GPS azimuth can be computed theoretically using the same assumptions about time-correlation made in section 3.1.3 where the accuracy of the GPS distance is presented.

The GPS azimuth ϕ_{GPS} is computed as:

$$\phi_{GPS} = \arctan(\frac{dE}{dN}) = f(dE, dN) \tag{4.30}$$

For variance propagation we have the following error equations:

$$d\phi_{GPS} = \frac{\partial f}{\partial dE} \cdot ddE + \frac{\partial f}{\partial dN} \cdot ddN = \mathbf{F}^T \cdot \begin{bmatrix} ddist_E \\ ddist_N \end{bmatrix} \tag{4.31}$$

with

$$\mathbf{F}^T = \begin{bmatrix} \frac{dE}{dE^2+dN^2} & \frac{dN}{dE^2+dN^2} \end{bmatrix} \tag{4.32}$$

Hence, the variance is obtained as:

105

$$\sigma^2_{\phi_{GPS}} = \mathbf{F}^T \cdot \mathbf{Q_{dd}} \cdot \mathbf{F} \tag{4.33}$$

where

$\mathbf{Q_{dd}}$ is computed as presented in equation (3.21).

The correlation ρ needed to compute $\mathbf{Q_{dd}}$ is also based on a correlation length α of 220s. As shown in Fig.4.14 this correlation length α can have a great influence on the precision of the GPS azimuth.

Fig.4.13 illustrates the accuracy of the ϕ_{GPS} in function of the time between the two GPS positions for different values of the time-correlation factor α, eventually fixed to 220s for the used receiver. Fig.4.14 illustrates the accuracy of the ϕ_{GPS} in function of the time between the two GPS positions for different correlations ρ_{EN} between E and N. This correlation depends on the constellation and appears within the matrix $\mathbf{Q_{x_P x_P}}$ computed in equation(3.11).
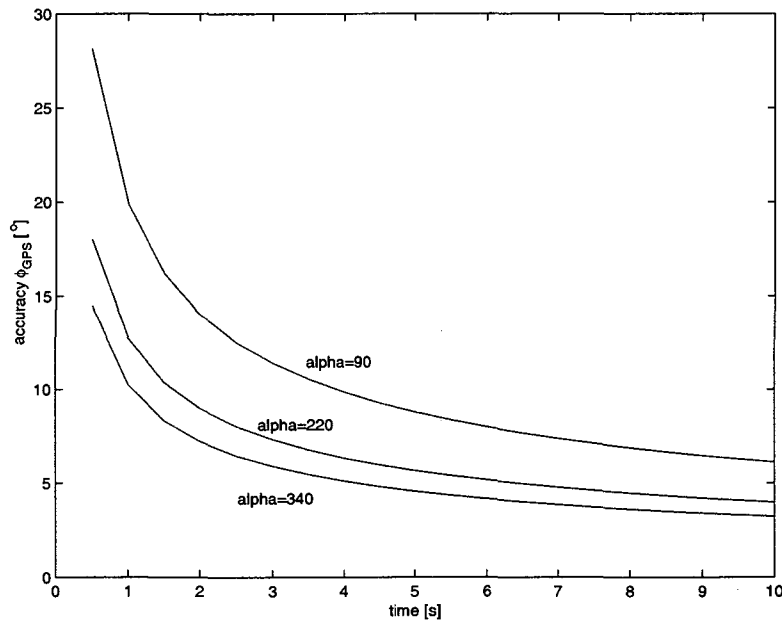
Figure 4.13: Theoretical accuracy of the GPS azimuth in function of time and for different values of the correlation time α (East and North correlation =0)

For a walking person, it is necessary to compute the azimuth over a short time, i.e. for a short travelled distance. If the pedestrian is turning, the
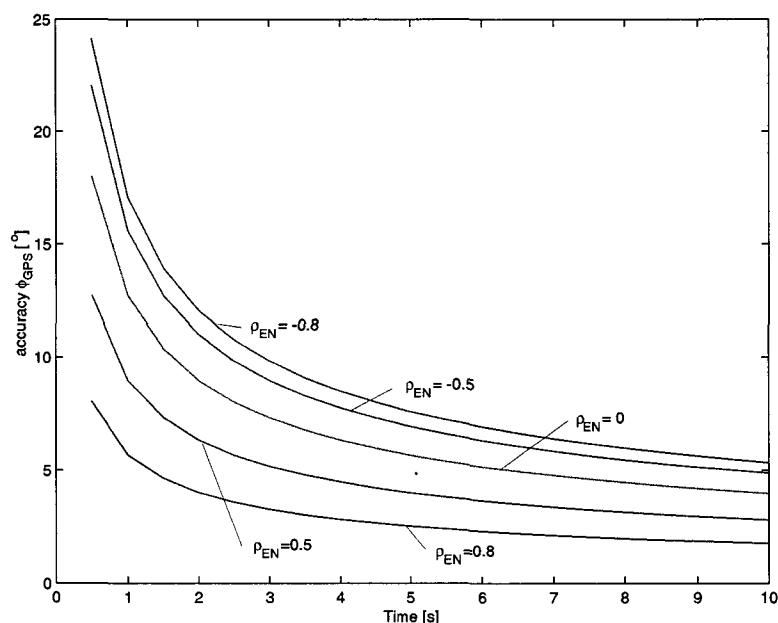
Figure 4.14: Theoretical accuracy of the GPS azimuth in function of time and correlation between the East and North coordinate ($\alpha = 220$)

computed azimuth is not equal to the walking azimuth but to the azimuth of the rope of the curve. If the elapsed time is short then the computed azimuth is assumed to be equal to the walking azimuth.

The theoretical accuracy of the GPS azimuth can be compared with real data. Fig.4.15 shows real azimuth data (light line) computed every 0.5 second. Two important assumptions are made:

1. the theoretical accuracy is pessimistic. The standard deviation of the GPS azimuth, when measured on a straight walking line at $1Hz$, is 8°.

2. the azimuth error is a white noise, uncorrelated in time.

The raw GPS azimuth is not precise enough to calibrate the parameters of the gyroscope efficiently. At this point, a Kalman Filter that accounts for the motion of the pedestrian and for the white noise aspect of the azimuth error is built to improve the GPS azimuth and its accuracy. The result of such a filter is also shown in Fig.4.15.

The theoretical accuracy of the GPS azimuth is improved from 8 to 2° by the Kalman filter. The filter is designed to eliminate the noise. Even better

107

results can be achieved by incrementing the weight of the kinematic model of the KF versus the observation model. However a strong kinematic model will produce a large reaction delay when the pedestrian is turning. The filter will be presented in details in the Chapter 5 as an integrated part of the centralised Kalman Filter.

4.7 Coupling GPS and Gyro azimuth

The idea to integrate gyroscope and GPS for navigation application is not new [Eissf89]. However their integration for pedestrian navigation has not been investigated yet. In this domain, the fact that the sensors are placed on a non-rigid platform forces to find new solutions. However, even after filtering, both data still have an inaccuracy that may lead to large errors when they are combined. A short smoothing algorithm is then proposed to improve the accuracy of the azimuth.

4.7.1 Comparing GPS and gyro azimuths

At this point, a first and simple method to integrate GPS and gyro azimuth is presented. The aim of this integration is to fix or correct the gyroscope bias and then the azimuth. The bias correction can be computed as:

$$db_k = \frac{\phi_{GPS_k} - \phi_{gyro_k}}{time_{k-1}^k} \tag{4.34}$$

And then the corrected bias is:

$$b_k = b_{k-1} + db_k \tag{4.35}$$

Once the bias is corrected, it can be applied to the next gyroscope measurement. It is also possible to correct the azimuth itself. The correction is computed as:

$$d\phi_{gyro_k} = db_k \cdot time_{k-1}^k \tag{4.36}$$

and then the azimuth ϕ_{gyro} at time k is corrected as:

$$\phi_{gyro_k} = \phi_{gyro_{k-1}} + d\phi_{gyro_k} \tag{4.37}$$

The previous four formulae (4.34) to (4.37) form a very simple integration of GPS and gyro data. The full integration process will be presented in a more sophisticated form in the next chapter where the covariance of each information source, as well as a kinematic model for the bias, will be taken into account.
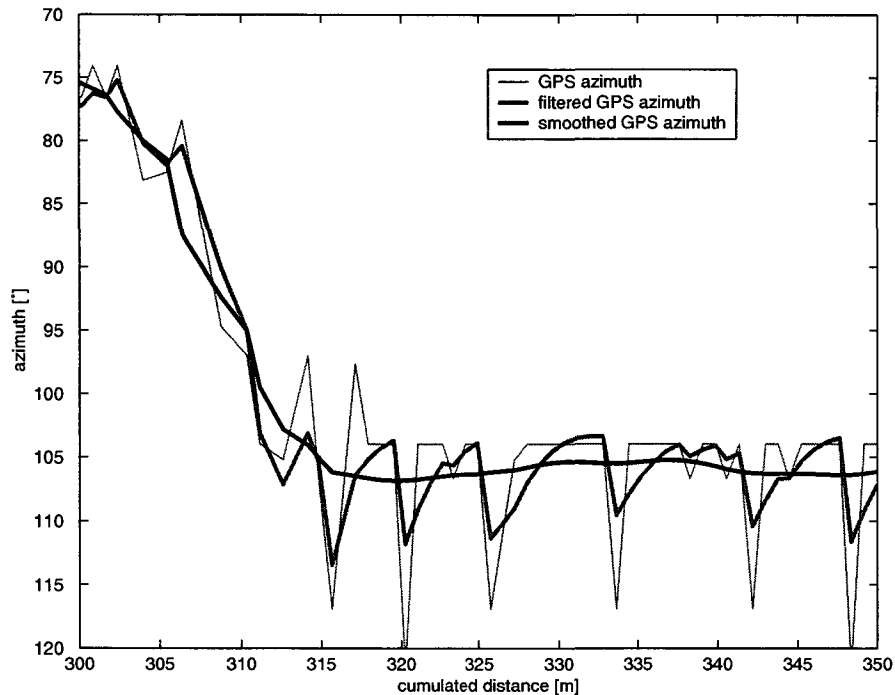
Figure 4.15: GPS azimuth filtered and smoothed with a KF

4.7.2 Smoothing

When both filtered azimuths (ϕ_{GPS} and ϕ_{gyro}) are compared, they still contain some errors. However, the residuals are completely uncorrelated and can yield big differences when they are opposed. For ϕ_{GPS}, the residuals are white noise. For ϕ_{gyro}, the residuals still contains the pattern of the steps, that is not completely eliminated by the filter. To attenuate these differences a smoothing process is proposed. Fig.4.15 illustrates the methodology with a concrete example where the smoothing is performed on the GPS azimuth.

When, at time k, an update is decided (i.e. a comparison between ϕ_{GPS} and ϕ_{gyro} through a KF to calibrate the bias) the filter and DR process continue for some seconds (say 5 seconds) instead of performing it with the current filtered value of the azimuth. During these 5 seconds, some additional values must be stored as required by all the smoothing algorithms. Generally these values are:

- the predicted and filtered state vector at each epoch

- the covariance matrix of the predicted and filtered state vector

- the transition matrix

Merminod proposed another smoothing algorithm where observations and their weight matrix as well as the design matrix must be stored instead of the predicted parameter and associated covariance matrix [Mermi89].
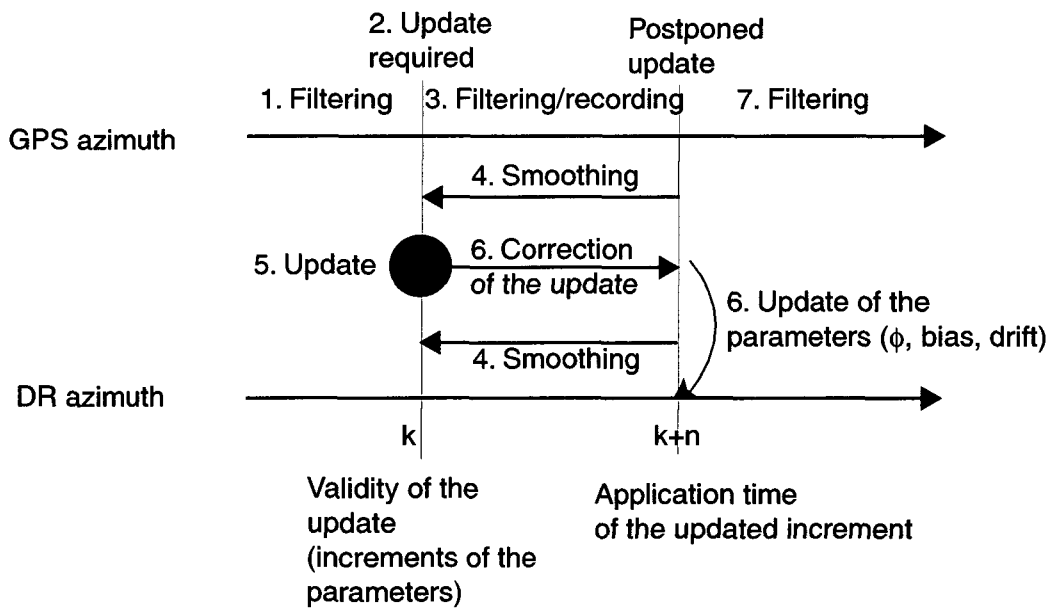
Figure 4.16: Short-smoothing process applied to GPS and gyro azimuth to improve their integration

After the 5 seconds, at time $k + 5s$, the smoothing process is performed to obtain a smoothed values of the GPS and gyro azimuths at time k. Then, the comparison is done with these two values. The increments of parameters (for example db) are computed with these values. Fig.4.16 illustrates this short-smoothing process.

At this point the correction parameter (for example db) can be combined with the bias b to provide the new bias value in two different manners. The first one consists in computing the new bias at time k and then to re-process the DR-algorithm from time k to time $k + n$. Another way is to assume that the importance of the error in the bias (db) is not too big and that the new bias can be applied directly at time $k + n$ without computing again the DR process from time k to time $k + n$.

Fig.4.17 shows a concrete example of the back smoothing process performed in order to compute a new estimation of the parameters of the gyroscope and of the azimuth.

There are important advantages when smoothing:

- The variance of the smoothed azimuths is smaller than the variance of the filtered azimuths.

- The pattern of the gait disappears.

- The GPS errors are reduced.

The drawback is of course the computation time and the storing space required by the smoothing algorithm. Indeed, during the computation of the smoothed value, the DR process must continue.
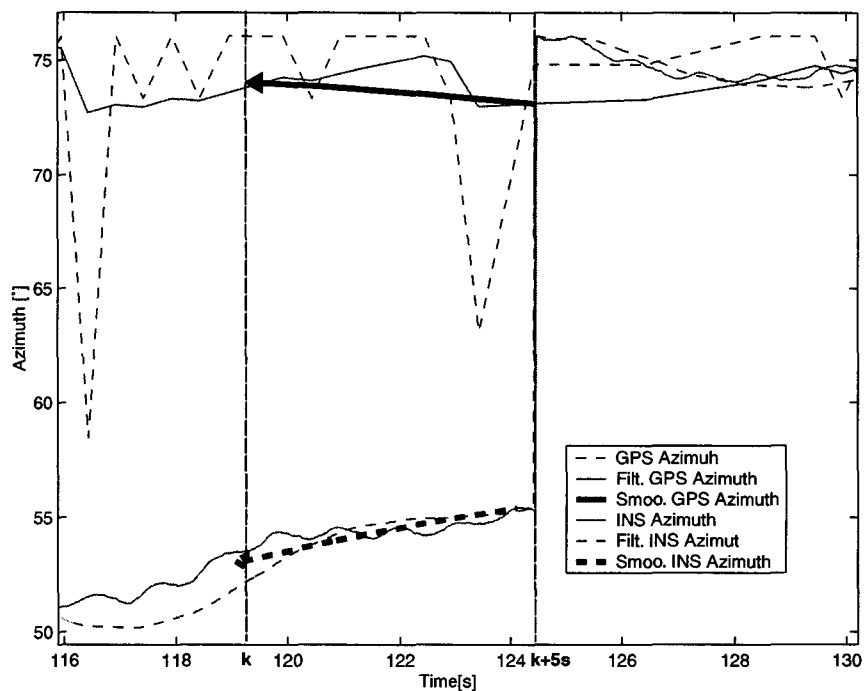
Figure 4.17: Smoothing of GPS and gyro azimuth with bias and azimuth update.

111

From a stochastic point of view, the short-smoothing process allows to improve the standard deviation of the GPS azimuth from 8 to 3 and then to $1.5°$. For ϕ_{gyro} the Kalman filter and smoothing process have another goal: to eliminate the pattern of the body oscillation, while keeping a good reaction of the filter to real changes of the walking azimuth.

4.8 Azimuth from compass

A magnetic compass is another way to provide external azimuth information to the proposed DR system. This device indicates the magnetic North sensing the earth magnetic field. Most of the pedestrian navigation systems, already developed or under development, use a magnetic compass for orientation. This device is often combined with GPS because it gives directly an azimuth, which GPS can accomplish correctly only when the receiver is moving. However the compass have some important drawbacks. Indeed magnetic disturbances are numerous, particularly in urban environment. The sources of these disturbances are numerous and vary with time [Denne79, Carus00].

4.8.1 Combination gyro and compass

The combination of gyroscope and magnetic compass has already been applied in different areas such as car navigation [Mclel92, Harve98]. For pedestrian navigation, this concept has been presented in [Gabag01a, Ladet01a, Ladet01b]. It is also adopted by the research group at the University of Tampere, Finland [Kappi01, Leppa01, Colli01].

The different tests conducted in parallel with the two sensor systems show clearly that the weaknesses of one system are the advantages of the other one (see Tab.4.1).

	Advantages	Disadvantages
Magnetic compass	absolute azimuth long term stable accuracy	unpredictable external disturbances
Gyroscope	no external disturbances short term accuracy	relative azimuth drift

Table 4.1: Comparison between compass and gyroscope

According to this remark, an optimal and more reliable system can be obtained by coupling the gyroscopes with the magnetic compass. The gyroscope will provide a useful indication to identify magnetic disturbances, while the compass will be useful to determine the bias of the gyros and the initial orientation, even when no GPS is available.

From an algorithmic point of view, different integration strategies are possible. The first one, proposed by McLellan [Mclel92], is to implement a heading filter with the following state vector:

$$\mathbf{x} = \begin{bmatrix} \phi & \dot{\phi} \end{bmatrix} \tag{4.38}$$

The observations that update the filter come from the different sensors, and undergo previously through a local filtering. A design matrix is formed for each type of update:

compass update:
$$\mathbf{H} = \begin{bmatrix} 1 & 0 \end{bmatrix} \tag{4.39}$$

gyroscope update:
$$\mathbf{H} = \begin{bmatrix} 0 & 1 \end{bmatrix} \tag{4.40}$$

GPS update:
$$\mathbf{H} = \begin{bmatrix} 1 & 0 \end{bmatrix} \tag{4.41}$$

In this thesis, the proposed implementation is similar to the GPS-gyro integration filter. The GPS azimuth ϕ_{GPS} is replaced by the compass azimuth $\phi_{compass}$. However, before processing such an update the azimuth provided by the magnetic compass must be free of disturbances.

When the pedestrian is walking, the influence of perturbation sources varies continuously, creating a varying error in the compass azimuth. A constant influence can occur only with big magnetic sources or by sources attached to the pedestrian (other sensors, batteries, iron structures...). This second type of sources produces errors that can be eliminated by a calibration procedure [Gnepf99, Carus00]. The variation can be observed via the azimuth angular rate:

$$\omega_{compass_k} = \frac{\phi_{compass_k} - \phi_{compass_{k-1}}}{time_{k-1}^k} \tag{4.42}$$

These disturbances can be detected with the gyroscope comparing the $\omega_{compass_k}$ with the gyroscope angular rate ω_z. This comparison requires that both data sources are perfectly synchronised.

Fig.4.18 shows the gyro and compass azimuth and Fig.4.19 illustrates, for the same sample, the difference between the angular rate measured by the gyroscope and the one computed from the compass outputs. When the amplitude of this difference reaches a certain threshold value the magnetic field is considered as disturbed and the outputs of the magnetic compass are not considered.
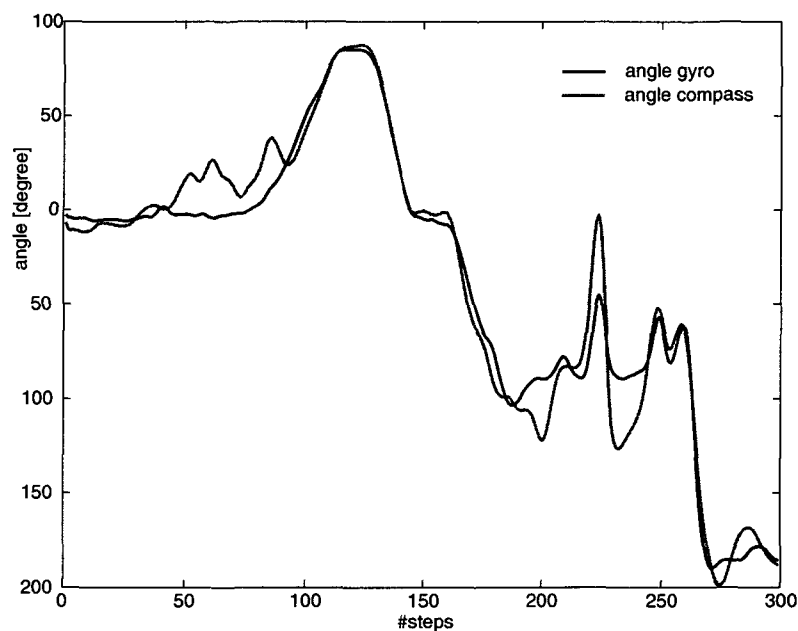
Figure 4.18: Angle obtained by the gyroscope and by the magnetic compass

Finally the integration of the gyroscope and the magnetic compass data can be represented in the scheme presented in Fig.4.20.

The main difference between the GPS-gyro and the compass-gyro integration consists in the capacity of each one to detect the body oscillations. In the second case, both sensors detect the body oscillation. Furthermore, if both sensors are mounted together and if they are perfectly synchronised, they will have the same oscillation signal. Thus no smoothing process is needed to eliminate it because the oscillation signal will disappear when subtracting one sensor azimuth from the other. Then the key issue is to calibrate the magnetic disturbances induced by the electronic circuit included in the gyroscope and to synchronise both sensors. It is interesting to note that the body oscillation itself is a good synchronisation tool because of its sinusoidal pattern which is easy to detect and match with the pattern of the second
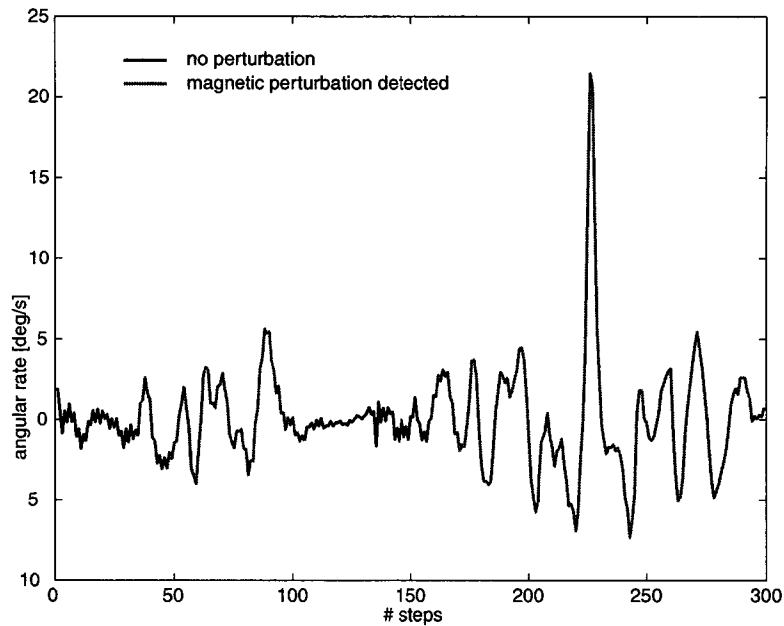
Figure 4.19: Difference between the angular rate of the gyroscope (raw data) and of the compass (computed) with detected perturbation.
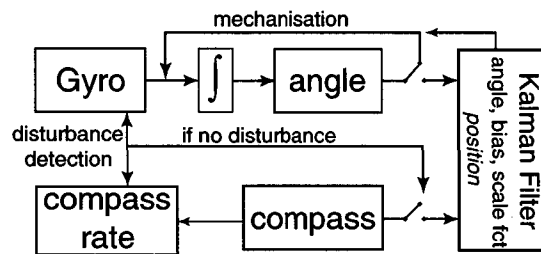
Figure 4.20: Scheme for an integration of gyroscope and magnetic compass

sensor. A simple cross-correlation algorithm can give the lag between the two sources.

4.9 Conclusion

In this chapter, the way to obtain an azimuth from different sensors has been presented. Different solutions have been proposed to obtain an accurate and

115

reliable orientation. Considering the evolution of the sensors it appears that the best solution is to combine gyroscope, magnetic compass and satellite positioning system. When GPS signals are not available due to sky obstructions for a long period of time, the compass only or gyro only solution may quickly accumulate important errors due to magnetic disturbances, respectively non-stability of the bias that lead to a drift in the angle. Moreover a combined gyro and compass offers a powerful DR orientation and can provide a more accurate and reliable azimuth. Furthermore, thanks to the continuous availability of the compass and to the short duration of most of perturbations, a gyroscope with an lesser accuracy (and then an inferior price) may be used. In other words, the compass is used to determine the azimuth in the long term and the gyroscope in the short term. GPS at this point becomes unnecessary for the adjustment of the bias and scale factor of the gyroscope. However it is still needed to determine the offset of the azimuth compass. This offset is the angle formed by the pedestrian's line of walk and the axis of the compass.

Chapter 5

DR algorithm and integration with GNSS

In this chapter the fusion process of distance and orientation will be presented. Firstly, a special attention is brought to the synchronisation between all the data sources. Then, the Dead Reckoning algorithm is presented as well as the error propagation that occurs through this process. The link between the error propagation and the kinematic model of the Kalman Filter is then made. A centralised Kalman filter is presented that allows to consider all the sensors data source and the DR parameters. The external measurement of the Kalman Filter are the GPS measurements: position, velocity, azimuth. Considerations are made about the implementation of the filter and a specific section is dedicated to the integrity that can be of interest for some specific applications of pedestrian navigation. Results of tests are then presented.

5.1   DR algorithm

The two elements of a DR approach have been presented. The folding process of those elements is done in the following mechanisation, that furnishes the navigation parameters:

$$E_k = E_{k-1} + dist_k \cdot sin(\phi_k)$$
$$N_k = N_{k-1} + dist_k \cdot cos(\phi_k)$$

(5.1)

where

E	is the East coordinate
N	is the North coordinate
$dist_k = speed_k \cdot dt$	is the travelled distance
$speed_k$	is the velocity
ϕ_k	is the azimuth
dt	is the processing rate of the distance and azimuth (0.5 s)

The next two sections will present two elements linked to this algorithm. The first one is the problem of the time synchronisation between the different data sources. The second one is a study of the error propagation in this model. This study will introduce the next section about the centralised Kalman filter.

5.2 Synchronisation and real-time

The system and the algorithm have been designed to work close to real-time. The notion of real-time is itself ambiguous while pure real-time is not possible due to computation time. Furthermore, if numeric filters are used, they induce delays. Other data processing, such as data transmission, communication or display create a lag. As we will see, the way to treat and combine the different sensors and algorithms produces a delay of 1 to 2 seconds, which is acceptable for most of the applications in pedestrian navigation.

Indeed as presented in the previous chapters both elements, distance and orientation, produce a computational delay. For distance the computational time is driven by the time or step interval needed to compute the distance. In chapter 3 the ideal interval has been defined as four steps or 2 seconds. Actually the computed speed at time k is representative of the velocity at the middle of the interval, i.e. at time $k - 1$ second or $k - 2$ steps.

For the orientation, the delay is due to the filtering of the azimuth. As presented in chapter 4, the filter delay is 1 second. If a Kalman filter is used the filter delay is more difficult to estimate. However, a comparison between the azimuth computed with low-pass and Kalman filters allows to estimate the delay produced by the KF at 1 second. When the gyroscope azimuth is integrated with GPS the smoothing algorithm is initiated and consumes additional time that provokes a delay of a few seconds.

Fig.5.1 illustrates the computational time of distance and orientation. At time k, the velocity is computed with accelerometer data from time $k - 2$ to time k. The same applies for the orientation, with the gyroscope data.

118
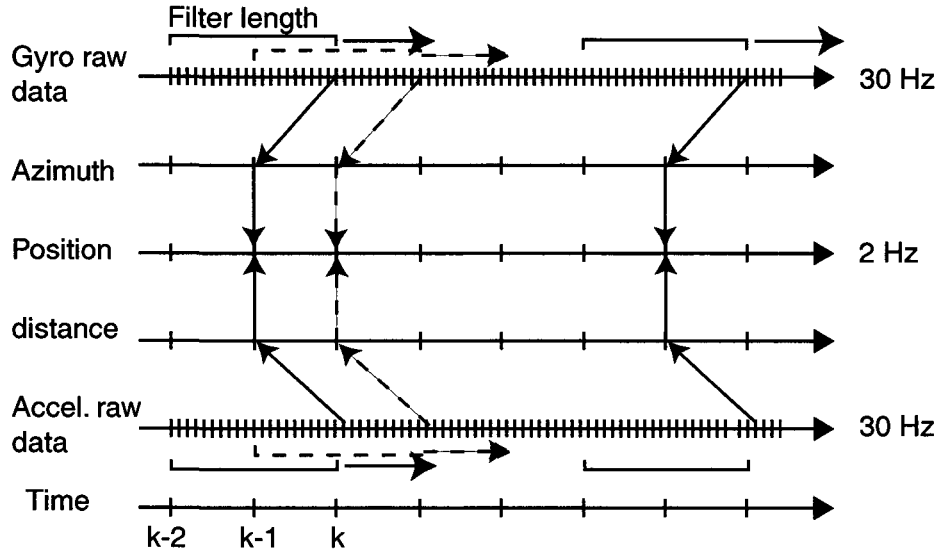
Figure 5.1: Synchronisation between gyroscope and accelerometers

Both values are representative of the velocity, respectively the orientation, at time $k - 1$. Thus the delay of the DR algorithm is 1 second. To this computational delay, it is necessary to add the process delay that depends on the characteristics of the processor and on the efficiency of the filtering algorithms.

5.3 Error propagation

The error propagation in the Dead Reckoning model is computed as presented below.

For orientation, the derivation in Taylor's series of equation (4.29) gives:

$$d\phi_k = \frac{\partial \phi_k}{\partial \phi_{k-1}} \cdot d\phi_{k-1} + \frac{\partial \phi_k}{\partial b} \cdot db + \frac{\partial \phi_k}{\partial \lambda} \cdot d\lambda \qquad (5.2)$$

$$d\phi_k = 1 \cdot d\phi_{k-1} + dt \cdot db + dt \cdot \omega \cdot d\lambda \qquad (5.3)$$

For distance, when the first model is used (3.28), the derivative gives:

$$ddist_k = \frac{\partial s}{\partial A} \cdot dA \cdot dt + \frac{\partial s}{\partial B} \cdot dB \cdot dt \qquad (5.4)$$

119

$$ddist_k = \sqrt{VAR} \cdot dA \cdot dt + 1 \cdot dB \cdot dt \qquad (5.5)$$

The propagation of errors on distance and orientation in the North coordinate is:

$$dN_k = \frac{\partial N_k}{\partial N_{k-1}} \cdot dN_{k-1} + \frac{\partial N_k}{\partial \phi_k} \cdot d\phi_k + \frac{\partial N_k}{\partial dist_k} \cdot ddist_k \qquad (5.6)$$

where $d\phi_k$ is replaced by equation (5.3) and $ddist_k$ by equation (5.5).

For East and North we have then:

$$\begin{cases} dN_k = 1 \cdot dN_{k-1} - dist \cdot sin(\phi_k) \cdot d\phi_k + cos(\phi_k) \cdot ddist_k \\ dE_k = 1 \cdot dE_{k-1} + dist \cdot cos(\phi_k) \cdot d\phi_k + sin(\phi_k) \cdot ddist_k \end{cases} \qquad (5.7)$$

In matrix notation we obtain:

$$\begin{bmatrix} dN_k \\ dE_k \end{bmatrix} = \mathbf{F}_{DR}^T \begin{bmatrix} dN_{k-1} & dE_{k-1} & d\phi_k & ddist_k \end{bmatrix}^T \qquad (5.8)$$

To illustrate, in a simple way, the error propagation, the experiences on an athletic ring are considered again. The computed distance can be considered without error ($ddist = 0$), the A and B parameter are perfectly calibrated (the same day, on the same surface), the surface is ideal and the walker maintains a constant speed during the walk. For the orientation we consider only an error in the bias but not in the scale factor ($d\lambda = 0$). The initial orientation ($d\phi_0$) is also considered without error.

The bias increment db is computed every $time_{k-1}^k$ seconds comparing the azimuth mechanised with the gyroscope raw data (ϕ_{gyro}) and the external azimuth (ϕ_{ext}) provided here by GPS, both at time k.

$$d\hat{b}_k = \frac{\phi_{gyro_k} - \phi_{ext_k}}{dt} \qquad (5.9)$$

Using equations (5.3) and (5.7), the correction $d\hat{\phi}$, $d\hat{N}$ and $d\hat{E}$ are computed:

$$d\hat{\phi}_k = dt \cdot d\hat{b}_k \qquad (5.10)$$

$$d\hat{N}_k = -dist \cdot sin(\hat{\phi}_k) \cdot d\hat{\phi}_k = -dist \cdot sin(\hat{\phi}_k) \cdot dt \cdot d\hat{b}_k \qquad (5.11)$$

$$d\hat{E}_k = dist \cdot cos(\hat{\phi}_k) \cdot d\hat{\phi}_k = dist \cdot cos(\hat{\phi}_k) \cdot dt \cdot d\hat{b}_k \qquad (5.12)$$

and added to the navigation parameter: ϕ, N and E respectively:

$$\hat{\phi}_k = \phi_{DRk} + d\hat{\phi}_k \qquad (5.13)$$

$$\hat{N}_k = N_{DR} + d\hat{N}_k \qquad (5.14)$$

$$\hat{E}_k = E_{DR} + d\hat{E}_k \qquad (5.15)$$

These corrections are illustrated in Fig.5.2. The external azimuth can be provided by a magnetic compass or by a GPS receiver. At each update, the equation (5.9) to (5.15) are performed and and the two last equation create the jump that is visible in the Fig.5.2. The equation (5.13) provides the new azimuth to continue with the DR process.
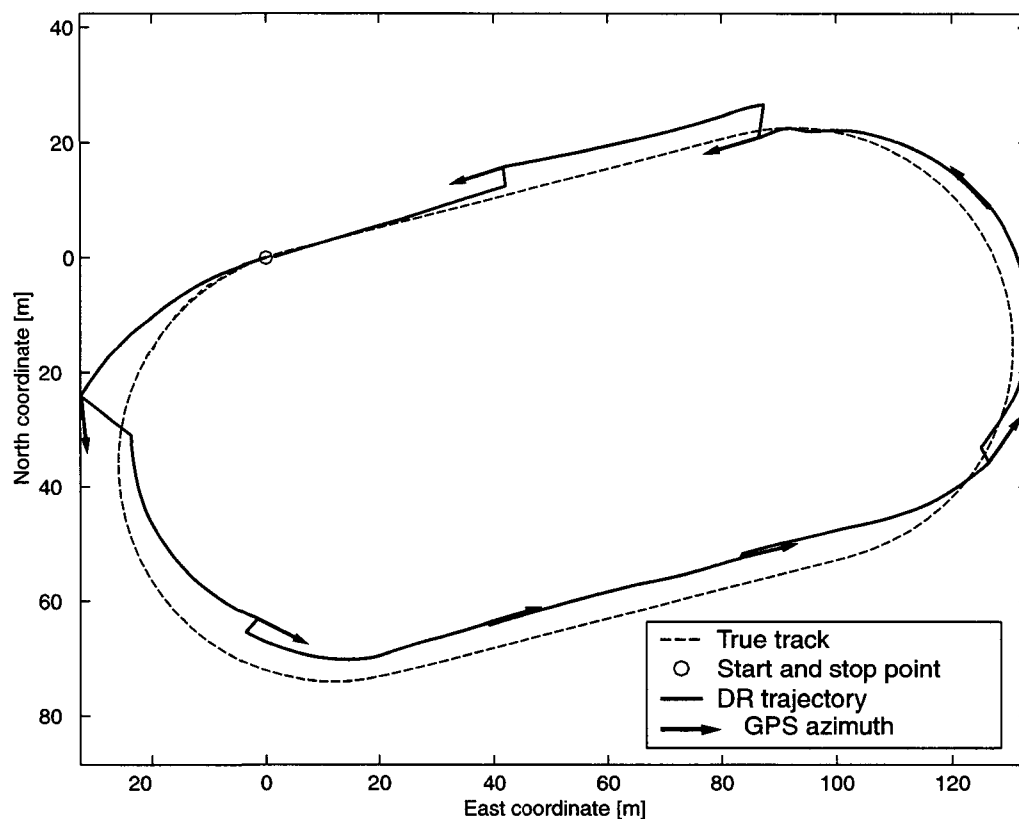
Figure 5.2: Bias, azimuth and position correction computed by comparing the gyro and an external azimuth

The following equation provides the covariance matrix of the corrected parameter $\mathbf{C}_{DR}$:

$$\mathbf{C}_{DR} = \mathbf{F}_{DR}^T \cdot \mathbf{C_{xx}} \cdot \mathbf{F}_{DR} \tag{5.16}$$

where $\mathbf{C_{xx}}$ is the covariance matrix of the position, azimuth and distance increments $(d\phi,\ dN,\ dE$ and $ddist)$.

The equation (5.9) is an integration between GPS and INS but at a very simple level. The next paragraph proposes a more efficient algorithm for a better integration of all the sensors.

5.4   Centralized Kalman Filter

The Kalman filter (KF) is the optimal combination, in term of minimisation of variance, between the prediction of parameters from a previous time instant and external observations at the present instant [Brown97]. KF is built around two independent models: the kinematic model and the observation model. Each one has a functional part and a stochastic part.

5.4.1   Kinematic model

The functional part of the kinematic model represents the prediction of the parameters. The considered parameters in the GPS-gyro-accelerometer system form the following vector:

$$\mathbf{x} = [\ E\ N\ \phi\ b\ \lambda\ A\ B]^T \tag{5.17}$$

Unlike other navigation applications, the trajectory of a pedestrian is difficult to predict. Changes in speed and orientation are sudden and can be of great amplitude. Therefore it is preferable for the prediction of the parameter to consider only the DR mechanisation. No other navigation parameters, such as speed or acceleration, are introduced in the state vector. The functional part of the kinematic model is then the DR mechanisation.

Concerning the stochastic part of the model, the equations presented for the error propagation can be reused. This time, however, only the changes of the parameters (called increments) are considered rather then their absolute value. The state vector is:

$$d\mathbf{x} = [dE\ dN\ d\phi\ db\ d\lambda\ dA\ dB]^T \tag{5.18}$$

To build a rigorous stochastic model, the continuous kinematic equation is first considered. This step is just theoretical since we have only discrete

measurements, but it allows the correlation between the predicted parameters to be considered.

$$d\dot{\mathbf{x}} = \mathbf{F} \cdot d\mathbf{x} + \mathbf{G} \cdot u \qquad (5.19)$$

where u is a white noise.

The three first lines of the $\mathbf{F}$ matrix (concerning the first derivative of dE, dN and $d\phi$) are the time derivatives of the equations (5.3) and (5.7) developed for the DR mechanisation and error propagation. Concerning the lines 4 and 5 of the $\mathbf{F}$ matrix, the parameters of the sensors db, $d\lambda$ are modelled as Gauss-Markov processes. The driving noise w_b of db is greater than the w_λ of the scale factor λ.

$$\begin{aligned} d\dot{b} &= -\alpha_b \cdot db + w_b \cdot u \\ d\dot{\lambda} &= -\alpha_\lambda \cdot d\lambda + w_\lambda \cdot u \end{aligned} \qquad (5.20)$$

Regarding the lines 7 and 8 of the $\mathbf{F}$ matrix, dA and dB are modelled as random walk processes.

$$\begin{aligned} d\dot{A} &= 0 + w_A \cdot u \\ d\dot{B} &= 0 + w_B \cdot u \end{aligned} \qquad (5.21)$$

The choice of w_A and w_B is critical. Over the flat areas the pre-calibrated parameters can be taken into account and the two driving noises are low. When there is a slope larger than about 7% then it is better to re-estimate these parameters and to adapt the driving noise. This situation can be resolved through an adaptive Kalman filter, where the driving noise on dA and dB can be controlled by the slope angle determined for example with a barometer or by GPS. The slope can also be detected in analysing the signal itself, as proposed in Perrin et al. [Perri00]. However implementing such detection in real-time is still to be resolved. The $\mathbf{G}$ matrix contains the driving noise of the system i.e. the w in equations (5.20) and (5.21).

To build the Kalman Filter it is necessary to pass from the continuous equation to the discrete time equation [Mermi89]. This is done through the following equation:

$$\Phi_k = \mathbf{I} + \mathbf{F}_k \cdot dt + \frac{\mathbf{F}_k^2}{2!}dt^2 + \frac{\mathbf{F}_k^3}{3!}dt^3 \qquad (5.22)$$

$$\mathbf{C}_{ww} = \int_{t_{k-1}}^{t_k} \Phi_k \cdot \mathbf{G} \cdot q_{uu} \cdot \mathbf{G}^T \cdot \Phi_k^T dt \qquad (5.23)$$

where q_{uu} is the spectral density of the noise.

The three first lines of matrix $\mathbf{F}$ represents the same relation as in the equations (5.3) and (5.7). During the mechanisation phase, the parameters are computed through the DR equations. In parallel the following variance propagation is performed:

$$\mathbf{C}_{\tilde{x}\tilde{x}_k} = \mathbf{\Phi}_k \cdot \mathbf{C}_{\tilde{x}\tilde{x}_{k-1}} \cdot \mathbf{\Phi}_k^T + \mathbf{C}_{ww} \qquad (5.24)$$

The $\mathbf{C}_{\tilde{x}\tilde{x}_k}$ matrix contains the variance of the parameters at time k.

5.4.2 Observation model

The considered external observations are the GPS position (ℓ_E and ℓ_N) and the GPS azimuth (ϕ_{GPS}). They form the observation vector ℓ_k . In fact they are indirect observations computed from the GPS code and phase rate measurement. This is taken in account through the variance and correlation included in the covariance matrix of the observations $\mathbf{C}_{\ell\ell}$. Each observation is function of the parameters:

$$\ell_k - v = f(x) \qquad (5.25)$$

Working with the increase of the parameters, equation (5.25) becomes by decomposition in Taylor's series around the mechanised values:

$$\tilde{v}_k - v = \mathbf{H} \cdot dx \qquad (5.26)$$

where $\mathbf{H}$ is the design matrix:

$$\mathbf{H} = \begin{bmatrix} 1 & 0 & 0 & 0 & 0 & 0 & 0 \\ 0 & 1 & 0 & 0 & 0 & 0 & 0 \\ 0 & 0 & 1 & 0 & 0 & 0 & 0 \end{bmatrix} \qquad (5.27)$$

and

$$\tilde{v}_k = \ell_k - f(\tilde{x}) \qquad (5.28)$$

v is the vector of residuals of the observations and is the vector of the mechanised parameters at the observation time t_k.

In the equation (5.28) represents the difference between the GPS position and azimuth and the DR output after mechanisation. This vector can be used as a first reliability indicator. Large discrepancies could indicate a fault in the measurement or in a DR sensor.

It is also possible to consider the GPS velocity as an observation and to introduce the Kalman filter presented in Chapter 3. However, the GPS velocity and the GPS azimuth are also strongly correlated because they are both issued from the same measurement (doppler or phase rate). Furthermore, the introduction of the GPS position has also an effect on the distance and then on the dA and dB parameters. In this centralised Kalman filter the measurements of the GPS velocity are not considered. However, one can consider from time to time performing a local Kalman Filter, considering only the GPS velocity and the distance parameter, as developed in Chapter 3. Instead of a local Kalman, an enlargement of the centralised Kalman Filter can also be made. For that, the design matrix $\mathbf{H}$ must be modified as follows:

$$\mathbf{H} = \begin{bmatrix} 1 & 0 & 0 & 0 & 0 & 0 & 0 \\ 0 & 1 & 0 & 0 & 0 & 0 & 0 \\ 0 & 0 & 1 & 0 & 0 & 0 & 0 \\ 0 & 0 & 0 & 0 & 0 & RMS \cdot dt & dt \end{bmatrix} \tag{5.29}$$

The observation vector is then:

$$\ell_k = \begin{bmatrix} \ell_E & \ell_N & \phi_{GPS} & speed_{GPS} \end{bmatrix}^T \tag{5.30}$$

If the $speed_{GPS}$ is measured instantaneously then a few updates must occur because of the low precision of the instantaneous GPS velocity (20cm/s). Otherwise, as indicated in Chapter 3, the GPS velocity can be previously filtered and smoothed, following the same concept as for the GPS orientation presented in Chapter 4. Then the correlation between the GPS velocity and orientation must be considered in the covariance matrix of the observation $\mathbf{C}_{\ell\ell}$.

5.5 Implementation of the Kalman Filter

The question that remains is to know when to perform an update. It is possible to make it each time when an observation is available. However, if two observations occur in a brief delay, then the update is not useful because the data are strongly correlated.

125

The GPS speed measurements *speed$_{GPS}$* can be implemented in a local KF only for distances that allow the A and B parameter to be improved. Then, when it is needed, a full update is performed with the modified **H** matrix. In either case the control of the A and B parameter with the GPS velocity is also part of the integrity monitoring that is discussed in the next section.

The update phase is a combination of the two models presented above. It is an estimation that minimizes the variance of the errors in the observations and of the mechanised parameters. The update phase is performed when the following conditions are fulfilled:

- GPS is available

- The GPS position and azimuth have no gross error (fault)

- The accuracy (computed through the covariance matrix) of the three navigation parameters (position and azimuth) reach a predefined level (10m or 5 degree)

The GPS error is controlled during the computation by considering the comparison between the changes in the GPS azimuth and the gyro raw data. It avoids an update being performed when the person walks too slowly (the GPS azimuth is then too inaccurate).

At each update, a new state vector $d\hat{x}$ is computed. This vector offers all the parameters needed to continue the DR process until the next update.

5.6   Integrity monitoring

As seen above, the integration of two different systems brings a lot of advantages. Firstly it helps to provide continuous information about the position of the pedestrian. Secondly, from a stochastic point of view, it helps to improve the accuracy of the whole system. A third point that is discussed in the present section is the integrity.

The integrity of a system is its capacity to detect faults. The GPS system is not offering this service. However, by the integration of two independent systems, i.e. GNSS and INS, it is possible to determine the failure of one of the systems by comparing the two independent solutions.

The concept of integrity is also linked to the concept of reliability [Baard68]. The reliability is the 'measurement' of the trust that can be given to a solution. When two independent systems are giving solutions that are stochastically close, then one can consider the combined solution as reliable. The reliability is the capacity of the system to detect large errors. This is done by the overdetermination of the parameters.

Another concept is also often given together with the integrity concept: the continuity. A continuous system must fulfil the following condition: the system must furnish information continuously, without interruption. In a conceptual view, the conceived system, coupling DR and GPS, allows this condition to be fulfilled. However, the challenge is then more on the hardware side, ensuring a continuous power supply and choosing robust components.

One of the main problems with GPS is that this system does not give any information about its integrity. If a fault occurs, the users are only informed a few hours after the failure. This lack of integrity can be covered by three different techniques.

- The Augmentation System. This technique needs the implementation on the ground of one or more receivers measuring continuously the signals emitted by the GPS satellites. When a fault is detected, it warns the users by broadcasting the integrity information. Generally, the source of errors can be the satellite itself (problem with the clock) or the influence of the atmosphere on the signal. The signal can be perturbed mainly in the ionosphere where electrical phenomena can occur.

- The Receiver Autonomous Integrity Monitoring (RAIM) is an applicable technique when the receiver tracks more than 4 satellites [Mcbur88]. After the computation of the coordinate (usually done through a least squares adjustment), each estimated residual (one per satellite) is examined. If one of them is greater than a certain number, then the satellite is considered as non-integer.

- Integration of GPS with another navigation system, INS being the most common example [Palmq96]. This technique is based on the comparison of two different solutions (positions) provided by two independent systems. If there is a discrepancy between both solutions, an integrity alarm is switched on.

In the studied case, the integrity of GPS can be given by comparing the GPS solution with the DR solution. However, the DR solution depends

on the GPS solution because of all the interactions between both systems made through the Kalman Filters. To keep the two systems independent, the comparison has to be made with the raw data, before the Kalman filter. The comparison between the gyroscope raw data and the change of GPS azimuth is a good way to check possible faults of the GPS solution. These faults, or systematic errors, can be produced either by the GPS system itself (satellite clock) or by external conditions (ionosphere, multipath...).

Special techniques to detect and ignore faults in measurement can be introduced directly into the Kalman Filter [Wang97, Wang98]. This capacity to eliminate faults is called the robustness [Koch98]. However, this procedure is heavy and requires a lot of storage space and computation time. The approach adopted is simpler and consumes less processing time.

5.7   Algorithm structure

Fig.5.3 describes the algorithm structure for an integrated GNSS-INS system used for pedestrian navigation. The initial point is the activity monitoring determination based on raw measurements from the accelerometer and the gyroscope. The implemented algorithm considers only three states of activity: walk, run or stop. The basic concept of the algorithm consists on fixing a threshold value on the VAR charcteristics. If the VAR is smaller than the threshold, the pedestrian is considered as stopped. A second value makes the difference between walk and run. The activity is also cross-checked with another threshold value on the gyroscope outputs. Other activities, such as climbing stairs, can be detected through different algorithms that have not been implemented in the algorithm developed in the frame of this thesis. If the activity is considered as walk, then the rest of the algorithm is implemented, otherwise during the stop activity, the GPS data are considered only.

First the raw data of the accelerometers are filtered. Then, using the individual parameters, the velocity and the distance are computed.

On the gyroscope side, the raw data, corrected for the bias and the drift, are integrated over time to obtain the azimuth change. Then, the azimuths are filtered to eliminate partially the body movement. The filtered azimuths are combined with the distance and the previous position to have the pedestrian's position.

On the GNSS receiver side, the following parameters are deduced: position, velocity and azimuth. They are combined with the previous parameters

through a single Kalman filter that combines two of the three KF illustrated in the figure.
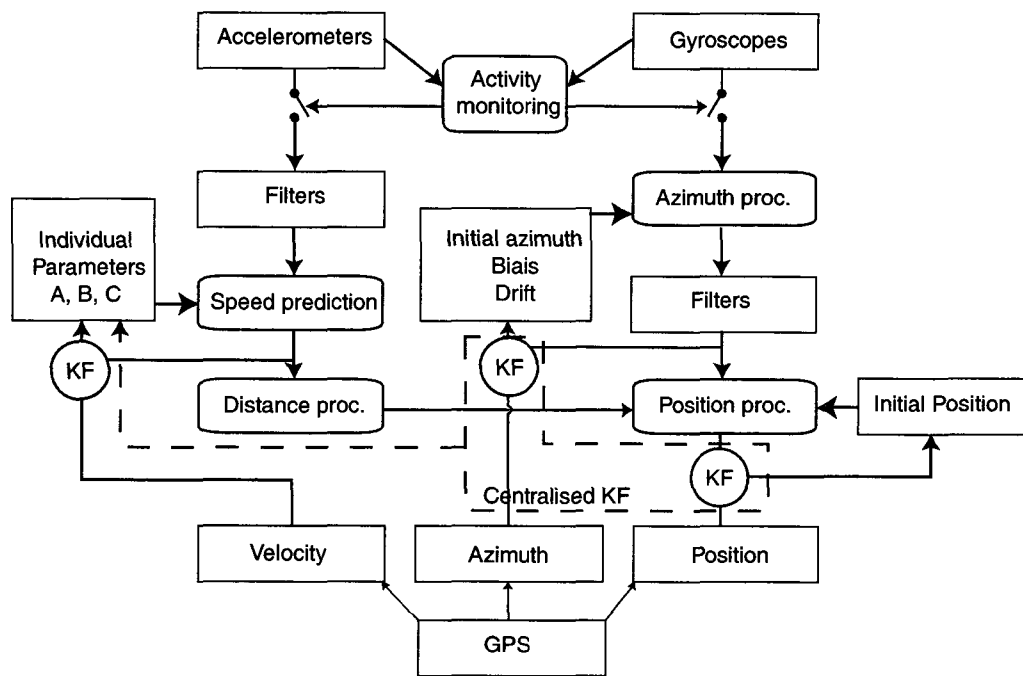
Figure 5.3: Algorithm structure

5.8 Results of tests

Several tests have been performed in different environments. The test presented below consists in following a track around a building on the EPFL campus (Fig.5.4). Other tests have been made on the athletic ring (400m) and in a residential area (2500m) to validate the algorithms.

The pedestrian walks about 400m at the average speed of 1.6 m/s on a flat area. He follows a track situated between the dashed lines of the Fig.5.4 and passes under the building. GPS signals from at least 4 satellites are available for the first part of the track. They provide an initial orientation to the system and allow the first update to be performed (this is essential for the bias calibration). The interruption of the GPS signal is due to obstruction caused by the building. When the GPS signals reappear multipath effects perturb them. The next and last update is done when the conditions presented above are fulfilled. The reliability of the GPS is observed comparing the
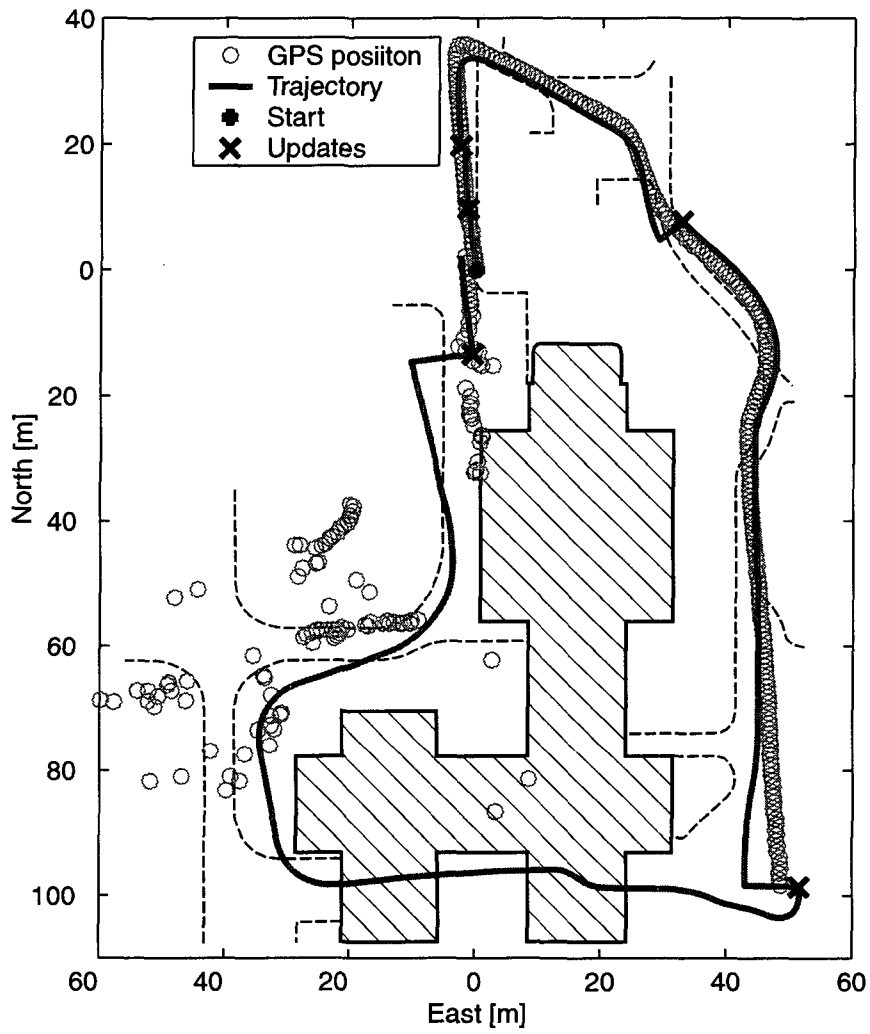
Figure 5.4: Trip around a building on the EPFL campus

change of GPS azimuth with the gyro raw data. The comparison between DR position and GPS position is also taken into account. The control of the GPS solution by the DR system is the precursor of a more mathematical and powerful integrity monitoring.

The different analysis made with this type of test show that the degradation of the accuracy of the system with time when no GPS is present is mainly due to the bias of the gyroscope. During the update procedure, the difference between the DR solution and the GPS solution are distributed mainly to the bias.

Chapter 6

Perspectives and conclusion

6.1 Perspectives

The pedestrian navigation domain was not a common domain and was not well documented at the beginning of this thesis. During this work a lot of different aspects have been introduced and analysed. Only a part of them have been more deeply investigated. Therefore, the door is let open for investigations in several fields. This section is mentioning a few of them.

Activity monitoring

A basic algorithm for activity monitoring has been implemented. However, this task plays an important role for many applications. It can improve also the system itself. Algorithms already exist. Some of them are presented in the Chapter 2. They could be implemented in the presented method to improve the system so that it can react correctly in some special situations as climbing stairs, jumping ... The challenge is to base the activity monitoring algorithms on the same sensors as those used for navigation.

Magnetic compass and gyroscope integration

The aspect of integration of magnetic compass and gyroscope has been presented in the Chapter 4 of this thesis report. However, the algorithm have not been completely developed and validated. Further tests are needed to improve this integration. This activity has been undertaken in the Unité de Topométrie and are presented in the thesis report of Quentin Ladetto

[Ladet03]. The first results reveal that this integration can provide very good performances.

The third dimension

All the concepts presented until now focus on a two dimensional positioning. This paragraph gives some indication about the third dimension: how it can be measured and which role it plays for pedestrian navigation.

The distance computation models are valid only if the slope is not too great. In the same way as for car navigation, the model is adjusted through the individual parameters.

However, the lack of direct information about the third dimension can be tricky in some situations. When the pedestrian is in a building, it is important for some applications to know at which level he is. This vertical information can be obtained through different techniques.

- Barometer. This instrument is very convenient for altitude determination. It must be calibrated from time to time and is sensitive to pressure modification due to weather changes.

- Activity monitoring. Using the accelerometer signal, it is possible to detect 'climbing' or 'going down' stairs and then to 'count' the number of stairs.

- Neural network. An algorithm based on this theory has been developed in [Herre99]. It allows the pedestrian's speed and the slope of the path to be computed from the accelerometer signal.

The choice of the technique depends on the situation. If the barometer suits a lot of situations, the second solution (activity monitoring) is more appropriate and accurate in buildings when the pedestrian used the stairs and not the lift! The third one (neural network) is convenient for walking on slopes.

DR distance model establishment

Concerning the establishment of the model for the determination of the distance presented in section 3.2.3, the choice has been made to include only the *VAR* characteristics of the acceleration. This choice is based on the good correlation between this characteristic and the pedestrian's velocity. However,

the other characteristics present also strong correlation and a combination of different characteristics inside a single model must not be excluded. To choose the best combination, a Principal Component Analysis (PCA) could be considered. PCA is a Multi-Variate Statistical Process Control (MSPC) method that allows to monitor the correlated output of different sources [Ogaja01]. In the actual study, the sources are the different characteristics and the speed. This analysis will allow to determine which characteristics are significantly different to be introduce simultaneously in a single model.

Integration with communication tool

Finally, the majority of applications in the pedestrian navigation field needs a communication tool. Often the position is of interest for external persons or systems. Therefore, it is worth to investigate the combination of the developed system with a communication tool as global as possible to fulfill also the initial requirements.

6.2   Conclusion

The work performed during this Ph.D. study and presented in this report demonstrates the feasibility of a pedestrian navigation system combining Global Navigation Satellite System (GNSS) and Inertial Navigation System (INS). The solution to mix the signal from three different types of sensors (accelerometers, gyroscope and a GPS receiver) has been chosen regarding the major constraint of the continuous availability of location information. If the requirements change (more precise, cheaper, ...), then the proposed technical solution will certainly be different and the proposed system must be adapted. We have seen that the proposed solution offers the best compromise for providing continuous location capability. It has been selected after an analysis of all existing systems able to provide a navigation service.

The way to combine the INS measurement and the GPS measurement differs drastically from the classical mechanisation. There is no double integration and the number of sensors used is different. The number of sensors (one gyroscope and two accelerometers) is an important aspect of the system. The utilisation of only one accelerometer is also a possible solution. However, the determination of the distance would be less precise, as shown in the first method for distance determination. The accuracy of the system could also be improved by adding more sensors, for example the magnetic

compass or a third accelerometer, but the cost and the energy consumption of the system would be affected.

The determination of the distance is one of the main added value of this thesis. To compute the distance, the utilisation of the accelerometers changes a lot in comparison with the classical double integration. It varies also from the classical pedometer utilisation that has limited capability. This new way to use accelerometers to compute a distance (through the determination of the velocity) is inspired by the medical research into walking and into energy expenditure.

In fact the proposed methodology is the result of a mix of medical and navigation investigation, as illustrated in Fig.6.1.

Figure 6.1: Pedestrian navigation is a mix of existing results and methodology issued form the Medical domain and the navigation domain.

Finally, the developed algorithm for the distance computation provide a relative accuracy of about 2% of the travelled distance.

Concerning the orientation, the gyroscope is utilised in a classical way to compute the azimuth. The main difference is that the system is based only on one gyroscope instead of three. This simplification has been made possible because the attitude (i.e. 3D orientation in space) of a pedestrian is quite constant and varies in a symmetrical way. The algorithm for the integration of GPS and gyroscope proposes a small smoothing of both signal before the adjustment through a Kalman Filter. This original proposition is

possible due to the small kinematics of the pedestrian. A lag of five seconds between the request of an update and the actual update is acceptable.

The result obtained in the frame of this thesis shows that the chosen methodology can fulfill the initial requirements. The integration of a GNSS receiver and INS sensors is an adapted solution for many applications in the domain of Pedestrian Navigation.

Bibliography

[Abous93] ABOUSALEM M. A. (1993). Development of a robust GPS kinematic positioning module for automatic vehicule location and navigation systems. Department of Geomatics Engineering, University of Calgary: M. Sc. thesis.

[Amini99] AMINIAN K., ROBERT P., BUCHSER E.E., RUTSCHMANN B., HAYOZ D., DEPAIRON M. (1999). Physical Activity Monitoring based on Accelerometry: Validation and Comparison with Video Observation. Medical and Biological Engineering and Computing. 37 (3) (May): pp 304-308.

[Ander01] ANDERSON R.S., HANSON D.S., KOUREPENIS A.S. (2001). Evolution of Low Cost MEMS/GPS Inertial System Technologies. ION GPS 2001, Salt Lake City (USA), 11-14 September 2001.

[Ansel98] ANSEL Y. (1998). Operation Limits of Micromachined Inertial Sensors. Département de microtechnique. Lausanne, EPFL: 152p.

[Anton85] ANTONSSON E. K., and MANN R. W. (1985). The frequency content of gait. Journal of Biomech., 18, pp 39-47.

[Aoki99] AOKI H., SCHIELE B. and PENTLAND A. (1999). Realtime Personal Positioning System for a Wearable Computer. The third international Symposium on Wearable computers, San Fransisco CA, pp37-43.

[Ayazi01] AYAZI F., NAJAFI K. (2001). A HARPSS polysilicon vibrating ring gyroscope. Journal of Microelectromechanical Systems, Volume: 10 Issue: 2 , June 2001, pp 169-179.

[Ayen88] AYEN T.G. and MONTOYE H.J. (1988). Estimation of energy expenditure with a simulated three-dimensional accelerometer. Journal of Ambulatory Monitoring, vol 1. pp 293-301.

[Baard68] BAARDA W. (1968). A testing procedure for use in geodetic networks. Delft, Publications on geodesy, Netherland Geodetic Commission.

[Balog88] BALOGUN J. A., AMUSA L. O. and ONEWADUME M. A. (1988). Factors affecting Caltrac and Calcount accelerometer output. Phys. Ther., 68, pp 1500-1504.

[Barbo01a] BARBOUR N.M. (2001). Inertial Components - Past, Present and Future. Guidance, Navigation, and Control Conference. Montreal, Québéc, Canada, August 6-8. Sponsored by: AIAA. (Draper Report no. P-3925).

[Barbo01b] BARBOUR N.M. (2001). MEMS for Navigation - a Survey Institute of Navigation National Technical Meeting. Long Beach, CA, January 22-24. Sponsored by: ION. (Draper Report no. P-3871)

[Bened02] BENEDICTO J., OOSTERLINCK R. (2002). Status of the GALILEO Program. GNSS 2002, Copenhagen, May.

[Boute97a] BOUTEN C.K., VERDUIN K.M., KODDE R.M., JANSSEN J.D. (1997). A tri-axial Accelerometer and Portable Data Processing unit for the Assessment of Daily Physical Activity. IEEE Transactions on Biomedical Engineering 44 (3)(March): 136-147.

[Boute97b] BOUTEN C.K., SAUREN, A.A., VERDUIN K.M., JANSSEN J.D. (1997). Effects of Placement and Orientation of body-fixed Accelerometers on the Assessment of Energy Expenditure during Walking. Medical and Biological Engineering and Computing 35: 50-56.

[Britt71] BRITTING K. R. (1971). Inertial Navigation System Analysis. New York, Wiley-Interscience.

[Brown88] BROWN R. G. (1988). Loran-Aided GPS Integrity. ION GPS 1988, Colorado Springs, September 1988.

[Brown97] BROWN R. G. and HWANG P.Y.C (1997). Introduction to Random Signal and Applied Kalman Filtering. Third Edition, J.W. Sons. 1997, New York. 484 p.

[Brouh60] BROUHA L. (1960). Evaluation of requirements of jobs in Physiology in Industry. Oxford, U.K.: Pergamon pp 94-108.

[Campb99] CAMPBELL N., MULLER H., RANDELL (1999). Combining positional information with visual media. The Third International Symposium on Wearable Computers. Digest of Papers. pp: 203-205.

[Cappo82] CAPPOZZO A. (1982). Low frequency self-generated vibration during ambulation in normal men. Journal of Biomech., 15, pp 599-609

[Carle1872] CARLET (1872). Essai expérimental sur la locomotion humaine, étude de la Marche. Ann. Des Scienses Nat., Sect. Zool. XV.

[Carus00] CARUSO M.J. (2000). Applications of magnetic sensors for low cost compass systems. IEEE Position Location and Navigation Symposium (PLANS), pp 177-184.

[Cavag64] CAVAGNA G., SAIBENE F. and MARGARIA R. (1964). Mechanical work in running. Journal of Applied Physiol. 19:249-256.

[Cavag76] CAVAGNA G. A., THYS H., ZAMBONI A. (1976). The Sources of external Work in Level Walking and Running. Journal of Physiol. 262, p. 639-657.

[Cgali02] CGALIES (2002). Support group to the European Commission for the implementation of the E-112 service in Europe. http://www.telematica.de/cgalies

[Chen99] CHEN T., SHIBASAKI R. (1999). A versatile AR type 3D mobile GIS based on image navigation technology. Systems, Man, and Cybernetics, IEEE SMC '99 Conference Proceedings. Vol. 5, pp 1070-1075.

[Chui92] CHUI, C. K. An introduction to Wavelets. Academic Press, New York.

[Cohen95] COHEN C. E. (1995). Attitude Determination. in Global Positionning System, Theory and Application, Volume II, Parkinson and Spickler, Progress in Astronautics and Aeronautics. 164p.

[Colli01] COLLIN J., KAPPI J., SAARINEN J. (2001). Unaided MEMS-Based INS Application in a Vehicular Environment. Tampere University of Technology, Finland, ION GPS 2001, Salt Lake City, Spetember 2001.

[Denne79] DENNE W. (1979). Magnetic Compass Deviation and Correction. 3rd Ed. Brown, Son & Fergusson Ltd, Scotland. 165p.

[Dodso99] DODSON A. H., MOORE T., MOON G. V. (1999). A Navigation System for the Blind Pedestrian. Proc GNSS 99, 3rd European Symp on Global Navigation Satellite Systems, Genoa, Italy, October, pp 513-518.

[Drane98] DRANE C., RIZOS C. (1998). Positioning Systems in Intelligent Transportation Systems. ITS series, Artech House, London. 369p.

[Dunn01] DUNN R. W., SHABALIN D. E., THIRKETTLE R. J., MAC-DONALD G. J. , STEDMAN G. E. and SCHREIBER K. U. (2001). Design and initial operation of a 367 m2 rectangular ring laser. Submitted to Appl. Opt., Jan 2001.

[Eissf89] EISSFELLER B. (1989). Basic Filter Concepts for the Integration of GPS and an Inertial Ring Laser. Manuscripta Geodaetica 14 No.3: 166-182.

[Elwel99] ELWELL J. (1999). Inertial Navigation for the Urban Warrior. Digitization of the Battlespace. 4th. Held in Orlando, FL, April 7-8. pp 196-204.

[Farri87] FARRIS D. S. (1987). Prototype development of a system providing for initial assessment of the dynamics/kinematic of bipedal motion. Proc. 10th Ann. Conf. RESNA, San Jose, California. pp 726-728.

[Feine97] FEINER S., MacINTYRE B., HOLLERER T. and WEBSTER A. (1997). A Touring Machine: Prototyping 3D Mobile Augmented Reality Systems for Exploring the Urban Environment. The First International Symposium on Wearable computers, Boston, MA, pp 74-81.

[FGS98] GERMAN RESEARCH GROUP FOR SPACE GEODESY (1998). Earth Rotation. Sonderheft. Bundesamt für Kartographie und Geodäsie, Frankfurt am Main. http://www.ifag.de

[Fisch97] FISCHER S. (1997). Multi-Scale Analysis for Pattern Recognition. Signal Processing Laboratory (LTS). Internal report. Swiss Federal Institute of Technology, Lausanne.

[Fonta01] FONTANA R. J. (2001). Recent Apllication of UBW Radar and Communication Systems. EuroEM200, Edinburgh, Scotland. May 30.

[Frenc96] FRENCH R. L. (1996). Land Vehicle Navigation and Tracking. in Global Positionning System, Theory and Application, Volume II, Parkinson and Spickler, Progress in Astronautics and Aeronautics, 164p.

[Gabag97a] GABAGLIO V. (1997). Orientation d'un système multi-antennes GPS. Lausanne, Unité de Topométrie, Institut de Géomatique, Département de Génie Rural, EPFL.

[Gabag97b] GABAGLIO V. (1997). Orientation d'un système multi-antennes GPS. Vermessung, Photogrammetrie, Kulturwissenschaft - Mensuration Photogrammétrie et Génie Rural 95(juillet): 453-458.

[Gabag99] GABAGLIO V., MERMINOD B. (1999). Real-Time Calibration of Length of Steps with GPS and Accelerometers. GNSS'99 Conference Proceedings, Genova, Italy.

[Gabag00] GABAGLIO V. and MERMINOD B. (2000). Using Satellite Positioning Systems and Inertial Sensors for Human Navigation. GNSS 2000 Conference Proceedings, Edinburgh, 1-4 May.

[Gabag01a] GABAGLIO V., LADETTO Q., MERMINOD B., (2001) Kalman filter mechanization for GPS-INS Pedestrian Navigation, GNSS 2001 Conference Proceedings, Sevilla (E), 8-11 May 2001.

[Gabag01b] GABAGLIO V. (2001) "Centralised Kalman Filter for Augmented GPS Pedestrian Navigation", ION 2001 Conference Proceedings, Salt Lake City (USA), 11-14 September 2001

[Garaj01] GARAJ V. (2001). The Brunel Navigation System for Blind: Determination of the Most Appropriate Position to Mount the External GPS Antenna on the Users Body. ION GPS 2001 Conference Proceedings, Salt Lake City, September 2001.

[Garci00] GARCIA E. (2000). Exoskeletons for Human Performance Augmentation (EHPA), DARPA/DSO research program, BAA00-34. http://www.darpa.mil/DSO/thrust/md/Exoskeletons/index.html .

[Geige98] GEIGER W., FOLKMER B., MERZ J., SANDMAIER H., LANG W. (1998). A new silicon rate gyroscope Electro Mechanical System. The Eleventh Annual International Workshop on MEMS 98, Conference Proceedings. pp 615 -620.

[Gelb74] GELB A. (1974). Applied Optimal Estimation. MIT Press, Cambridge, Mass. 374p.

[Gille00] GILLET J., SCHERZINGER B. M., LITHOPOULOS E. (2000). Inertial/GPS System for Seismic Survey. SEG Convention and Trade Show, August, Calgary, Canada. Available on http://www.applanix.com .

[Glori01] GLORIA (2001). Project of the 5th Framework Program of the European Commission. http://www.eu-gloria.org

[Gnepf99] GNEPF S. (1999). Leica Digital Magnetic Compass, System Integration Handbook. Leica product litterature.

[Goldi99] GOLDING A. R. and LESH N. (1999). Indoor navigation using diverse set of cheap, wearable sensors. Proceedings of the 3rd International Symposium on Wearable Computers, San Fransisco, CA. pp 29-36.

[Golle91] GOLLEDGE R.G., LOOMIS J. M., KLATZKY R.L., FLURY A. and YANG X. L. (1991). Designing a personal guidance system to aid navigation without sight: progress on the GIS component. International Journal of Geographical Information Systems, Taylor and Francis Ltd., London, 5(4): pp 373-395.

[Golle98] GOLLEDGE R.G., KLATZKY R.L., LOOMIS J. M., SPIEGLE J. and TIETZ J. (1998). A geographical information system for a GPS based personal guidance system. International Journal of Geographical Information Science, Taylor and Francis Ltd., London, 12(7): pp 727-749.

[Grewa93] GREWAL, M., ANDREWS, A. (1993). Kalman Filtering : Theory and Practice, Prentice Hall Information. 416p.

[Grewa00] GREWAL M. S., WEILL L. R., ANDREWS A. P. (2000). Global positioning systems and Inertial Navigation Integration. John Wiley & Sons, Inc. 416p.

[Haddr01] HADDRELL T., PRATT T. (2001). Understanding the Indoor GPS Signal, Parthus Ltd (UK), ION GPS 2001, Salt Lake City, September 2001.

[Hagan80] HAGAN R. D., STRATHMAN T., STRATHMAN L. and GRETTMAN L. R. (1980). Oxygen uptake and energy expenditure during horizontal treadmill running. Journal of Appl. Physiol. 49:571-575.

[Han97] HAN S. (1997). Quality-control issues relating to instantaneous ambiguity resolution for real-time GPS kinematic positioning. Journal of Geodesy Vol. 71, No. 6(May): 351-361.

[Harri90] HARRIS C. B. (1990). Prototype for a land based vehicle location and navigation system. M. Sc. Thesis, Vol. 20033, University of Calgary, Canada

[Harte94] HARTER A. and HOPPER A. (1994). A distributed location system for the active office. IEEE Network, January/February 1994, pp 62-70.

[Harve98] HARVEY R. S. (1998). Developement of a Precision Pointing System Using an Integrated Multi-sensor Approach. Department of Geomatics Engineering. Calgary, University of Calgary: 140p.

[Hatch82] HATCH R. R. (1982). The synergism of GPS Code and carrier Measurement. Proceedings of the Fourth International Geodetic Symposium on Satellite Positioning, Las Cruces.

[Hein01] HEIN G. W., EISSFELLER B., OEHLER V., WINKEL J. O. (2001). Synergies between Satellite Navigation and Location Services of Terrestrial Mobile Communication. Proceedings of Locellus 2001, Munich, Germany, Februar 5-7. pp 211-225.

[Heinr01] HEINRICH G., EISSFELLER B. (2001). Radiofrequency Ranging Techniques for Indoor Positioning. Proceedings of Indoornav 2001, Munich, Germany, July 4-5. pp 31-51.

[Helal01] HELAL A., MOORE S. E., RAMACHANDRAN B. (2001) Drishti: An Integrated Navigation System for Visually Impaired and Disabled, Proceedings of the 5th International Symposium on Wearable Computers, October, Zurich, Switzerland.

[Herre99] HERREN R., SPARTI A., AMINIAN A., SCHUTZ Y. (1999). The Prediction of Speed and Incline in Outdoor Running in Humans using Accelerometry. Medicine and science in sports and exercises 31 (7)(July): 1053-1059.

[Hoffm01] HOFFMAN G.S., MILLER M.M. (2001). Real-Time Personal Positioning and Physiological Monitoring System. Locellus, Munich, Germany, February 5-7.

[Jiraw00] JIRAWIMUT R., SHAH M. A., PTASINSKI P., CECELJA F., BALACHANDRAN W. (2000). Integrated DGPS and Dead Reckoning for A Pedestrian Navigation System in Signal Blocked Environments, ION GPS, Salt Lake City, Utah, September 19-22.

[Jiraw01] JIRAWIMUT R., PTASINSKI P., GARAJ V., CECELJA F. and BALACHANDRAN W. (2001). A Method for Dead Reckoning Parameter Correction in Pedestrian Navigation System. Proc. of IEEE Instrumentation and measurement Technology conference. Budapest, hungary, May 21-21. pp 1554-1558.

[Judd97] JUDD T. (1997). A Personal Dead Reckoning Module. ION GPS. Kansas City. September.

[Kalma60] KALMAN R. E. (1960). A New Approch to Linear Filtering and Prediction Problems. Journal of Basic Engineering, Vol. 82 (Transaction of the American Society of Mechanical Engineers): pp 35-45.

[Kalma61] KALMAN R. E. (1961). New Results in Linear Filtering and Prediction Theory. Journal of Basic Engineering Vol. 83 (Transaction of the American Society of Mechanical Engineers): pp 95-107.

[Kappi01] KAPPI J., COLLIN J., SAARINEN J., SYRJARINNE J. (2001). MEMS-IMU Based Pedestrian Navigator for Handheld Devices. ION GPS. Salt Lake City. September.

[Kee01] KEE C., YUN D., JUN H. (2001). Autonomous Navigation and Attitude Control of a Miniature Vehicle Using Indoor Navigation System. ION GPS. Salt Lake City. September.

[King98] KING A. D. (1998). Inertial Navigation: Forty Years of Evolution. GEC Review, Vol. 13, No. 3.

[Kitaz95] KITAZAKI S. and GRIFFIN M. J. (1995). A data correction method for the surface measurement of vibration on the body. Journal of Biomech., 28, pp 885-890.

[Koch98] KOCH K. R., YANG Y. (1998). Robust Kalman Filter for Rank Deficient Observation Models. Journal of Geodesy 72(1998): 436 - 441.

[Koure98] KOUREPENIS A., BORENSTEIN J., CONNELLY J., ELLIOTT R., WARD P., WEINBERG M. (1998). Performance of MEMS inertial sensors. Position Location and Navigation Symposium (PLAN), IEEE.

[Ladet99] LADETTO Q., MERMINOD B., TERRIER P., SCHUTZ Y. (1999). On foot navigation: When GPS is not enough. GNSS'99, Genova, Italy.

144

[Ladet00a] LADETTO Q., GABAGLIO V., MERMINOD B., TERRIER P., SCHUTZ Y. (2000). Human Walking Analysis Assisted by DGPS. GNSS, Edinburgh, 1-4 May.

[Ladet00b] LADETTO Q. (2000). On Foot Navigation: Continuous Step Calibration Using Both Complementary Recursive Prediction and Adaptive Kalman Filtering. ION GPS, Salt Lake City, Utah, September 19-22.

[Ladet01a] LADETTO Q., GABAGLIO V., MERMINOD B. (2001). Two different approaches for Augmented GPS Pedestrian Navigation. Locellus, Munich, Germany, February 5-7.

[Ladet01b] LADETTO Q., GABAGLIO V., MERMINOD B. (2001). Combining Gyroscopes, Magnetic Compass and GPS for Pedestrian Navigation. Int. Symposium on Kinematic Systems in Geodesy, Geomatics and Navigation (KIS 2001), Banff, Canada, June 5-8.

[Ladet03] LADETTO Q. (2003). Capteurs et algorithmes pour la localisation autonome en mode pédestre. Thesis report. EPFL.

[Ladin91] LADIN Z. and WU G. (1991). Combining position and acceleration measurements for joint force estimation. Journal of Biomech, 24, pp 1173-1187.

[Lapor79] LAPORTE R. E., KULLER L. H., and KUPFER D. J. (1979). An objective measure of physical activity for epidemiological research. Am. J. Epidemiol., 109, pp 158-167.

[Lauri76] LAURILYA S. H. (1976). Electronic surveying and navigation. Wiley-Interscience publication. John Wiley & Sons, New-York.

[Lawre98] LAWRENCE A. (1998). Modern Inertial Technology. Guidance and Control. ed. Springer-Verlag. 2nd ed. New York. 268p.

[Lechn01] LECHNER W., BAUMANN S., LEGAT K. (2001). Pedestrian Navigation - Bases for the Next Mass Market in Mobile Positioning. Proceedings of Locellus 2001, Munich, Germany, Februar 5-7. pp 79-90.

[Legat00] LEGAT K. AND LECHNER W. (2000). Navigation systems for pedestrians - a basis for various value-added services. ION GPS, Salt Lake City, Utah, September 19-22.

[Leppa01] LEPPAKOSKI H., SAARINEN J., SYRJARINNE J. (2001). Personal Positioning Using Wireless Assisted GPS with Low-Cost INS. ION GPS. Salt Lake City. September.

[Locus01] LOCUS (2001), Project of the 5th Framework program of the European Comission. http://www.telematica.de/locus

[Loehn01] LOEHNERT E., WITTMANN E., PIELMEIER J. (2001). PARAMOUNT - Public Safety & Commercial Info-Mobility Applications & Services in the Mountains. ION GPS. Salt Lake City. September.

[Makik95] MAKIKAWA M. and IIZUMI H. (1995). Development of an ambulatory physical activity memory device and its application for categorization of actions in daily life. Medinfo 95 Proceedings, pp 747-750.

[Mao00] MAO G., GU Q. (2000). Design and implementation of microminiature inertial measurement system and GPS integration. Proceedings of the IEEE National Aerospace and Electronics Conference (NAECON). pp 333 -338.

[Marga76] MARGARIA R. (1976). Biomechanics and Energetics of Muscular Exercise. Oxford: Clarendon Press, pp 67-139.

[Markl78] MARKLEY F. L. (1978). Parametrization of the Attitude. Spacecraft Attitude Determination and Control. J. R. Wertz. Dordrecht, Kluwer Academic Publishers: 410-420.

[Marse96] MARSELLI C. (1996). Error Correction to Microsensors in a Navigation Application. 3ème Congrès France-Japon/1er Congrès Europe-Asie en mécatronique, Besançon, Institut de Microtechnique, Neuchâtel.

[Marse97] MARSELLI C. (1997). Error Modelling of a Silicon Angular Rate Sensor. Symposium Gyro 97, Stuttgart.

[Marse98a] MARSELLI C. (1998). Data processing of a navigation microsystem, Ph. D. Thesis, Institut de microtechnique, Université de Neuchâtel, Switzerland.

[Marse98b] MARSELLI C. and Al. (1998). Application of Kalman Filtering to Noise Reduction on Microsensor Signals, Institute of Microtechnology, Neuchâtel.

[Matla98] MATLAB (1998). Wavelet Toolbox User's Guide. The MathWorks Inc., Natick, Mass.

[Maybe94] MAYBECK P. S. (1994). Stochastic models, estimation and control. Mathematics in science and engineering, Vol 141, ed. R. Bellman, University of Southern California.

[Mcbur88] McBURNEY P. W. (1988). Self-Cointained GPS Integrity Monitoring Using a Censored Kalman Filter. ION GPS. Colorado Springs.

[Mclel92] Mc LELLAN J. F. (1992). Design and Analysis of a Low Cost GPS Aided Navigation System. UCGE Reports number 20097. University of Calgary, Alberta, Canada.

[Meije89] MEIJER G. A. L., WERSTERTEP K. R., KOPER H., and TEN HOOR F. (1989). Assessment of energy expenditure by recording heart rate and body acceleration. Med. Sci. Sports Exerc., vol. 21, pp 343-347.

[Mermi88] MERMINOD B. (1988). Resolution of the Cycle Ambiguities. School of Surveying, University of New South Wales, Sydney.

[Mermi89] MERMINOD B. (1989). The Use of Kalman Filters in GPS Navigation. School of Surveying. University of New South Wales. Sydney. 203p.

[Monto83] MONTOYE H., WASHBURN R., SERVAIS S., ERTL A., WEBSTER J.G. and NAGLE F. J. (1983). Estimation of energy expenditure by a portable accelerometer. Med. Sci. Sports Exerc., vol. 15, pp 403-407.

[Morri73] MORRIS J. R. W. (1973). Accelerometry - A technique for the measurement of human body movements. Journal of Biomech. vol 6. pp 729-736.

[Najaf99] NAJAFI B., AMINIAN K., BLANC Y., ROBERT P. (1999). A New Method For Body Posture Detection Using A Kinematic Sensor. EMBC'99 (Supplement of the Journal "Medical and Biological Engineering and Computing"), Vienna.

[NATO91] NATO Team (1991). Navstar GPS User Equipment, an Introduction. GPS Joint Program Office.

[Nels01] http://www.nels.org/source/newsletter.html

147

[Ogaja01] OGAJA C., WANG J., RIZOS C. (2001). Principal Component Analysis of Wavelet Transformed GPS Data for Deformation Monitoring, Proc. IAG Scientific Assembly, 2-7 Spetember, Budapest, Hungary.

[Olivi91] OLIVIER R., VETTERLI M. (1991). Wavelets and Signal Processing, IEEE Signal Processing, October, pp 14-38.

[Opsha01] OPSHAUG G.R., ENGE P. (2001). GPS and UWB for Indoor Navigation. ION GPS. Salt Lake City. September.

[Palmq96] PALMQVIST J. (1996). Integrity Monitoring of Integrated Satellite/Inertial Navigation Systems Using the Likelihood Ratio. ION GPS. Kansas City. September.

[Parki95] PARKINSON B. W., SPICKLER J. J. (1995). Global Positioning System, Theory and Application. Volume I and II. P. Zarchan. Washington, American Institute of Astronautics and Aeronautics. Volume 163. 793&643p.

[Perri00] PERRIN O., TERRIER P., LADETTO Q., MERMINOD B., SCHUTZ Y. (2000). Improvement of Walking Speed Prediction by Accelerometry using Altimetry, validated by DGPS. Med biol Eng Comp. 38: 164-168.

[Petri96] PETRIE H., JOHNSON V., STROTHOTTE T., RAAB A., FRITZ S. and MICHEL R. (1996). MOBIC: Designing a Travel Aid for Blind and Elderly People. Journal of Navigation, Royal Institute of Navigation, London, 49(1): pp 45-52.

[Ram98] RAM S. and SHARF J. (1998). The People Sensor: A Mobility Aid for the Visually Impaired. The Second International Symposium on Wearable computers, Pittsburgh, PA, 1998, pp 166-167.

[Rande00] RANDELL C. and MULLER H. (2000). Context Awareness by Analysing Accelerometer Data. The Fourth International Symposium on Wearable computer, Atlanta, GA, pp 175-176.

[Redmo85] REDMOND D. P. and HEGGE F. W. (1985). Observations on the design and specification of a wrist-worn human activity monitoring system. Behav. Res. Meth. Instr. Comp., 17, pp 659-669.

[Reswi78] RESWICK J., PERRY J., ANTONELLI D., SU N., and FREEBORN, C. (1978). Preliminary evaluation of the vertical acceleration gait analizer (VAGA). in Proc. 6th Annu. Symp. External Control Extremities, Dubrovnik, pp 305-314.

[Rober01] ROBERTS G.W., EVANS A., DODSON A., DENBY B., HOL-LANDS R., COOPER S. (2001). Integrating GPS, INS and Augmented Reality for Sub-surface Visualisation. ION GPS. Salt Lake City. September.

[Sagna13a] SAGNAC G. (1913). L'éther lumineux démontré par l'effet du vent relatif d'éther dans un interféromètre en rotation uniforme. C. R. Acad. Sci., 95, pp 708-710.

[Sagna13b] SAGNAC G. (1913). Sur la preuve de la réalité de l'éther lumineux par l'expérience de l'interférographe tournant. C. R. Acad. Sci., 95, pp 1410-1413.

[Sauer94] SAUER D. B. (1994). Phase Measurement in Kinematic GPS Applications Theory and Summary of Processing Strategies. Bern, Astronomische Institüt Universität Bern. Switzerland.

[Schut97] SCHUTZ Y. AND CHAMBAZ, A. (1997). Could a satellite based navigation system (GPS) be used to assess the physical activity of individuals on earth ? Eur. J. Clin. Nutr. 51:338-339.

[Schwa83] SCHWARZ K. P. (1983). Inertial Surveying and Geodesy. Reviews of geophysics and space physics Vol. 21 No. 4(May): 878-890.

[Shust93] SHUSTER M. D. (1993). "A survey of Attitude Representations." Journal of Astronauticals Sciences Vol. 41 No 4, Oct-Dec. pp 437-517.

[Skalo99] SKALOUD J. (1999). Optimising Georeferencing of Airborne Survey Systems by INS/DGPS. Department of Geomatics Engineering, University of Calgary. 160p.

[Smidt71] SMIDT G. L., ARORA J. and JOHNSTON R. C. (1971). Accelerographic analysis of several types of walking. Am. J. Phys. Med., 50, pp 285-300.

[Soehr00] SOEHREN W. and KEYES CH. (2000). Human-Motion Based-Navigation Algorithm Development. IEEE Positioning, Location and Navigation Symposium (PLANS), SanDiego, March 13-16.

[Stran97] STRANG G. and Borre K. (1997). Linear Algebra, Geodesy, and GPS. Wellesley-Cambridge Press.

[Tanak94] TANAKA S., YAMAKOSHI K. and ROLFE P. (1994). New portable instrument for long-term ambulatory monitoring of posture

change using miniature electro-magnetic inclinometer. Med. Biol. Eng. Comp., 32, pp 357-360.

[Terri99] TERRIER P., AMINIAN K., SCHUTZ Y. (1999). Can Accelerometry Accurately Predict Energy Cost of Walking in Uphill & Downhill Conditions? International Journal of Obesity and related Metabolism Disorder 23(Suppl 5): 60.

[Tiber97] TIBERIUS C. C. J. M. (1997). Kinematic GPS: Performance and Quality Control. Int. Symposium on Kinematic Systems in Geody, Geomatics and Navigation (KIS'97), Banff, Canada.

[Titte97] TITTERTON D. H. (1997). Strapdown Inertial Navigation Technology. IEE Radar, Sonar, Navigation and Avionics Series 5, ed. E.D.R. Shearman. London: Peter Peregrinus Ltd. 455 p.

[Vanlo78] Van LOAN C. F. (1978). Computing Integrals Involving the Matrix Exponential. IEEE Trans. on Automatic Control, Vol ac-23, 3, pp 395-404.

[Velti96] VELTINK P. H., BUSSMANN H. B. J., DE VRIES W., MERTENS W. L. J. and VAN LUMMEL R. C. (1996). Detection of static and dynamic activities using uniaxial accelerometers. IEEE Trans. Rehabil. Eng., 4, pp 375-385.

[Vidal01] VIDAL J., JATIVA R., CABRERA M. (2001). Positioning Limits for UMTS Mobiles in Delay & Angular Dispersive Channels. Proceedings of Locellus 2001, Munich, Germany, Februar 5-7. pp 92-106.

[Viita99] VIITANEN P, (1999). Indoor and local positioning systems, Short overview. Personal Navigation Technology Group. VTT Automation.

[Wang97] WANG J. G. (1997). Filtermethoden zur fehlertoleranten kinematischen Positionsbestimmung. Studiengang Vermessungewesen. München, Universität der Bundeswehr: 135p.

[Wang98] WANG J. G. (1998). Identifikation und Kompensation Systematischer Sensorfehler im Kalman-Filter. Allgemeine Vermessungs-Nachrichten 7, September: pp 224-230.

[Want92] WANT R. et al. (1992) The active badge location system. ACM Transactions on Information Systems, 10(1):91-102, Jan 1992.

[Ward97] WARD A., JONES A. and HOPPER A. (1997). A New Location Technique for the Active Office. IEEE Personnel Communications, 4(5):42–47, October 1997.

[Washb88] WASHBURN R. A. and LAPORTE R. E. (1988). Assessment of walking behaviour: effects of speed and monitor position on two objective physical activity monitors. Res. Q. Exerc. Sports, 59, pp 83-85.

[Webst82] WEBSTER J. B., MESSIN S., MULLANEY D. J. and KRIPKE D. F. (1982). Transducer design and placement for activity recording. Med. Biol. Eng. Comp. 20, pp 741-744.

[Wei90] WEI M. (1990). A Strapdown Inertial Algorithm Using an Earth-Fixed Cartesian Frame. Navigation, Journal of the ION 37 No.2 (Summer 1990). pp 153-167.

[Wickm90] WICKMAN J. and HAKANSSON A. (1990). Localisation with GSM. Land Navigation and Informations Systems. Conf. of Royal Institute of Navigation, Warwick.

[Wolf97] WOLF R. (1997). A Kalman Filter for the Integration of a Low Cost INS and An Attitude GPS. Int. Symposium on Kinematic Systems in Geodesy, Geomatics and Navigation (KIS'97), Banff, Canada.

[Wong81] WONG T.C., WEBSTER H.J., MONTOYE H. and WASHBURN, R. (1981). Portable accelerometer device for measuring human energy expenditure. IEEE Trans. Biomed. Eng., vol. 28 pp 467-471.

[Yang99] YANG J., YANG W., DENECKE M. and WAIBEL A. (1999). Smart Sight: A Tourist Assistant System. The Third International Symposium on Wearable computers, San Francisco CA, pp 73-78.

[Yazdi98] YAZDI N., AYAZI F., NAJAFI K. (1998). Micromachined inertial sensors. Proceedings of the IEEE , Volume: 86 Issue: 8 , Aug. 1998. pp 1640-1659.

[Zhao97] ZHAO Y. (1997). Vehicle Location and Navigation Systems. ITS series, Artech House. London.

Acknowledgments

To become a doctor is a long way that looks sometimes very "walkable" and sometimes like a long and obscure tunnel. As I reach the end of it, I would like to thank sincerely the people who help me and accompany me during this part of my life.

First, I would like to thank Professor Bertrand Merminod, my supervisor. From the beginning, he trusts in my capacity and gives me the chance to accomplish this work. I appreciate the freedom he gave me to perform this research, giving the opportunity to put my attention in various field and to learn a lot. He find always the time to provide fruitful recommendation with his clear approach of the problems and fine reasoning. I also greatly appreciate the chance he offered me to present my research at different seminars and conferences all over the world.

To these thanks, I would like also to associate all the team of the Unit of Topometry: Pierre-Yves Gilliéron, Hubert Dupraz, Jean-Robert Gros for his continuous availability and help, Lionel Gostelli, Véronique Boillat Kireev, Dorette Fasoletti, Cristina Benagli, Mounir Azouzi who paves the way to become a doctor in the Unit, and all the people who have worked within the Unit during these last years.

Special thanks to Jan Skaloud who provides always very profitable input to the work with his unbeatable skills in a lot of fields like Kalman filter, INS, wavelet, etc .

Last but not least, I would like to place huge and infinite thanks to my officemate Quentin Ladetto. We share a lot of time and discussion together in the office but also outside, in the "normal" life. I really appreciate his continuous friendship and dynamism.

During my thesis work, I had also the opportunity to supervise student for their diploma thesis. It was always a great experience for me. The work they have done was also very helpful for the thesis. Thanks then to Laurent

Claude, David Brugger, Cedric Moullet and Yannick Levet whose work has been very appreciated for the thesis.

All the team of the Unit and the nice infrastructure in Lausanne provides a very comfortable and friendly environment to perform this work.

I would like also to thanks Mario El Khoury and Jens Krauss who were in charge of the project at CSEM. I always appreciate their constructive remarks and suggestions during the different meeting we held on the project.

To Michele Zehnder and Emmanuel Marthe, I thank them for their friendship and the company during the long train travel between Fribourg and the EPFL.

Thank you also to Guy Banim and John Swann, they dedicated time for the proof-read of the PhD report.

Thank you also to the people in ESA. They offer my first position outside university and they have placed confidence in me. I appreciate also the days provided to accomplish the last steps of this Ph.D thesis. In particular I would like to thanks Alex Steciw, head of the Galileo Interim Support Structure in Brussels and all my colleagues of the GISS.

Enfin, un tout grand merci à ma famille. A Mireille tout d'abord, merci pour tout ce que tu m'as apporté durant ces "longues" années. Merci pour ton soutien permanent et sans faille. Merci aussi à nos trois filles: Marie, Lucie et Pauline, rayons de soleil permanent. A vous quatre, vous m'avez donné toute l'énergie nécessaire pour accomplir ce travail.

Appendix A

Appendix: Kalman filter

This appendix presents the algorithmic part of the Kalman Filter [Kalma60, Kalma61]. All the historical background of the filter (Wiener filter) are not exposed and can be found in [Brown97]. A special attention is focused on the extended Kalman filter with non-linear observation model [Grewa93].

A.1 Theoretical development

A Kalman filter is composed by two model:

1. an observation model

2. a kinematic model

Each model have a stochastic part and a functional part.

The common part of the two model are the parameters, expressed in the state vector $\mathbf{x}$.

Observation model

The functional part of the observation model build the n relations $f = (f_1, f_2, \ldots, f_n)$ between the n observations $\ell = (\ell_1, \ell_2, \ldots, \ell_n)$ and the u parameters.

$$\ell - \mathbf{v} = f(\mathbf{x}) \tag{A.1}$$

where **v** is an error on the observation.

If the equation is not linear, it is linearised using a Taylor series. The value around which the function will be linearised is the approached value $\mathring{x}$. The best approached value is generally the estimated value $\tilde{x} = \mathring{x}$. This implies $d\tilde{x} = 0$ .The linearised equation is then:

$$\tilde{\mathbf{v}} - \mathbf{v} = \mathbf{H} \cdot d\mathbf{x} \tag{A.2}$$

where

$$\mathbf{H} = \begin{bmatrix} \frac{\partial f_1(\mathbf{x})}{\partial x_1} & \cdots & \frac{\partial f_1(\mathbf{x})}{\partial x_u} \\ \vdots & & \vdots \\ \frac{\partial f_n(\mathbf{x})}{\partial x_1} & \cdots & \frac{\partial f_n(\mathbf{x})}{\partial x_u} \end{bmatrix} \tag{A.3}$$

and the vector $\tilde{\mathbf{v}}$ is computed as:

$$\tilde{\mathbf{v}} = \ell - f(\tilde{\mathbf{x}}) \tag{A.4}$$

The stochastic model is the covariance matrix of the observation $\mathbf{Q}_{\ell\ell}$.

Kinematic model

The kinematic model expresses the evolution of the parameter in function of their actual state. It build a relation between parameters at time k and the same parameters at time $k + 1$. The model include also random process to characterise its stochastic part.

The kinematic model can be described in two different forms:

1. continuous form

2. discrete form

In the continuous form, both the functional and the stochastic models are expressed in the following stochastic differential equation:

$$\dot{\mathbf{x}} = \mathbf{F} \cdot \mathbf{x} + \mathbf{G} \cdot u \tag{A.5}$$

The passage from the continuous (**F** and **G**) to the discrete form (Φ and $\mathbf{Q}_{ww}$) is done by resolving the homogeneous equation (stochastic differential equation) from Equation A.5:

$$\dot{\mathbf{x}} = \mathbf{F} \cdot \mathbf{x} \tag{A.6}$$

We have:

$$\Phi(t_k, t_{k-1}) = e^{\mathbf{F}\Delta t} \approx I + \mathbf{F} \cdot \Delta t + \frac{1}{2!}\mathbf{F}^2 \Delta t^2 + \ldots + \frac{1}{n!}\mathbf{F}^n \Delta t^n \tag{A.7}$$

For the stochastic part we have:

$$\mathbf{Q}_{ww} = \int_{t_{k-1}}^{t_k} \Phi \mathbf{G} q_{uu} \mathbf{G}^T \Phi^T dt \tag{A.8}$$

where q_{uu} is the spectral density of u.

The resolution of those two last equations can also be done using exponential matrix [Brown97, Vanlo78].

The discrete form is:

$$\begin{cases} \tilde{\mathbf{x}}_k = \Phi \cdot \hat{\mathbf{x}}_{k-1} \\ \mathbf{Q}_{ww} \end{cases} \tag{A.9}$$

Filter

From the two models described above, we have at time k on one hand observations that allow to compute the parameters $\mathbf{x}$ and on the other hand predicted increments of the parameters at time k based on the increment of the parameters at time $k - 1$. These predicted parameters can be considered as pseudo-observations.

The filter is actually the combination of both model with the task to minimize the errors $\mathbf{v}$ on observations and the increments $d\mathbf{x} = (\mathbf{x} - \tilde{\mathbf{x}})$ on the parameters.

State and covariance update:

The gain matrix $\mathbf{K}$ is computed as

$$\mathbf{K} = \mathbf{Q}_{\tilde{\mathbf{x}}\tilde{\mathbf{x}}} \mathbf{H}^T (\mathbf{H} \mathbf{Q}_{\tilde{\mathbf{x}}\tilde{\mathbf{x}}} \mathbf{H}^T + \mathbf{Q}_{\ell\ell})^{-1} \tag{A.10}$$

The updated increments $d\hat{\mathbf{x}}$ are:

$$d\hat{\mathbf{x}} = d\tilde{\mathbf{x}} + \mathbf{K}(\tilde{\mathbf{v}} - \mathbf{H} \cdot d\tilde{\mathbf{x}}) \tag{A.11}$$

With the assumption $\tilde{\mathbf{x}} = \mathring{\mathbf{x}}$, we have:

$$d\hat{\mathbf{x}} = \mathbf{K} \cdot \tilde{\mathbf{v}} \tag{A.12}$$

The updated parameters are then computed as:

$$\hat{\mathbf{x}} = \tilde{\mathbf{x}} + d\hat{\mathbf{x}} \tag{A.13}$$

For the stochastic model, the covariance matrix is computed as:

$$\mathbf{Q}_{\hat{\mathbf{x}}\hat{\mathbf{x}}} = (\mathbf{I} - \mathbf{KH})\mathbf{Q}_{\tilde{\mathbf{x}}\tilde{\mathbf{x}}} \tag{A.14}$$

State and covariance propagation:

After the update of the parameters, the kinematic model makes the propagation until the next update. For the parameters, we have:

$$\tilde{\mathbf{x}}_{k+1} = \boldsymbol{\Phi} \cdot \hat{\mathbf{x}}_k \tag{A.15}$$

and for the stochastic part, the covariance matrix is computed as:

$$\mathbf{Q}_{\tilde{\mathbf{x}}\tilde{\mathbf{x}}} = \boldsymbol{\Phi}\mathbf{Q}_{\hat{\mathbf{x}}\hat{\mathbf{x}}}\boldsymbol{\Phi}^T + \mathbf{Q}_{ww} \tag{A.16}$$

A.2 Example of using a Kalman filter

After exposing the Kalman filter theory, this section gives a few example of the use of a Kalman filter.

A.2.1 KF as a low pass filter to eliminate noise

KF filter can be used as a low past filter to eliminate noise issued by a sensor. in the thesis we have many example where this type of KF is used: step detection (3.1.2), filtering RMS (3.4), filtering (and smoothing) the GPS azimuth (4.6) and INS azimuth (4.4).

In these cases the observation is the sampled signal itself and the kinematics model is generally composed by a random process. Relation between parameters appears when different order of the random process are involved.

A.2.2 KF as an integration tool to combine DR and/or INS with GPS

This sort of Kalman filter have been used in the thesis in some application: pedometer and GPS integration to determine the averaged step length (3.1.3).

Here the state propagation is in completely replaced by the DR algorithm or the INS mechanisation that will give better result than any model of movement.

The considered observation are the difference between GPS position and INS position and the parameter are the increment dx. At each update the predicted parameter is reset to nil and only the stochastic part is propagated.

Curriculum Vitae

Name:	**GABAGLIO**
Surname:	**Vincent**
Born:	24th June 1973 in Fribourg (Switzerland)
Citizen:	Swiss
E-mail:	Vincent.Gabaglio@a3.epfl.ch

Education

1997–2001	Ph.D candidate at the Geodetic Engineering Lab at the Institute of Geomatics of the Swiss Federal Institute of Technologye in Lausanne (EPFL). *Thesis Director:* Prof. Bertrand Merminod
January 2003	Ph.D. thesis defense: "INS/GPS integration for Pedestrian Navigation".
Nov. 1997 - May 1998	Visiting Fellow in the Satellite And Positioning Group (SNAP), headed by Prof. Chris Rizos, at the University of New South Wales, Sydney, Australia
1992–1997	Engineering EPF diploma in Rural Engineering - Geomatics (Ingénieur diplômé EPFL en génie rural, spécialisation mensuration).
April 1997	*Diploma Thesis* : "Détermination d'attitude à l'aide de GPS / Attitude determination with GPS". *Supervisor:* Prof. Bertrand Merminod.
June 1992	*Federal Maturity (Baccalaureat) Scientific Type*, Collège St-Michel, Fribourg.

Professional experiences

Since November 2001	Receivers Services and User Application Expert at the European Space Agency for the Galileo program
1997-2001	First assistant for the courses Adjustement and Navigation Supervision of diploma thesis and semester student projects

Awards

2001	Prize APLE for the invention EPFL 2000 for the patent *Pedestrian Navigation Method and Apparatus Operative in a Dead Reckoning Mode.*
2001	Winner of the *ION-GPS 2001 Student Competition*, Salt Lake City
2001	Best presentation Award (session New Application) at the *ION-GPS 2001 conference*, Salt Lake City
1997	Winner of the prize SSMAF (Société Suisse des Mensuration et des Amlérioration foncière) awarding the excellent quality of the Diploma thesis in the Rural Engineering section.
1997	Winner of the prize AVIG (Association vaudoise des Ingénieur Géomètre) awarding the student in the rural engineering section having the best marks at diploma and propedeutical exams.

Language

French (mother language)
English (good knowledge)
German (knowledge)
Italian (good speaking knowledge)

Main publications

Gabaglio V. (2001) *Centralised Kalman Filter for Augmented GPS Pedestrian Navigation*, GPS-ION Conference, Salt Lake City, Utah, September 12-15.

Ladetto Q., Gabaglio V., Merminod B. (2001) *Combining Gyroscopes, Magnetic Compass and GPS for Pedestrian Navigation*, Int. Symposium on Kinematic Systems in Geody, Geomatics and Navigation (KIS 2001), Banff, Canada, June 5-8, p. 205-212.